Physical Metallurgy

1

Robert W. Cahn and Peter Haasen (†), editors

FOURTH, REVISED AND ENHANCED EDITION

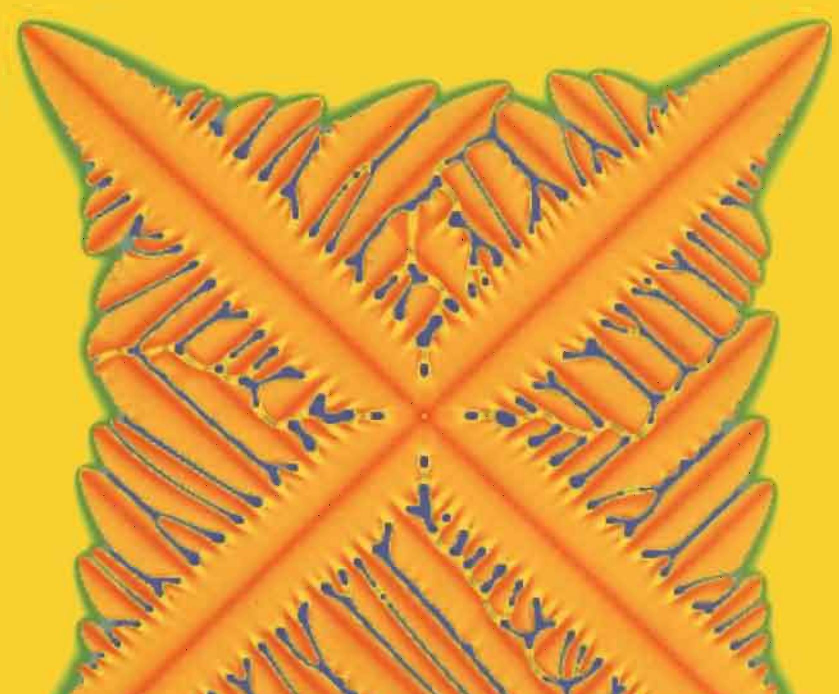

NORTH-HOLLAND

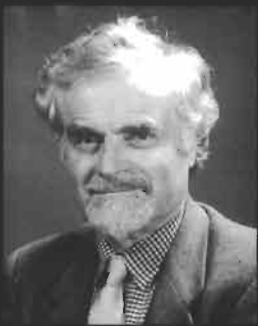

Prof. Robert W. Cahn, editor

PHYSICAL METALLURGY

VOLUME I

LIST OF CONTRIBUTORS

A. S. Argon
E. Arzt
H. K. D. H. Bhadeshia
H. Biloni
J. L Bocquet
W. J. Boettinger
G. Brebec
R. W. Cahn
G. Y. Chin†
T. W. Clyne
R. D. Doherty
H. E. Exner
R. Ferro
D. R. Gaskell
H. Gleiter
A. L. Greer
P. Haasen†
J. P. Hirth
S. Hofmann
E. D. Hondros
E. Hornbogen
G. Kostorz
C. Laird
P. Lejček
W. C. Leslie
Y. Limoge
J. D. Livingston
F. E. Luborsky
T. B. Massalski
J. R. Nicholls
A D. Pelton
D. G. Pettifor
D. P. Pope
M. Rühle
A. Saccone
S. R. J. Saunders
M. P. Seah
W. Steurer
J.-L. Strudel
R. M. Thomson
C. M. Wayman
M. Wilkens
A. H. Windle
H. J. Wollenberger

PHYSICAL METALLURGY

Fourth, revised and enhanced edition

Edited by

Robert W. CAHN
University of Cambridge

Peter HAASEN†
University of Göttingen

VOLUME I

1996

NORTH-HOLLAND
AMSTERDAM—LAUSANNE—NEW YORK—OXFORD—SHANNON—TOKYO

ELSEVIER SCIENCE B.V.
Sara Burgerhartstraat 25
P.O. Box 211, 1000 AE Amsterdam, The Netherlands

ISBN: 0 444 89875 1

This book is printed on acid-free paper.

Printed in The Netherlands

Regretfully unnoticed, in the final printing process a layout error has occurred on the original page v, due to which the authors' names of chapters 15-19 are not correctly aligned with their chapter titles. Please use this corrected page instead.

SYNOPSIS OF CONTENTS

Volume 1

1. Crystal structure of the metallic elements	*Steurer*
2. Electron theory of metals	*Pettifor*
3. Structure and stability of alloys	*Massalski*
4. Structure of intermetallic compounds and phases	*Ferro, Saccone*
Appendix: Quasicrystals	*Steurer*
5. Metallurgical thermodynamics	*Gaskell*
6. Phase diagrams	*Pelton*
7. Diffusion in metals and alloys	*Bocquet, Limoge, Brebec*
8. Solidification	*Biloni, Boettinger*
9. Microstructure	*Gleiter*

Volume 2

10. Surface microscopy, qualitative and quantitative	*Exner*
11. Transmission electron microscopy	*Rühle, Wilkens*
12. X-ray and neutron scattering	*Kostorz*
13. Interfacial and surface microchemistry	*Hondros, Seah, Hofmann, Lejček*
14. Oxidation, hot corrosion and protection of metallic materials	*Saunders, Nicholls*
15. Diffusive phase transformations in the solid state	*Doherty*
16. Nondiffusive phase transformations	*Wayman, Bhadeshia*
17. Physical metallurgy of steels	*Leslie, Hornbogen*
18. Point defects	*Wollenberger*
19. Metastable states of alloys	*Cahn, Greer*

Volume 3

20. Dislocations	*Hirth*
21. Mechanical properties of single-phase crystalline media: deformation at low temperatures	*Argon*
22. Mechanical properties of single-phase crystalline media: deformation in the presence of diffusion	*Argon*
23. Mechanical properties of solid solutions	*Haasen*†
24. Mechanical properties of intermetallic compounds	*Pope*
25. Mechanical properties of multiphase alloys	*Strudel*
26. Fracture	*Thomson*
27. Fatigue	*Laird*
28. Recovery and recrystallization	*Cahn*
29. Magnetic properties of metals and alloys	*Livingston, Luborsky, Chin*†
30. Metallic composite materials	*Clyne*
31. Sintering processes	*Exner, Arzt*
32. A metallurgist's guide to polymers	*Windle*

SYNOPSIS OF CONTENTS

Volume 1

1. Crystal structure of the metallic elements	*Steurer*
2. Electron theory of metals	*Pettifor*
3. Structure and stability of alloys	*Massalski*
4. Structure of intermetallic compounds and phases	*Ferro, Saccone*
Appendix: Quasicrystals	*Steurer*
5. Metallurgical thermodynamics	*Gaskell*
6. Phase diagrams	*Pelton*
7. Diffusion in metals and alloys	*Bocquet, Limoge, Brebec*
8. Solidification	*Biloni, Boettinger*
9. Microstructure	*Gleiter*

Volume 2

10. Surface microscopy, qualitative and quantitative	*Exner*
11. Transmission electron microscopy	*Rühle, Wilkens*
12. X-ray and neutron scattering	*Kostorz*
13. Interfacial and surface microchemistry	*Hondros, Seah, Hofmann, Lejček*
14. Oxidation, hot corrosion and protection of metallic materials	*Saunders, Nicholls*
15. Diffusive phase transformations in the solid state	
16. Nondiffusive phase transformations	*Doherty*
17. Physical metallurgy of steels	*Wayman, Bhadeshia*
18. Point defects	*Leslie, Hornbogen*
19. Metastable states of alloys	*Wollenberger*
	Cahn, Greer

Volume 3

20. Dislocations	*Hirth*
21. Mechanical properties of single-phase crystalline media: deformation at low temperatures	*Argon*
22. Mechanical properties of single-phase crystalline media: deformation in the presence of diffusion	*Argon*
23. Mechanical properties of solid solutions	*Haasen*†
24. Mechanical properties of intermetallic compounds	*Pope*
25. Mechanical properties of multiphase alloys	*Strudel*
26. Fracture	*Thomson*
27. Fatigue	*Laird*
28. Recovery and recrystallization	*Cahn*
29. Magnetic properties of metals and alloys	*Livingston, Luborsky, Chin*†
30. Metallic composite materials	*Clyne*
31. Sintering processes	*Exner, Arzt*
32. A metallurgist's guide to polymers	*Windle*

PREFACE TO THE FOURTH EDITION

The first, single-volume edition of this Work was published in 1965 and the second in 1970; continued demand prompted a third edition in two volumes which appeared in 1983. The first two editions were edited by myself alone, but in preparing the third, which was much longer and more complex, I had the crucial help of Peter Haasen as co-editor. The third edition came out in 1983, and sold steadily, so that the publishers were motivated to propose the preparation of yet another version of the Work; we began the joint planning for this in early 1992. We agreed on the changes and additions we wished to make: the responsibility for commissioning chapters was divided equally between us, but the many policy decisions, made during a series of face-to-face discussions, were very much a joint enterprise. Peter Haasen was able to commission all the chapters which he had agreed to handle, and this task (which involved detailed discussions with a number of authors) was completed in early 1993. Thereupon, in May 1993, my friend of many years was suddenly taken ill; the illness worsened rapidly, and in October of the same year he died, at the early age of 66. When he was already suffering the ravages of his fatal illness, he yet found the resolve and energy to revise his own chapter and to send it to me for comments, and to modify it further in the light of those comments. He was also able to examine, edit and approve the revised chapter on dislocations, which came in early. These were the very last professional tasks he performed. Peter Haasen was in every sense co-editor of this new edition, even though fate decreed that I had to complete the editing and approval of most of the chapters. I am proud to share the title-page with such an eminent physicist.

The first edition had 22 chapters and the second, 23. There were 31 chapters in the third edition and the present edition has 32. The first two editions were single volumes, the third had to be divided into two volumes, and now the further expansion of the text has made it necessary to go to three volumes. This fourth edition is nearly three times the size of the first edition thirty years ago; this is due not only to the addition of new topics, but also to the fact that the treatment of existing topics has become much more substantial than it was in 1965. There are those who express the conviction that physical metallurgy has passed its apogee and is in steady decline; the experience of editing this edition, and the problems I have encountered in holding enthusiastic authors back from even more lengthy treatments (to avoid exceeding the agreed page limits by a wholly unacceptable margin), have shown me how mistaken this pessimistic assessment is! Physical metallurgy, the parent discipline of materials science, has maintained its central status undiminished.

The first three editions each opened with a historical overview. We decided to omit this in the fourth edition, for two main reasons: the original author had died and it would have fallen to others to revise his work, never an entirely satisfactory proceeding; it had also become plain (especially from the reaction of the translators of the earlier editions into Russian) that the overview was not well balanced between different parts of the world. I am engaged in writing a history of materials science, as a separate venture, and this will incorporate proper attention to the history of physical metallurgy as a principal constituent. — It also proved necessary to leave out the chapter on superconducting alloys: the ceramic superconductor revolution has virtually removed this whole field from the purview of physical metallurgy. — Three entirely new topics are treated in this edition: one is oxidation, hot (dry) corrosion and protection of metallic materials, another is the dislocation theory of the mechanical behavior of intermetallic compounds. The third new topic is a leap into very unfamiliar territory: it is entitled “A Metallurgist’s Guide to Polymers”. Many metallurgists — including Alan Windle, the author of this chapter — have converted in the course of their careers to the study of the more physical aspects of polymers (regarded by many materials scientists as *the* “materials of the future”), and have had to come to terms with novel concepts (such as “semicrystallinity”) which they had not encountered in metals: Windle’s chapter is devoted to analysing in some depth the conceptual differences between metallurgy and polymer science, for instance, the quite different principles which govern alloy formation in the two classes of materials. I believe that this is the first treatment of this kind.

Six of the existing chapters (now numbered 1, 4, 21, 22, 27, 30) have been entrusted to new authors, while another five chapters have been revised by the previous authors with the collaboration of additional authors (8, 13, 16, 17, 19). Chapter 19, originally entitled “Alloys rapidly quenched from the melt” has been broadened and retitled “Metastable states of alloys”. A treatment of quasicrystals has been introduced in the form of an appendix to chapter 4, which is devoted to the solid-state chemistry of intermetallic compounds; this seemed appropriate since quasicrystallinity is generally found in such compounds. — Only three chapters still have the same authors they had in the first edition, written some 32 years ago.

27 of the 29 new versions of existing chapters have been substantially revised, and many have been entirely recast. Two chapters (11 and 25) have been reprinted as they were in the third edition, except for corrected cross-references to other chapters, but revision has been incorporated in the form of an Addendum to each of these chapters; this procedure was necessary on grounds of timing.

This edition has been written by a total of 44 authors, working in nine countries. It is a truly international effort.

I have prepared the subject index and am thus responsible for any inadequacies that may be found in it. I have also inserted some cross-references between chapters (internal cross-references within chapters are the responsibility of the various authors), but the function of such cross-references is better achieved by liberal use of the subject index.

As always, the editors have been well served by the exceedingly competent staff of North-Holland Physics Publishing (which is now an imprint of Elsevier Science B.V. in

Amsterdam; at the time of the first two editions, North-Holland was still an independent company). My particular thanks go to Nanning van der Hoop and Michiel Bom on the administrative side, to Ruud de Boer who is responsible for production and to Chris Ryan and Maurine Alma who are charged with marketing. Mr. de Boer's care and devotion in getting the proofs just right have been extremely impressive. My special thanks also go to Professor Colin Humphreys, head of the department of materials science and metallurgy in Cambridge University, whose warm welcome and support for me in my retirement made the creation of this edition feasible. Finally, my thanks go to all the authors, who put up with good grace with the numerous forceful, sometimes impatient, messages which I was obliged to send in order to "get the show on the road", and produced such outstanding chapters under pressure of time.

I am grateful to Dr. W.J. Boettinger, one of the authors, and his colleague Dr. James A. Warren, for kindly providing the computer-generated dendrite microstructure that features on the dust-cover.

The third edition was dedicated to the memory of Robert Franklin Mehl, the author of the historical chapter and a famed innovator in the early days of physical metallurgy in America. I would like to dedicate this fourth edition to the memory of two people: my late father-in-law, *Daniel Hanson* (1892–1953), professor of metallurgy at Birmingham University for many years, who did more than any other academic in Britain to foster the development and teaching of modern physical metallurgy; and the physical metallurgist and scientific publisher — and effective founder of Pergamon Press — *Paul Rosbaud* (1896–1963), who was retained by the then proprietor of the North-Holland Publishing Company as an adviser and in 1960, in the presence of the proprietor, eloquently urged upon me the need for a new, advanced, multiauthor text on physical metallurgy.

November 1995 Robert W. CAHN
Cambridge

PREFACE TO THE THIRD EDITION

The first edition of this book was published in 1965 and the second in 1970. The book continued to sell well during the 1970s and, once it was out of print, pressure developed for a new edition to be prepared. The subject had grown greatly during the 1970s and R. W. C. hesitated to undertake the task alone. He is immensely grateful to P. H. for converting into a pleasure what would otherwise have been an intolerable burden!

The second edition contained twenty-two chapters. In the present edition, eight of these twenty-two have been thoroughly revised by the same authors as before, while the others have been entrusted to new contributors, some being divided into pairs of chapters. In addition, seven chapters have been commissioned on new themes. The difficult decision was taken to leave out the chapter on superpure metals and to replace it by one focused on solute segregation to interfaces and surfaces — a topic which has made major strides during the past decade and which is of great practical significance. A name index has also been added.

Research in physical metallurgy has become worldwide and this is reflected in the fact that the contributors to this edition live in no fewer than seven countries. We are proud to have been able to edit a truly international text, both of us having worked in several countries ourselves. We would like here to express our thanks to all our contributors for their hard and effective work, their promptness and their angelic patience with editorial pressures!

The length of the book has inevitably increased, by 50% over the second edition, which was itself 20% longer than the first edition. Even to contain the increase within these numbers has entailed draconian limitations and difficult choices; these were unavoidable if the book was not to be priced out of its market. Everything possible has been done by the editors and the publisher to keep the price to a minimum (to enable readers to take the advice of G. Chr. Lichtenberg [1775]: "He who has two pairs of trousers should pawn one and buy this book".).

Two kinds of chapters have been allowed priority in allocating space: those covering very active fields and those concerned with the most basic topics such as phase transformations, including solidification (a central theme of physical metallurgy), defects and diffusion. Also, this time we have devoted more space to experimental methods and their underlying principles, microscopy in particular. Since there is a plethora of texts available on the standard aspects of X-ray diffraction, the chapter on X-ray and neutron scattering has been designed to emphasize less familiar aspects. Because of space limitations, we regretfully decided that we could not include a chapter on corrosion.

This revised and enlarged edition can properly be regarded as to all intents and purposes a new book.

Sometimes it was difficult to draw a sharp dividing line between physical metallurgy and process metallurgy, but we have done our best to observe the distinction and to restrict the book to its intended theme. Again, reference is inevitably made occasionally to nonmetallics, especially when they serve as model materials for metallic systems.

As before, the book is designed primarily for graduate students beginning research or undertaking advanced courses, and as a basis for more experienced research workers who require an overview of fields comparatively new to them, or with which they wish to renew contact after a gap of some years.

We should like to thank Ir. J. Soutberg and Drs. A.P. de Ruiter of the North-Holland Publishing Company for their major editorial and administrative contributions to the production of this edition, and in particular we acknowledge the good-humoured resolve of Drs. W.H. Wimmers, former managing director of the Company, to bring this third edition to fruition. We are grateful to Dr. Bormann for preparing the subject index. We thank the hundreds of research workers who kindly gave permission for reproduction of their published illustrations: all are acknowledged in the figure captions.

Of the authors who contributed to the first edition, one is no longer alive: Robert Franklin Mehl, who wrote the introductory historical chapter. What he wrote has been left untouched in the present edition, but one of us has written a short supplement to bring the treatment up to date, and has updated the bibliography. Robert Mehl was one of the founders of the modern science of physical metallurgy, both through his direct scientific contributions and through his leadership and encouragement of many eminent metallurgists who at one time worked with him. We dedicate this third edition to his memory.

April 1983

Robert W. Cahn, Paris
Peter Haasen, Göttingen

PREFACE TO THE FIRST AND SECOND EDITIONS

This book sets forth in detail the present state of physical metallurgy, which is the root from which the modern saience of materials has principally sprung. That science has burgeoned to such a degree that no one author can do justice to it at an advanced level; accordingly, a number of well-known specialists have consented to write on the various principal branches, and the editor has been responsible for preserving a basic unity among the expert contributions. This book is the first general text, as distinct from research symposium, which has been conceived in this manner. While principally directed at senior undergraduates at universities and colleges of technology, the book is therefore also appropriate for postgraduates and particularly as a base for experienced research workers entering fields of physical metallurgy new to them.

Certain topics have been left to one side or treated at modest length, so as to limit the size of the book, but special stress has been placed on others which have rarely been accorded much space. For instance, a good deal of space is devoted to the history of physical metallurgy, and to point defects, structure and mechanical properties of solid solutions, theory of phase transformations, recrystallization, superpure metals, ferromagnetic properties, and mechanical properties of two-phase alloys. These are all active fields of research. Experimental techniques, in particular diffraction methods, have been omitted for lack of space; these have been ably surveyed in a number of recent texts. An exception has however been made in favour of metallographic techniques since, electron microscopy apart, recent innovations have not been sufficiently treated in texts.

Each chapter is provided with a select list of books and reviews which will enable readers to delve further into a particular subject. Internal cross-references and the general index will help to tie the various contributions together.

I should like here to acknowledge the sustained helpfulness and courtesy of the publisher's staff, and in particular of Mr. A. T. G. van der Leij, and also the help provided by Professor P. Haasen and Dr. T. B. Massalski in harmonising several contributions.

Brighton, June 1965 (and again 1970) R. W. CAHN

CONTENTS

List of contributors ii

Synopsis of contents v

Preface to the fourth edition vii

Preface to the third edition xi

Preface to the first and second editions xiii

VOLUME I

Chapter 1. Crystal structure of the metallic elements, by W. Steurer 1

1. Introduction 2

2. Factors governing a crystal structure 2
   - 2.1. Chemical bond factor 3
     - 2.1.1. The covalent bond 3
     - 2.1.2. The metallic bond 4
   - 2.2. Geometrical factors 5
     - 2.2.1. Coordination 7
     - 2.2.2. Space filling 7
     - 2.2.3. Layer stackings, polytypism 7
     - 2.2.4. Polymorphism 10

3. Crystal structure of metallic elements 12
   - 3.1. Nomenclature 13
   - 3.2. Group 1 and 2, alkali and alkaline earth metals 15
   - 3.3. Groups 3 to 10, transition metals 18
   - 3.4. Groups 11 and 12, copper and zinc group metals 21
   - 3.5. Groups 13 to 16, metallic and semi-metallic elements 22
   - 3.6. Lanthanides and actinides 28

References 45

Further reading 46

Chapter 2. Electron theory of metals, by D. G. Pettifor 47

1. Introduction 48

2. Band formation 50
   - 2.1. The constituent atoms 50
   - 2.2. Bond formation 59
   - 2.3. Band formation 63

3. Simple-metal bands 64
   - 3.1. The free-electron approximation 64
   - 3.2. Nearly-free-electron approximation 67
   - 3.3. Volume dependence 72

4. Transition-metal bands 77
   - 4.1. Tight-binding approximation 77
   - 4.2. Hybrid NFE-TB bands 82
   - 4.3. Volume dependence 84

5. Bulk properties 87
   - 5.1. Simple metals 87
   - 5.2. Transition metals 90

6. Structural stability 95
   - 6.1. Elemental metals 95
   - 6.2. Binary intermetallic phases 102

7. Heat of formation 111

8. Band theory of magnetism 123

References 129

Further reading 133

Chapter 3. Structure and stability of alloys, by T. B. Massalski 135

1. Solid solubility 136

2. Terminology (types of solid solutions) 138

3. Energy of solid solutions and phase stability considerations 140

4. Factors governing solid solubility (Hume–Rothery rules for primary solid solutions) 144

5. The meaning of "electron concentration" 147
   - 5.1. Progress in the electronic theories of metals and alloys 149

6. Termination of primary solid solubility 150
   - 6.1. Electronic theories of primary solid solutions based on noble metals 150
   - 6.2. Primary solid solubility in transition metal alloys 154

7. The atomic size in solid solutions 154
   - 7.1. The size factor 157
   - 7.2. The measurement of atomic size in terms of volume 159
   - 7.3. Combined effects of size and electronegativity 161
   - 7.4. Strain in solid solutions 161
   - 7.5. Deviation from Vegard's law 164
   - 7.6. Measurement of actual atomic sizes in solid solutions 165

8. Intermediate phases with wide solid solubility 166
   - 8.1. The electron phases 166
   - 8.2. Electron phases with cubic symmetry 168

8.3. Electron phases with hexagonal symmetry 170
8.4. Laves phases 176
8.5. Phases with wide solubility formed by the transition elements 178

9. Lattice spacings in solid solutions 180
9.1. Lattice spacings in primary solid solutions 180
9.2. The relationship between lattice spacings and magnetic properties 184

10. Defect structures 186
10.1. Vacancies and vacant sites in structures of alloys 186
10.2. Stacking faults 189
10.3. Metastable structures 192

11. Order in solid solutions 193
11.1. Types of superlattices 194
11.2. Long-period superlattices 195
11.3. Long-range order and short-range order 198

References 199

Further reading 203

Chapter 4. Structure of intermetallic compounds and phases, by R. Ferro and A. Saccone 205

1. Introduction 206
1.1. Preliminary remarks and definition of an intermetallic phase 206
1.2. Identification of the intermetallic phases 209

2. Chemical composition of the intermetallic phase and its compositional formula 210

3. Crystal structure of the intermetallic phase and its representation 214
3.1. Unit cell description (general remarks, lattice complexes) 214
3.2. Structural types 220
3.3. Unit cell Pearson symbol 223
3.4. Structure trivial names and symbols 224
3.5. Rational crystal structure formulae 227
3.5.1. Coordination and dimensionality symbols in the crystal coordination formula ... 228
3.5.2. Layer stacking sequence representation 231
3.5.3. Assembly of polyhedra 237
3.5.4. Modular aspect of crystal structure 240
3.5.5. An exercise on the use of alternative structural notations ($AuCu_3$ type as an example) 241

4. Relationships between structures and structure "families" 247
4.1. Degenerate and derivative structures, superstructures (defect, filled-up, derivative structures) 247
4.1.1. Ordering-disordering transformation 251
4.2. Antiphase domain structures 256
4.3. Homeotect structure types (polytypic structures) 256
4.4. Chimney-ladder structures (structure commensurability, structure modulation) 258
4.5. Recombination structures, intergrowth structure series 260
4.6. Group-subgroup relations for the representation of crystal-chemical relationships 263

5. Elements of systematic description of structure types. General remarks and references 264

6. Description of a few selected structural types 267
6.1. bcc W-type structure and derivative structures 268
6.1.1. Structural type: cI2–W 268

6.1.2. Structural type: cP2–CsCl 268
6.1.3. Structural type: cF16–$MnCu_2Al$ 271
6.1.4. Structural types: cF16–Li_3Bi and cF16–NaTl 272
6.1.5. Comments on the bcc derivative structures 273
6.2. Close-packed structures and derivative structures 275
6.2.1. Structural type: cF4–Cu 275
6.2.2. Cu–derivative, substitutional and interstitial superstructures (tetrahedral and octahedral holes) 275
6.2.3. Structural type: cP4–$AuCu_3$ 279
6.2.4. Structural types: tP2–AuCu (I) and oI40–AuCu(II) 279
6.2.5. Structural type: tP4–Ti_3Cu 279
6.2.6. Structural types: hP2–Mg, hP4–La and hR9–Sm 280
6.2.7. Structural type: hP8–Ni_3Sn 281
6.2.8. Structural type: hP6–$CaCu_5$ 281
6.3. Tetrahedral structures 283
6.3.1. cF8–C (diamond) and tI4–βSn structural types 283
6.3.2. Structural types: cF8–ZnS sphalerite and hP4–ZnO (ZnS wurtzite) 285
6.3.3. General remarks on "tetrahedral structures" and polytypes. tI16–FeCuS2, hP4–C lonsdaleite, oP16–BeSiN2 types and polytypes 286
6.3.4. An important non-tetrahedral C structure. The hP4–C graphite 288
6.4. cF8–NaCl, cF12–CaF_2, and cF12–AgMgAs types 288
6.4.1. cF8–NaCl type structure and compounds 288
6.4.2. cF12–CaF_2 type and antitype structures and compounds 291
6.4.3. Structural type: cF12–AgMgAs 293
6.5. hP4–NiAs, cP3–CdI_2, hP6–Ni_2In, oP12–Co_2Si, oP12–TiNiSi types; hP2–WC, hP3–AlB_2, hP6–$CaIn_2$, hP9–Fe_2P types, tI8–NbAs, tI8–$AgTlTe_2$ and tI10–$BaAl_4$ ($ThCr_2Si_2$) types, tI12–$ThSi_2$ and tI12–LaPtSi types 293
6.5.1. Structural type: hP4–NiAs 294
6.5.2. Structural type: hP3–CdI_2 294
6.5.3. Structural type: hP6–Ni_2In 294
6.5.4. Structural types: oP12–Co_2Si ($PbCl_2$) and oP12–TiNiSi 295
6.5.5. Structural type: hP2–WC 295
6.5.6. Structural types: hP3–AlB_2 and hP3–BaPtSb; hP3-ω, Cr-Ti phase 296
6.5.7. Structural type: hP6–$CaIn_2$ 297
6.5.8. Structural type: hP9–Fe_2P 299
6.5.9. Structural types: tI8–NbAs, tI8–$AgTlTe_2$ and tI10–$BaAl_4$ ($ThCr_2Si_2$) 299
6.5.10. Structural types: tI12–$\alpha ThSi_2$ and tI12–LaPtSi 304
6.6. Tetrahedrally close-packed, Frank–Kasper structures, Laves phases, Samson phases 307
6.6.1. General remarks 307
6.6.2. cP8–Cr_3Si type cP8–Cr_3Si type structure 309
6.6.3. σ phase type structure, (tP30–σCr-Fe type) 309
6.6.4. Laves phases: cF24–Cu_2Mg (and cF24–Cu_4MgSn and cF24–$AuBe_5$), hP12–$MgZn_2$ (and hP12–U_2OsAl_3) and hP24–Ni_2Mg types 311
6.6.5. Structures based on frameworks of fused polyhedra, Samson phases 314

7. On some regularities in the intermetallic compound formation and structures 315
7.1. Preliminary remarks 315
7.2. On some factors which control the structure of intermetallic phases 317
7.2.1. Chemical bond factor and electrochemical factor 322
7.2.2. Energy band factor, electron concentration 325
7.2.3. Geometrical principles and factors, Laves' stability principles 326
7.2.4. Atomic dimensions and structural characteristics of the phases 328
7.2.5. Reduced dimensional parameters 334
7.2.6. Alternative definitions of coordination numbers 338
7.2.7. Atomic-environment classification of the structure types 342

8. Semi-empirical approaches to the prediction of (intermetallic) compound formation 345
8.1. General remarks on procedures of prediction of compound and structure formation in alloy systems 345
8.2. Stability diagrams, structure maps 345
8.3. Savitskii–Gribulya–Kiselyova method (cybernetic computer-learning prediction system) . 346
8.4. Villars, Villars and Girgis approaches (analysis of the dependence of the behaviour of alloy systems on the properties of the component elements) 347
8.5. Miedema's theory and structural information 349
8.6. Prediction of the properties of selected families of alloys: Gschneidner's relations as an example 351
8.7. Pettifor's chemical scale and structure maps 352

Appendix 1. Gazetteer, in alphabetic order, of intermetallic phases cited in this chapter. 355

References 363

Appendix to chapter 4. The structure of quasicrystals, by W. Steurer 371

1. Introduction 372

2. Description of quasiperiodic structures 374
2.1. Decoration of quasiperiodic tilings 374
2.2. Higher-dimensional approach 376
2.3. Symmetry of quasicrystals 378

3. The structure of quasicrystals and approximants 379
3.1. One-dimensional quasicrystals 380
3.2. Two-dimensional quasicrystals 381
3.2.1. Octagonal phases 381
3.2.2. Decagonal phases 382
3.2.3. Dodecagonal phases 391
3.3. Icosahedral phases 391
3.3.1. Primitive hypercubic icosahedral phases 395
3.3.2. Face-centered hypercubic icosahedral phases 401

References 408

Further reading 411

Chapter 5. Metallurgical thermodynamics, by D. R. Gaskell 413

1. Introduction 414
1.1. The First and Second Laws of Thermodynamics 414
1.2. Auxiliary thermodynamic functions 415

2. Metallurgical thermochemistry 417
2.1. The measurement of changes in enthalpy 417
2.2. The measurement of entropy 419

3. Phase equilibrium in a one-component system 422

4. Chemical reaction equilibrium 424

5. Ellingham diagrams 429

6. The thermodynamic properties of solutions 435
6.1. Mixing processes 435
6.2. Regular solution behavior 439

7. The thermodynamic origin of phase diagrams 443

8. Reaction equilibrium involving solutions and the Gibbs phase rule 447
8.1. The dependence of the equilibrium state on activity 447
8.2. The Gibbs phase rule 450

9. The thermodynamics of surfaces and interfaces 453
9.1. The Gibbs adsorption isotherm 453
9.2. The Langmuir adsorption isotherm 456
9.3. Curved interfaces 458

10. The measurement of thermodynamic activity 460
10.1. Determination of activity by experimental measurement of vapor pressure 461
10.2. Determination of activity by establishing heterogeneous equilibrium 464
10.3. Electrochemical measurement of activity 467

Bibliography 469

Chapter 6. Phase diagrams, by Arthur D. Pelton 471

1. Introduction 472

2. Binary phase diagrams 472
2.1. The thermodynamic origin of phase diagrams 474
2.2. Minima and maxima in two-phase regions 477
2.3. Miscibility gaps 478
2.4. Simple eutectic systems 480
2.5. Binary phase diagrams with no intermediate phases 481
2.5.1. Thermodynamic origin illustrated by simple regular solution theory 481
2.5.2. Liquid–liquid immiscibility – monotectics 483
2.5.3. Peritectics 483
2.5.4. Syntectics 485
2.6. Limited mutual solid solubility 485
2.7. Calculation of limiting slopes of phase boundaries 488
2.8. Intermediate phases 489
2.9. Topology of binary phase diagrams 492
2.9.1. Order-disorder transformations 494
2.10. Application of thermodynamics to phase diagram analysis 495
2.10.1. Polynomial representation of excess properties 496
2.10.2. Least-squares optimization 496
2.10.3. Calculation of metastable phase boundaries 500
2.11. Solution models 500
2.12. Binary phase diagrams involving a gaseous phase 502

3. Ternary phase diagrams 503
3.1. The ternary composition triangle 503
3.2. Ternary space model 504
3.3. Polythermal projections of liquidus surfaces 506
3.4. Ternary isothermal sections 509
3.4.1. Topology of ternary isothermal sections 511
3.5. Ternary isopleths (constant composition sections) 512

4. Multicomponent phase diagrams 514
4.1. Zero phase fraction lines 515
4.2. Nomenclature for invariant reactions 515

5. Thermodynamic calculation of ternary and multicomponent phase diagrams 516

6. Phase diagrams with potentials as axes 518
6.1. Classification of phase diagrams 524

7. Experimental techniques of measuring phase diagrams ... 525
7.1. Thermal analysis ... 526
7.2. Sampling techniques and quenching techniques ... 528
7.3. Other techniques ... 529

8. Bibliography 530
8.1. Compilations of phase diagrams ... 530
8.2. Texts and review articles ... 530

9. Acknowledgements ... 531

References ... 531

Chapter 7. Diffusion in metals and alloys, by J. L Bocquet, G. Brebec and Y. Limoge .. 535

1. Macroscopic and microscopic theories of diffusion ... 536
1.1. The mechanisms of diffusion ... 536
1.1.1. Exchange mechanisms ... 536
1.1.2. Mechanisms involving point defects ... 536
1.1.2.1. Interstitial mechanisms ... 537
1.1.2.2. Vacancy mechanisms ... 538
1.1.2.3. Mixed mechanisms ... 538
1.1.2.4. Short-lived Frenkel pairs ... 539
1.1.3. Mechanisms involving extended defects ... 539
1.2. The macroscopic theory of diffusion ... 539
1.2.1. Generalities ... 539
1.2.2. Binary alloys and the vacancy mechanism ... 539
1.2.3. Some special cases ... 541
1.2.3.1. Chemical diffusion ... 541
1.2.3.2. Dilute systems ... 542
1.2.4. The various diffusion coefficients ... 543
1.2.5. Fick's second Law ... 545
1.3. The random walk theory of diffusion ... 546
1.3.1. Einstein relation and flux expression ... 546
1.3.2. Calculation of $\overline{X}$ and $\overline{X^2}$ in terms of jump frequencies ... 547
1.3.2.1. Expression for $\overline{X^2}$ ... 548
1.3.2.2. Expression for $\overline{X}$ ... 548
1.3.3. Binary alloys and vacancy mechanism ... 550
1.3.4. Correlation effects ... 550
1.3.5. The limitation of Fick's Law ... 552
1.4. Jump frequency and diffusion coefficient calculation ... 553
1.4.1. Vacancy concentration ... 553
1.4.2. Vacancy jump ... 554
1.4.2.1. Rate theory of jumps ... 554
1.4.2.2. Dynamic theory of jumps ... 555
1.4.3. Macroscopic parameters of diffusion ... 557
1.4.3.1. Variation with temperature ... 557
1.4.3.2. Variation with pressure ... 558
1.4.3.3. Variation with atomic mass ... 558
1.5. Numerical simulation approaches ... 559
1.5.1. Molecular Dynamics method ... 560
1.5.2. Monte Carlo method ... 561

2. Experimental methods ... 562
2.1. Macroscopic methods ... 563
2.1.1. D from the *C(x)* curve ... 563

2.1.1.1. C(x) by sample sectioning 563
2.1.1.2. Non-destructive techniques 563
2.1.2. Other macroscopic methods 564
2.2. Microscopic (or local) methods 564
2.2.1. Relaxation methods 565
2.2.1.1. Thermodynamic aspects of relaxation 565
2.2.1.2. Anelasticity 566
2.2.1.3. Snoek relaxation 567
2.2.1.4. Zener relaxation 567
2.2.1.5. Gorsky effect 568
2.2.1.6. Magnetic relaxation in ferromagnetic alloys 569
2.2.1.7. Kinetics of short-range ordering 570
2.2.2. Spectroscopic methods 570
2.2.2.1. Nuclear magnetic resonance 570
2.2.2.2. Mössbauer effect 571
2.2.2.3. Quasi-elastic neutron scattering 572

3. Self-diffusion in pure metals 572
3.1. Self-diffusion in fcc and hcp metals 574
3.2. Diffusion in bcc metals 580
3.3. Prediction of the self-diffusion coefficients 581
3.3.1. Theoretical calculations of D 581
3.3.2. Empirical relations 582

4. Self- and solute-diffusion in dilute alloys 582
4.1. Vacancy diffusion in dilute A-B alloys 583
4.1.1. Standard models for bcc and fcc alloys 583
4.1.2. Kinetic expressions of the phenomenological coefficients L_{AA}, L_{AB}, L_{BA} and L_{BB} 584
4.1.2.1. Kinetic theory 584
4.1.2.2. Linear response method 586
4.1.3. Experimentally accessible quantities 588
4.1.4. Determination of vacancy jump frequencies 589
4.1.5. Determination of the solute–vacancy binding energy 592
4.2. Dumb-bell interstitial diffusion in dilute A-B alloys 592
4.3. A-B alloys with a high solute diffusivity 593
4.3.1. Purely interstitial solutes 593
4.3.2. Complex diffusion mechanisms 594

5. Diffusion in concentrated alloys 595
5.1. Diffusion of A* and B* tracers in homogeneous disordered alloys 595
5.1.1. Experimental results 595
5.1.2. Manning's random alloy model 596
5.1.3. Atomic models for diffusion in non-random disordered alloy 598
5.2. Diffusion of A^* and B^* tracers in ordered binary alloys 599
5.2.1. Ordered alloys with B2 structure 602
5.2.1.1. Experimental results 603
5.2.1.2. Atomic mechanisms for diffusion in ordered B_2 alloys 604
5.2.2. Ordered alloys with $L1_2$ structure 604
5.2.3. Ordered alloys with $L1_0$ structure 606
5.2.4. Ordered alloys with DO_3 structure 606
5.2.5. Ordered alloys with B8 structure 606
5.2.6. Ordered alloys with $B3_2$ structure 607
5.2.7. Ordered alloys with A15 structure 607
5.3. Chemical diffusion 607
5.3.1. Chemical diffusion in binary systems and Kirkendall effect 608
5.3.1.1. Description and interpretation of a typical experiment 608

5.3.1.2. Vacancy wind effect — Manning's approximation ... 609
5.3.1.3. Experimental check of vacancy wind effect ... 611
5.3.2. Ternary alloys ... 611

6. Electro- and thermomigration ... 612
6.1. Thermodynamic aspects ... 612
6.2. Microscopic analysis ... 613
6.3. Experimental methods ... 614
6.4. Experimental results and discussion ... 615
6.4.1. Thermomigration ... 615
6.4.2. Electromigration ... 616
6.5. Electromigration in short-circuits ... 617
6.6. Electromigration as a purification process ... 618

7. Diffusion along short-circuits ... 619
7.1. Phenomenological approach ... 619
7.1.1. Semi-infinite bicrystal ... 621
7.1.2. Semi-infinite crystal with an isolated dislocation ... 621
7.1.3. Short-circuit networks ... 622
7.1.4. Experimental results ... 623
7.2. New advances in grain-boundary diffusion ... 623
7.2.1. Impurity effects ... 623
7.2.2. Diffusion-induced grain-boundary migration (DIGM) ... 623
7.3. Atomistic approach to diffusion in short-circuits ... 624
7.3.1. Atomic model for grain-boundary diffusion ... 624
7.4. Surface diffusion ... 626
7.4.1. Atomic structure and point defects ... 626
7.4.2. Experimental results ... 630
7.4.2.1. Microscopic data ... 630
7.4.2.2. Macroscopic data ... 631

8. Diffusion under non-equilibrium defect concentrations ... 633
8.1. Quenched-in vacancies ... 633
8.2. Cold-work-induced defects ... 634
8.3. Irradiation-induced defects ... 635
8.3.1. Irradiation-enhanced diffusion ... 635
8.3.1.1. Defect creation ... 636
8.3.1.2. Collisional diffusion ... 637
8.3.1.3. Diffusion by thermally activated jumps ... 638
8.3.2. Irradiation-induced segregation and precipitation ... 640
8.3.3. Irradiation-induced phase transformations ... 643

9. Diffusion in amorphous metallic alloys ... 643
9.1. A primer of metallic glasses ... 644
9.1.1. Experimental portrait of the diffusion behaviour ... 645
9.1.2. Mechanism proposals ... 648
9.2. Simulation approach of the self-diffusion process ... 648
9.3. Random walk on a random array ... 649

References ... 651

Further reading ... 666

Chapter 8. Solidification, by H. Biloni and W. J. Boettinger ... 669

1. Introduction ... 670

2. Heat flow in solidification ... 670

2.1. Heat transfer within the solid/liquid metal system 670
2.2. Heat transfer at the metal-mould interface 673
2.3. Heat flow in one dimensional solidification geometries 675
2.3.1. Freezing at mould wall 676
2.3.2. Rapid freezing in contact with a cold substrate with initial melt supercooling 677
2.4. Heat flow in more complex solidification geometries 679
2.4.1. Heat flow in controlled directional solidification of metals 679
2.4.2. Powder solidification 679
2.5. Software packages 680
2.6. Experimental methods involving controlled solidification 681

3. Thermodynamics of solidification 682
3.1. Hierarchy of equilibrium 682
3.2. T_0 curves 686

4. Nucleation 687
4.1. Nucleation in pure liquids 687
4.1.1. Calculation of the critical radius and energy barrier 688
4.1.2. Nucleation rate 691
4.2. Effect of melt subdivision 693
4.3. Experiments on nucleation in pure metals 693
4.4. Alloy nucleation 695
4.5. Experiments on heterogeneous nucleation 697
4.6. Formation of metastable phases by supercooling 699
4.7. Grain size predictions in castings 700

5. Interface kinetics 700
5.1. Pure materials 700
5.1.1. Interface structure 702
5.1.2. Continuous growth 704
5.1.3. Growth of a diffuse interface 707
5.1.4. Two dimensional nucleation controlled growth 707
5.1.5. Growth by screw dislocations 708
5.1.6. Transition between continuous growth and facetted growth 708
5.2. Binary alloys 709

6. Solidification of alloys with planar and nearly planar S–L interfaces 714
6.1. General formulation of diffusion controlled growth 714
6.2. Solute redistribution during one dimensional solidification 714
6.2.1. Equilibrium freezing 714
6.2.2. Complete liquid mixing, with no solid diffusion 715
6.2.3. Solid diffusion during solidification 716
6.2.4. Steady-state diffusion controlled freezing 717
6.2.5. Convection effects. Freezing with partial mixing in the liquid (Boundary Layer Approach) 718
6.2.6. Zone melting 719
6.3. Lateral segregation 720
6.4. Morphological stability of a planar interface 720
6.4.1. Theory 721
6.4.2. Relationship to constitutional supercooling 724
6.4.3. Experiments 725
6.4.4. Further theoretical developments 726
6.5. Coupled interface and fluid flow instabilities 729

7. Cellular and dendritic solidification 731
7.1. Alloy dendritic growth 732
7.1.1. Theory of the tip region 732

7.1.2. Anisotropy ... 737
7.1.3. Approximate theory for low supercooling ... 739
7.1.4. Experiments on dendritic growth ... 739
7.2. Cell and dendrite spacings ... 741
7.2.1. Numerical calculations of arrayed cell and dendrite primary spacings ... 741
7.2.2. Analytical expressions for primary spacings ... 743
7.2.3. Secondary dendrite arm spacing ... 746
7.2.4. Cell to dendrite transition ... 748
7.3. Microsegregation ... 749
7.4. Solidification of ternary alloys ... 752
7.5. New approaches to modeling dendritic growth ... 755

8. Polyphase solidification ... 755
8.1. Eutectic solidification ... 756
8.1.1. Eutectic classification ... 757
8.1.2. Non-facetted–Non-facetted eutectics ... 757
8.1.3. Non-facetted–facetted eutectics ... 763
8.1.4. Eutectic cells and dendrites ... 765
8.1.5. Competitive growth – coupled zone ... 765
8.1.6. Divorced eutectics ... 767
8.1.7. Rapid solidification of eutectic alloys ... 768
8.2. Monotectic solidification ... 771
8.2.1. Directional solidification of monotectic alloys ... 773
8.2.2. Rapid solidification of monotectic alloys ... 775
8.3. Peritectic solidification ... 775
8.3.1. Peritectic solidification during dendritic growth ... 776
8.3.2. Aligned peritectic growth ... 778
8.3.3. Rapid solidification of peritectic systems ... 779

9. Fluid flow and casting structure ... 780
9.1. Transport processes and fluid flow in casting ... 780
9.2. Ingot structure ... 781
9.2.1. Chill zone ... 781
9.2.2. Columnar zone ... 782
9.2.3. Equiaxed zone ... 785
9.2.3.1. Origin of the equiaxed nuclei ... 785
9.2.3.2. Columnar to equiaxed transition (CET) ... 786
9.3. Macrosegregation ... 789
9.3.1. Gravity segregation ... 789
9.3.2. Interdendritic fluid flow and macrosegregation ... 789
9.3.3. Further theoretical developments for flow in the mushy zone ... 792
9.4. Porosity and inclusions ... 792
9.4.1. Porosity ... 793
9.4.2. Inclusions ... 794
9.5. Fluidity ... 795
9.5.1. Maximum fluidity ... 796
9.5.2. Combined effects of surface tension and fluidity ... 797
9.5.3. Continuous fluidity length ... 797
10. Solidification processes ... 797
10.1. Continuous casting ... 797
10.1.1. Continuous casting of steels ... 799
10.1.2. Continuous casting of light alloys ... 801
10.2. Fusion welding structures ... 803
10.2.1. Weld pool geometry ... 806
10.2.2. Macro- and microstructures of welds ... 807
11. Structure manipulation and new processes ... 809

11.1. Single crystal growth from the melt 809
11.2. Grain refinement 810
11.2.1. Thermal methods 810
11.2.2. Innoculation methods 812
11.2.3. Energy-induced methods 814
11.3. Eutectic modification 815
11.3.1. Aluminum–silicon alloys 815
11.3.2. Cast iron 816
11.3.3. Cast iron eutectic morphology 817
11.4. Influence of rapid solidification processes (RSP) 820
11.4.1. Experimental and production methods 820
11.4.2. Relationships between RSP and solidification structures 821
11.5. Low gravity effects during solidification 821
11.6. Solidification processing of metal matrix composites 824
11.7. Semisolid metal forming processes 826

References 830

Further reading 842

Chapter 9. Microstructure, by H. Gleiter 843

1. Definition and outline 844

2. Elements of microstructure 844
2.1. Point defects, dislocations and stacking faults 844
2.2. Grain boundaries 844
2.2.1. Crystallography 844
2.2.1.1. Coincidence site lattice 844
2.2.1.2. O-lattice 845
2.2.1.3. DSC lattice 847
2.2.2. Coincidence models 847
2.2.3. Structural unit models 848
2.2.4. Broken bond model 850
2.2.5. Dislocation models 853
2.2.6. Polyhedral unit models 855
2.2.7. Limitations of existing models 856
2.3. Interphase boundaries 859
2.3.1. Bonding at interphase boundaries 859
2.3.2. Chemistry of interphase boundaries 862
2.3.2.1. Interfaces without reaction layers 862
2.3.2.2. Interfaces with reaction layers 862
2.3.3. Crystallographic structure: "lock-in" model 864

3. Characterization of microstructure 865

4. Development of microstructure 870
4.1. Basic aspects 870
4.2. Microstructural changes stimulated by interfacial-energy reduction 870
4.2.1. Microstructural changes in single-phase materials, stimulated by interfacial energy: domain and grain growth 870
4.2.2. Microstructural changes in polyphase materials with a dispersion structure, stimulated by interfacial energy: Ostwald ripening 873
4.2.2.1. Stability against coarsening 877
4.2.2.2. Technological applications of coarsening theory 878
4.2.3. Microstructural changes in polyphase materials with a duplex structure stimulated by interfacial energy 878

4.2.4. Coarsening by Brownian motion ... 882
4.2.5. Microstructural changes stimulated by interfacial energy in the presence of external potential fields ... 883
4.2.5.1. Temperature gradients ... 883
4.2.5.2. Temperature cycling ... 884
4.2.5.3. Magnetic fields ... 885
4.2.5.4. Stress field ... 885
4.2.5.5. Electric fields ... 886
4.3. Deformation ... 886
4.4. Multiphase microstructures generated by migrating lattice defects ... 887
4.4.1. Moving grain boundaries ... 887
4.4.2. Moving dislocations ... 889
4.5. Periodic microstructures in open, dissipative systems ("self-organization") ... 890
4.5.1. Periodic structures due to long-range interaction forces ... 892
4.5.1.1. Precipitate lattices ... 892
4.5.1.2. Void lattices ... 892
4.5.1.3. Dislocation-loop lattices ... 893
4.5.1.4. Point-defect lattices ... 894
4.5.1.5. Long-period antiphase boundary structures ... 894
4.6. Microstructure in the vicinity of point defect sources and/or sinks ... 894
4.6.1. Enhanced precipitation and precipitate-free zones ... 894
4.6.2. Irradiation-induced precipitation ... 896
4.6.3. Point-defect condensation ... 896
4.7. Microstructure due to lattice defects formed by migrating grain boundaries ... 896
4.8. Microstructure of glasses ... 897
4.8.1. Microstructure of amorphously phase-separated glasses ... 898
4.8.2. Microstructure of partially crystallized glasses ... 899

5. Nanostructured materials ... 900
5.1. Materials with reduced dimensionality, reduced dimensions and/or high densities of defect cores ... 901
5.2. Man-made superlattices and quantum-well structures ... 902
5.3. Semicrystalline polymers ... 903
5.4. Nanocrystalline and nanoglassy materials ... 908
5.4.1. Basic concepts ... 908
5.4.2. Generation of nanocrystalline materials ... 914
5.4.3. Atomic structure ... 916
5.5. Nanoglasses ... 921
5.6. Nanocomposites ... 923
5.6.1. Nanocomposites made up of crystallites with different chemical compositions ... 923
5.6.2. Nanocomposites made up of crystallites and glassy components with different chemical compositions ... 925
5.6.3. Nanocomposites with intercalated (doped) grain boundaries ... 925
5.7. Technological applications ... 928
5.7.1. Hard, wear-resistant nanocrystalline WC–Co materials ... 928
5.7.2. Near net shape forming of nanocrystalline ceramics/intermetallics ... 928
5.7.3. Soft ferromagnetic nanostructured materials ("Finemet") ... 930
5.7.4. Magneto-caloric cooling with nanostructured materials ... 931
5.7.5. Nanocrystalline magnetic recording materials ... 932
5.7.6. Giant magnetoresistance in nanostructured materials ... 932
5.7.7. Luminescence from porous Si ... 933
5.7.8. Catalytic materials ... 935

References ... 935

Further reading ... 942

VOLUME II

Chapter 10. Qualitative and quantitative surface microscopy, by H. E. Exner 943

1. Introduction 944

2. Optical microscopy 945
 2.1. Metallographic specimen preparation 945
  2.1.1. Sampling 945
  2.1.2. Mounting 947
  2.1.3. Grinding 947
  2.1.4. Polishing 948
  2.1.5. Replica techniques 950
 2.2. Etching and other contrasting techniques 950
  2.2.1. Chemical and electrolytic etching 950
  2.2.2. Thermal etching 951
  2.2.3. Ion-etching 951
  2.2.4. Staining (tinting) and anodic oxidation 952
  2.2.5. Interference–layer contrast 953
 2.3. Principles of light microscopy and optical contrast enhancement 954
  2.3.1. Resolution and depth of focus 955
  2.3.2. Bright-field illumination 955
  2.3.3. Oblique illumination, dark field and stop contrast 955
  2.3.4. Polarized-light microscopy 956
  2.3.5. Phase contrast and interference contrast 957
  2.3.6. Filters 958
 2.4. Special optical devices and accessories 958
  2.4.1. Stereomicroscopy 958
  2.4.2. Laser scanning and confocal microscopy 958
  2.4.3. Scanning near-field optical microscopy 959
  2.4.4. High-temperature microscopy 959
  2.4.5. Television cameras 960
  2.4.6. Microphotometry and ellipsometry 960
  2.4.7. Interferometry 960
  2.4.8. Microhardness 961

3. Scanning electron microscopy 961
 3.1. Basic features of scanning electron microscopy 961
 3.2. Specimen preparation 966
 3.3. Typical forms of contrast 967
  3.3.1. Topographic contrast 967
  3.3.2. Material (atomic number) contrast 968
  3.3.3. Electron channelling contrast, electron channelling and Kossel patterns 969
  3.3.4. Magnetic contrast 970
  3.3.5. Charge collection microscopy and electron-beam-induced current measurements . 970
  3.3.6. X-ray mapping 970
  3.3.7. Cathodoluminescence 971
 3.4. Accessory equipment 971
  3.4.1. Stereomicroscopy 971
  3.4.2. Dynamic and non-ambient-temperature SEM 972

4. Scanning tunneling, atomic force and related microscopies 972
 4.1. Basic principles and capabilities 974
 4.2. Atomic force microscopy 974
 4.3. Tunneling spectroscopy 976

4.4. Related scanning techniques 976
4.5. Applications 977

5. Other special techniques of surface microscopy 979
5.1. Scanning acoustic and thermal wave microscopy 979
5.1.1. Scanning laser acoustic microscopy 980
5.1.2. Thermal-wave microscopy 981
5.2. Field-ion and field-electron microscopy 981
5.2.1. Field-ion microscopy 981
5.2.2. Atom-probe field-ion microscopy 982
5.2.3. Field-electron microscopy 983
5.2.4. Applications of field-ion microscopy 983
5.3. Photo-electron emission microscopy 985
5.4. Scanning Auger-electron microscopy 986
5.5. X-ray microscopy, topography and fluorescence 987
5.6. Imaging by other types of spectroscopic information 988

6. Topochemical techniques and surface spectroscopy 988

7. Quantitative interpretation of microstructural geometry 996
7.1. Image analysis 996
7.2. Planar characteristics and stereology 1001
7.2.1. Volume-fraction analysis 1001
7.2.2. Interface density 1004
7.2.3. Size and distance 1005
7.2.4. Orientation, contiguity, shape and other complex parameters 1010
7.3. Mathematical morphology 1014
7.4. Further aspects 1016

References 1016

Further reading 1030

Chapter 11. Transmission electron microscopy, by M. Rühle and M. Wilkens 1033

1. Introductory remarks 1034

2. The instrument 1034

3. Information from the diffraction pattern 1038
3.1. Diffraction spot pattern 1038
3.1.1. Double diffraction 1038
3.1.2. Patterns from ordered crystals 1039
3.2. Kikuchi lines 1040
3.3. Convergent-beam diffraction 1040
3.4. Moiré pattern 1042

4. Theory of diffraction contrast 1042
4.1. Introduction 1042
4.2. Specimen, reciprocal lattice and excitation error 1043
4.3. Outline of the dynamical diffraction theory 1044
4.4. Normal and anomalous absorption 1046
4.5. Dynamical bright-field and dark-field intensities 1047
4.6. The column approximation 1050
4.7. Diffraction at imperfect crystals 1050
4.7.1. The displacement field 1050
4.7.2. The kinematical approach 1051
4.7.3. Dynamical diffraction theory in terms of plane waves 1052

4.7.4. Dynamical diffraction theory in terms of Bloch waves 1053
4.7.5. Properties of strain contrast in strong-beam images 1054
4.7.6. Structure-factor contrast 1056
4.8. Practical applications of the differential equations 1056

5. Dislocations 1056
5.1. Introduction 1056
5.2. The displacement field 1057
5.3. Contrast profiles of single perfect dislocations 1057
5.3.1. The $g \cdot b \neq 0$ contrast 1057
5.3.2. The $g \cdot b = 0$ contrast 1058
5.4. Contrast of dislocation pairs 1059
5.5. Determination of the dislocation Burgers vectors and the dislocation densities 1061
5.6. Elastic anisotropy 1062

6. Point-defect agglomerates, radiation damage 1063
6.1. Introduction 1063
6.2. Dislocation loops 1063
6.2.1. Formation of loops 1063
6.2.2. Analysis of large dislocation loops 1064
6.2.3. Small dislocation loops 1064
6.3. Stacking-fault tetrahedra 1066
6.4. Cavities 1066
6.5. Displacement cascades and disordered zones 1067

7. Precipitates 1067

8. Structure of grain boundaries and interfaces 1069
8.1. Transmission electron microscopy of pure translation interfaces 1072
8.2. Transmission electron microscopy of grain boundaries 1075
8.3. Diffraction studies on the structure of grain boundaries 1077
8.4. Direct imaging of grain boundaries 1077
8.5. TEM contrast of heterophase boundaries 1078

9. High-resolution TEM 1079
9.1. Introduction 1079
9.2. The optical transfer function 1081
9.3. Consequences of the wave aberration 1082
9.4. The weak-phase object approximation 1083
9.5. Some remarks to the high-resolution images of crystalline specimens 1085
10. Analytical electron microscopy 1086
10.1. Basic considerations 1086
10.2. Quantitative analytical electron microscopy of thin foils: analysis of X-rays 1088
10.2.1. Cross-section for inner-shell ionization 1089
10.2.2. Thin-film approximation 1089
10.2.3. Beam-spreading in the specimen 1090
10.2.4. Errors limiting the data of X-ray analysis 1090
10.2.5. Examples 1091
10.3. Quantitative analytical electron microscopy of thin foils — electron energy loss spectroscopy 1091
10.3.1. Examples 1093

Appendix. Elements of the kinematical diffraction theory 1094
A.1. Introduction 1094
A.2. Fundamental equations 1095
A.3. Real space and reciprocal space, description of perfect crystal structures 1097
A.4. The kinematical diffraction amplitude F(K) of a perfect crystal 1099
A.5. The Ewald sphere and Bragg's law 1101
A.6. The atomic scattering amplitudes and the Debye–Waller factor 1102

A.7. Imperfect crystals 1104
References 1105
General bibliography for transmission electron microscopy 1108
Addendum 1109
B.1. Instrumentation 1110
B.2. Conventional transmission electron microscopy including weak beam 1111
B.3. Analytical electron microsopy 1111
B.4. High-resolution transmission electron microscopy 1112
Addendum References 1112

Chapter 12. X-ray and neutron scattering, by G. Kostorz 1115
1. Introduction 1116
2. Scattering from real crystals 1117
2.1. General predictions of the kinematical theory 1117
2.2. X-rays and neutrons 1119
2.3. Magnetic scattering 1123
2.4. Inelastic and quasi-elastic scattering 1126
2.5. Some experimental considerations 1128
3. Bragg peaks and vicinity 1130
3.1. Peak shifts 1130
3.2. Peak broadening and intensity changes 1132
3.3. Diffuse scattering near Bragg peaks 1134
4. Between Bragg peaks 1139
4.1. Displacement scattering 1139
4.2. Short-range order 1144
5. Near the incident beam 1161
5.1. Small-angle scattering 1162
5.2. Alloys 1166
5.3. Defects 1179
5.4. Special topics 1181
6. Energy transfers 1183
6.1. Phonons in real crystals 1183
6.2. Diffuse motion 1187
References 1188
Further reading 1198

Chapter 13. Interfacial and surface microchemistry, by E. D. Hondros, M. P. Seah, S. Hofmann and P. Lejček 1201
1. Introduction — The chemistry of interfaces and physical metallurgy 1202
2. Thermodynamic features of interfacial adsorption 1205
3. Methods of measuring the microchemistry of interfaces 1209
3.1. The interfacial energy or Gibbsian approach 1210
3.2. Modern surface analysis techniques 1211
3.3. Micrographic techniques 1216
4. Theory of segregation processes 1218

4.1. Introduction: equilibrium and non-equilibrium segregation ... 1218
4.2. The Langmuir–McLean theory ... 1219
4.2.1. Prediction of the free energy of segregation to grain boundaries ... 1221
4.2.2. Prediction of the free energy of segregation to surfaces ... 1225
4.2.3. Segregation with adsorbate–adsorbate interactions ... 1229
4.2.4. Temperature dependence of the free energies of segregation ... 1230
4.3. Segregation in simple ternary systems: site competition ... 1232
4.4. Segregation in complex metallurgical systems ... 1233
4.5. Anisotropy of segregation ... 1234
4.5.1. Segregation at symmetrical grain boundaries ... 1235
4.5.2. Segregation at asymmetrical grain boundaries ... 1237
4.5.3. Computer simulation of grain-boundary segregation ... 1238
4.5.4. Correlation between grain-boundary and free-surface segregation ... 1240
4.6. The kinetics of segregation ... 1242
4.7. Non-equilibrium segregation ... 1244
4.7.1. Solute pile-up at growing precipitates ... 1244
4.7.2. Quench-induced segregation ... 1245
4.7.3. Stress-induced segregation ... 1248
4.7.4. Segregation at moving grain boundaries ... 1248
4.7.5. Radiation-induced segregation ... 1249

5. Segregation-related physicochemical properties ... 1249
5.1. Interfacial energetics ... 1249
5.2. Surface and grain-boundary kinetics ... 1254
5.3. Grain-boundary cohesion ... 1258

6. Metallurgical phenomena affected by segregation ... 1263
6.1. Surface free energy change: role in creep cavitation ... 1263
6.2. Grain-boundary diffusivity: role in diffusion creep ... 1268
6.3. Interfacial cohesion: role in temper-brittleness ... 1270
6.4. Further examples of metallurgical phenomena influenced by microchemical processes ... 1274
6.4.1. Microchemical barrier layers ... 1274
6.4.2. Creep-embrittlement ... 1275
6.4.3. Intergranular stress-corrosion cracking ... 1276
6.4.4. Intergranular hydrogen-embrittlement ... 1279
6.4.5. Inhibition of surface oxidation on alloys ... 1279

7. Interfacial microchemistry and materials design theory ... 1280

References ... 1284

Further reading ... 1288

Chapter 14. Oxidation, hot corrosion and protection of metallic materials, by S. R. J. Saunders and J. R. Nicholls ... 1291

1. Introduction ... 1292
1.1. Definitions ... 1292
1.2. General ... 1292
1.3. Outline ... 1293

2. Fundamentals of oxidation ... 1293
2.1. Thermodynamics ... 1293
2.2. Oxide structure ... 1296
2.2.1. Amorphous oxides ... 1296
2.2.2. Crystalline oxides ... 1296
2.3. Kinetics ... 1297
2.3.1. Thin film region ... 1298

2.3.2. Thick film region ... 1299
2.4. Properties of oxide layers ... 1303
2.4.1. Electrical properties (diffusion) ... 1303
2.4.2. Mechanical properties (stress generation and relief) ... 1304

3. Oxidation of alloys ... 1306
3.1. Selective oxidation ... 1306
3.2. Internal oxidation ... 1309
3.3. Intermetallic alloys ... 1309
3.4. Scale adhesion ... 1309

4. Multi-component atmospheres ... 1311
4.1. Phenomenology ... 1311
4.2. Prediction of reaction products ... 1312
4.3. Reaction path ... 1315

5. Hot-salt corrosion ... 1317
5.1. The environment ... 1317
5.2. Phenomenology of hot-salt corrosion ... 1319
5.3. Mechanism of attack ... 1319
5.3.1. Na_2SO_4-induced attack ... 1319
5.3.2. Vanadate-induced attack ... 1323
5.4. Coal-fired gas turbines ... 1325

6. Test and measurement methods ... 1326
6.1. Monitoring oxidation processes ... 1326
6.1.1. Isothermal testing ... 1326
6.1.2. Cyclic oxidation ... 1328
6.1.3. Mechanistic studies ... 1328
6.2. Mechanical failure of oxide scales ... 1330
6.2.1. Internal stress measurements ... 1330
6.2.2. Detection of scale failure ... 1333
6.2.3. Measurement of the macro defects (cracks, voids and pores) present in an oxide scale ... 1334
6.3. Mixed oxidant tests ... 1335
6.3.1. Control of gas composition ... 1336
6.3.2. Experimental procedures ... 1337
6.4. Attack by molten salts ... 1337
6.5. Attack by solid deposits ... 1338

7. Life prediction modelling ... 1338
7.1. Oxidation models ... 1338
7.2. A probabilistic model of corrosion loss ... 1339
7.3. Modelling extreme corrosion ... 1340
7.4. Development of a life prediction model ... 1341

8. Developments in coating technology ... 1343
8.1. Diffusion-coating processes ... 1345
8.2. Modified aluminide coatings ... 1347
8.3. Overlay coatings processes ... 1348
8.3.1. Physical vapor deposition ... 1349
8.3.2. Spraying processes ... 1350
8.3.3. Laser processes ... 1351
8.4. Oxidation and hot-salt corrosion resistance of diffusion and overlay coatings ... 1351
8.5. Thermal stability of diffusion and overlay coatings ... 1352
8.6. Mechanical properties of diffusion and overlay coatings ... 1353
8.7. Future trends in overlay coating design ... 1354

References 1357

Further reading 1361

Chapter 15. Diffusive phase transformations in the solid state, by R. D. Doherty 1363

1. General considerations 1364
   1.1. Introduction 1364
   1.2. Driving forces — free energy changes 1365
   1.3. Stable and unstable free-energy curves 1368
   1.4. Gibbs's two types of transformation 1369
   1.5. First order and higher order transformations 1371
   1.6. Short-range and long-range diffusion 1371
   1.7. Techniques for studying phase transformations 1372
2. Nucleation-and-growth transformations 1374
   2.1. Theory of nucleation 1374
      2.1.1. Interfacial structure and energy 1378
      2.1.2. Equilibrium shape 1380
      2.1.3. Strain energy 1383
      2.1.4. Heterogeneous nucleation 1385
      2.1.5. Experimental studies of nucleation 1389
   2.2. Growth processes 1395
      2.2.1. Growth without change of composition 1396
      2.2.2. Transformations involving long-range diffusion 1400
      2.2.3. Role of interface structure in growth processes 1405
      2.2.4. Growth of ledged interfaces 1409
      2.2.5. Quantitative experimental observations of growth rates 1415
         2.2.5.1. Interface-controlled growth rates, without change of composition 1415
         2.2.5.2. Reactions involving long-range solute diffusion 1418
      2.2.6. Growth instabilities 1421
         2.2.6.1. Initial instability 1421
         2.2.6.2. Linear growth models 1427
   2.3. Precipitate dissolution 1431
   2.4. Competitive growth 1434
      2.4.1. Growth from a supersaturated matrix after "soft" impingement 1435
      2.4.2. Competitive coarsening: Ostwald ripening 1437
      2.4.3. During initial nucleation and growth 1443
      2.4.4. Coarsening of Widmanstätten precipitates 1448
   2.5. Discontinuous reactions: moving two-phase boundary MTPB reactions 1451
      2.5.1. Eutectoidal decomposition 1451
      2.5.2. Discontinuous precipitation — MTPB precipitation 1456
      2.5.3. Discontinuous (MTPB) coarsening 1458
      2.5.4. Determination of lamellar spacing in discontinuous (MTB) reactions 1460
      2.5.5. Diffusion-induced grain-boundary migration (DIGM) 1461
      2.5.6. Experimental results on discontinuous eutectoidal reactions 1468
   2.6. Bainitic transformations 1468
3. Continuous transformations 1480
   3.1. Spinodal decomposition 1480
   3.2. Continuous ordering 1490
4. Application of phase transformation theory to specific alloy systems 1494
5. Problems in phase transformations 1495

References 1497

Further reading 1505

Chapter 16. Phase transformations, nondiffusive, by C. M. Wayman and H. K. D. H. Bhadeshia 1507

1. Overview 1508

2. Martensitic transformations 1508
   2.1. Introduction and general characteristics 1508
   2.2. Experimental observations of crystallographic features 1510
   2.3. The phenomenological crystallographic theory of martensitic transformations 1514
      2.3.1. Summary of Crystallographic Theory 1515
      2.3.2. The inhomogeneous shear and martensite substructure 1517
      2.3.3. Mathematical description of the phenomenological crystallographic theory 1518
      2.3.4. Some other crystallographic observations 1521
      2.3.5. Further observations on the martensite morphology and substructure 1522
   2.4. Martensite–parent interfaces 1524
   2.5. Energetics of martensitic transformations 1527
      2.5.1. Transformation hysteresis and the reverse transformation 1527
   2.6. Thermoelastic and non-thermoelastic martensitic transformations 1528
      2.6.1. Free energy change due to martensitic transformation 1529
      2.6.2. Nucleation of martensite 1530
   2.7. Mechanical effects in martensitic transformations 1531
      2.7.1. Introductory comments 1531
      2.7.2. Chemical and mechanical driving forces 1532
      2.7.3. Critical stress to induce martensitic transformation 1535
      2.7.4. Transformation-induced plasticity (TRIP) 1536
   2.8. Mechanical effects specific to thermoelastic martensitic transformations 1538
      2.8.1. General 1538
      2.8.2. The shape memory effect (SME) 1538
      2.8.3. The two-way shape memory effect 1540
      2.8.4. The engine effect in shape memory alloys 1541
      2.8.5. Pseudoelastic effects 1541
      2.8.6. Pseudoelastic effects: superelasticity 1541
      2.8.7. Pseudoelastic effects: rubber-like behavior 1542
      2.8.8. Martensite-to-martensite transformations 1543

3. Crystallographically similar transformations 1544
   3.1. The bainite transformation in steels 1544
   3.2. Oxides and hydrides 1544
   3.3. The CuAu II ordering reaction 1544

4. Omega phase formation 1546

5. Phase changes and charge density waves 1548

References 1552

General bibliography 1553

Chapter 17. Physical metallurgy of steels, by W. C. Leslie and E. Hornbogen 1555

1. Iron and steel 1556
   1.1. Introduction 1556
   1.2. Some properties of pure iron 1557

2. Alloys of iron 1561
   2.1. Interstitial alloys 1561
   2.2. Substitutional alloys 1566
   2.3. Interstitial plus substitutional alloys 1568

3. Transformation reactions ... 1570
3.1. Pearlite ... 1570
3.2. Martensite ... 1572
3.3. Bainite ... 1576
3.4. Transformation diagrams and hardenability ... 1577
3.5. Tempering of martensite ... 1579

4. Deformation and recrystallization ... 1583
4.1. Microstructure of deformed steel ... 1583
4.2. Recovery and recrystallization ... 1587

5. Mechanical properties ... 1589
5.1. Strength of ferrite ... 1589
5.2. Properties of structural steels ... 1594
5.2.1. High-strength low-alloy steels ... 1600
5.3. Strength of martensite ... 1602
5.4. Strength and ductility of tempered martensite ... 1604
5.5. Ultra-high-strength steels ... 1607
5.5.1. Maraging steels ... 1607
5.5.2. Modified standard steels ... 1608
5.5.3. Thermomechanically-treated steels ... 1609
5.6. Tool steels ... 1610
5.7. Austenitic steels ... 1610
5.8. Steels for low-temperature applications ... 1611
5.9. Segregation of solutes and steel purity ... 1612

6. Other physical properties ... 1613
6.1. Steels for nuclear applications ... 1613
6.2. Steels for electrical applications ... 1614

7. Solidification ... 1615
7.1. Rimming steel, killed steel ... 1615
7.2. Cast irons ... 1616

References ... 1618

Further reading ... 1620

Chapter 18. Point defects, by H. J. Wollenberger ... 1621

1. Introduction ... 1622

2. Vacancy properties ... 1623
2.1. Theoretical background ... 1623
2.2. Experimental methods and results ... 1625
2.2.1. Introductory remarks ... 1625
2.2.2. Enthalpy and entropy of formation ... 1626
2.2.2.1. Single vacancies and di-vacancies ... 1626
2.2.2.2. Differential dilatometry ... 1627
2.2.2.3. Positron-annihilation spectroscopy ... 1633
2.2.2.4. Resistivity measurements after quenching ... 1634
2.2.3. Activation enthalpy of migration ... 1635
2.2.3.1. Problems of methods of determination ... 1635
2.2.3.2. Two selected pieces of evidence for vacancy migration in stage III ... 1636
2.2.3.3. Experimental determination of ΔH_v^m ... 1639
2.2.4. Agglomeration ... 1642
2.2.5. Interaction with solutes ... 1644
2.3. Vacancies in ordered alloys ... 1646

3. Self-interstitials 1647
3.1. Production of interstitial atoms 1647
3.1.1. Introduction 1647
3.1.2. Atomic displacement cross-section for electron irradiation and the production of stable Frenkel defects 1648
3.2. Determination of Frenkel defect concentrations 1654
3.3. Interstitial properties 1654
3.3.1. Results of model calculations 1654
3.3.1.1. Activation enthalpies of formation in equilibrium and saddle-point configurations 1656
3.3.1.2. Dynamic properties 1658
3.3.1.3. Arrhenius behavior of diffusion 1661
3.3.1.4. Multiple interstitials 1662
3.3.2. Experimental methods and results 1663
3.3.2.1. Relaxation volume 1663
3.3.2.2. Configuration 1663
3.3.2.3. Formation enthalpy 1665
3.3.2.4. Activation enthalpy of migration 1666
3.3.2.5. The controversy on the interpretation of the recovery-stage III 1670
3.3.2.6. Dynamic properties 1672
3.3.2.7. Interstitial agglomeration 1673
3.3.2.8. Interstitial-solute interaction 1676

4. Miscellaneous radiation effects 1682
4.1. Introductory remarks 1682
4.2. Frenkel defect production by neutrons and ions 1683
4.2.1. Atomic displacement cross-section and cascade formation 1683
4.2.2. Intra-cascade defect reactions 1688
4.3. Fast heavy-ion irradiation 1690
4.4. Swelling 1695
4.5. Radiation-induced creep 1700
4.6. Self-organization of point defect agglomerates 1701
4.7. Radiation-induced solute segregation 1708

References 1710

Further reading 1720

Chapter 19. Metastable states of alloys, by R. W. Cahn and A. L. Greer 1723

1. Introduction 1724
1.1. General features 1724
1.2. Methods for achieving metastability 1725
1.3. The nature of metastability 1726

2. Formation of metallic glasses (amorphous alloys) 1728
2.1. Formation and thermodynamics 1728
2.2. Compositions of amorphous alloys 1736
2.3. Criteria for formation of amorphous phases 1739
2.3.1. Criteria for amorphization by irradiation, and mechanically aided and induced amorphization 1747

3. Practical methods of creating metastable phases and microstructures 1748
3.1. Rapid quenching from the melt 1748
3.1.1. Cooling rates in rapid solidification processing 1752
3.2. Solidification of highly undercooled liquids 1756
3.3. Deposition by evaporation or sputtering 1758

3.4. Amorphization by irradiation 1758
3.5. Rapid solidification processing of surfaces 1759
3.6. Electrochemical, electroless and sonochemical deposition of amorphous phases 1762
3.7. Solid-state amorphization reactions (SSAR) 1764
3.8. Amorphization by mechanical processing 1766
3.9. Pressure effects 1767

4. Metallic glasses: structure and properties 1769
4.1. Structure 1769
4.2. Relaxation 1778
4.3. Crystallization 1784
4.4. Plastic deformation and fracture 1796
4.4.1. Partially devitrified (nanostructured) metallic glasses 1800
4.4.2. Thermal embrittlement 1801
4.5. Other properties of metallic glasses 1804

5. Rapid-solidification-processed (RSP) and other metastable crystalline alloys 1805
5.1. Age-hardening of light alloys 1805
5.2. General characteristics of rapid-solidification-processed (RSP) crystalline alloys 1809
5.3. RSP light alloys 1812
5.4. Steels 1814
5.5. Superalloys 1817

References 1818

Further reading 1829

VOLUME III

Chapter 20. Dislocations, by J. P. Hirth 1831

1. Elementary geometrical properties 1832

2. Elastic fields of dislocations 1834
2.1. Displacements and stresses 1834
2.2. Peach–Koehler force 1836
2.3. Dislocation interactions 1837
2.4. Surface effects 1839
2.5. Line tension 1841

3. Crystal lattice effects 1843
3.1. Peierls barrier 1843
3.2. Core structure and energy 1844
3.3. Stacking faults and partial dislocations 1846
3.4. Ordered alloys 1850
3.5. Slip systems 1852
3.6. Jogs 1853

4. Dislocation behavior at low homologous temperatures 1854
4.1. Kink motion 1854
4.2. Point forces and bowout 1855
4.3. Granato–Lücke internal friction theory 1856
4.4. Dislocation sources 1857
4.5. Dislocation pile-ups 1858
4.6. Pinning in alloys 1860
4.7. Work-hardening 1862

5. Dislocation behavior at high homologous temperatures 1863
5.1. Osmotic climb forces 1863
5.2. Jog drag 1865
5.3. Climb 1866
5.4. Solute drag 1866

6. Grain boundaries 1869

References 1872

Chapter 21. Mechanical properties of single-phase crystalline media: deformation at low temperatures, by A. S. Argon 1877

1. Overview 1878

2. Kinematics of deformation 1879
2.1. Elasticity as an affine transformation 1879
2.2. Kinematics of inelastic deformation 1880
2.2.1. Plasticity resulting from transformations 1880
2.2.2. Plasticity resulting from dislocation glide 1881
2.3. Lattice rotations accompanying slip 1884

3. The mechanical threshold of deformation 1885
3.1. The critical resolved shear stress for glide 1885

4. Elements of thermally activated deformation 1887
4.1. General principles 1887
4.2. Principal activation parameters for plasticity 1891
4.3. Flow stress mechanisms 1894
4.3.1. Intrinsic mechanisms 1894
4.3.1.1. The lattice resistance 1894
4.3.1.2. The dislocation resistance 1895
4.3.2. Extrinsic mechanisms 1896
4.3.2.1. The solute resistance 1896
4.3.2.2. Particle resistances 1897
4.3.2.3. Cutting of forest dislocations 1903
4.4. Superposition of resistances 1905

5. Selection of slip systems in specific crystal structures 1906

6. Plastic deformation by shear transformations 1907
6.1. Types of transformations 1907
6.2. Deformation twinning 1907
6.3. Stress-induced martensitic transformations 1912
6.4. Kinking 1912

7. Evolution of plastic resistance with strain: strain hardening 1913
7.1. General overview 1913
7.2. Deformation features 1915
7.2.1. The stress–strain curves 1915
7.2.2. Slip distribution and dislocation microstructures 1918
7.2.3. Lattice elastic strains developing during deformation 1923
7.2.4. Dynamic recovery in Stage III 1924
7.3. Theoretical models of strain hardening 1924
7.3.1. The initial yield stress and strength differential effects 1924
7.3.2. Strain hardening rate in Stage I 1926
7.3.3. Strain hardening rate in Stage II 1926
7.3.4. Strain hardening rate in Stage III and dynamic recovery 1929

7.3.5. Strain hardening rate in stage IV ... 1930
7.3.6. Latent hardening ... 1932
7.3.7. Transient creep at low temperatures ... 1933
7.3.7.1. Logarithmic creep ... 1934
7.3.7.2. Andrade creep ... 1935
7.3.8. Bauschinger effect ... 1935
7.3.9. Balance between the inter-plane and intra-plane resistances and the mobile dislocation density ... 1937
7.3.10. Yield phenomena ... 1938

8. Deformation of polycrystalline solids ... 1940
8.1. Plastic resistance of polycrystals ... 1940
8.2. Evolution of deformation textures ... 1943

9. Phenomenological continuum plasticity ... 1946
9.1. Conditions of plastic flow in the mathematical theory of plasticity ... 1946
9.2. Transition from dislocation mechanics to continuum mechanics ... 1947

10. Deformation instabilities and strain localization ... 1949

11. Contrasting crystal plasticity with that in amorphous media ... 1950

References ... 1951

Further reading ... 1954

Chapter 22. Mechanical properties of single-phase crystalline media: Deformation in the presence of diffusion, by A. S. Argon ... 1957

1. Overview ... 1958

2. Phenomenology of power-law creep ... 1960
2.1. Measurement of creep strain ... 1960
2.2. The functional forms of the creep relation ... 1961

3. Creep in solid-solution alloys ... 1969

4. Harper–Dorn creep ... 1973

5. Static thermal recovery ... 1973

6. Processes in steady-state creep in pure metals and class II solid-solution alloys ... 1977
6.1. Overview ... 1977
6.2. Slip distribution and dislocation clustering into sub-boundaries ... 1978
6.3. Dynamic internal stresses ... 1984
6.4. Effect of stacking-fault energy ... 1986

7. Diffusional flow ... 1988

8. Grain-boundary sliding during creep ... 1993

9. Superplasticity ... 1997
10. Other creep related phenomena ... 1999
11. Isomechanical scaling laws of inelastic behavior ... 1999
12. Phenomenological descriptions of homogenized continuum deformation behavior ... 2001
12.1. The representative volume element ... 2001
12.2. Evolution of deformation resistance ... 2002
12.3. Three-dimensional constitutive material response to deformation ... 2003

References ... 2004

Further reading ... 2006

Chapter 23. Mechanical properties of solid solutions, by P. Haasen† 2009

1. Introduction 2010

2. Solid-solution hardening 2011
   2.1. Survey of stress–strain curves of fcc alloy single crystals 2011
   2.2. Slip lines, etch pits, and electron transmission observations 2013
      2.2.1. Slip lines and etch pits 2013
      2.2.2. Electron transmission pictures of fcc alloys 2014
   2.3. Theories of solid-solution hardening 2016
      2.3.1. Dislocation locking mechanisms 2016
      2.3.2. Summation of solute forces acting on moving dislocations 2018
   2.4. Solid-solution effect on fcc stress–strain curves 2023
      2.4.1. Critical shear stress τ_0 of fcc solid solutions 2024
      2.4.2. The yield phenomenon in fcc alloys 2028
      2.4.3. Easy glide and overshoot in fcc alloys 2029
      2.4.4. Linear hardening 2029
      2.4.5. Dynamic recovery 2030
      2.4.6. Deformation twinning in fcc alloys 2031
   2.5. Solid-solution hardening in hcp crystals 2032
   2.6. Solid-solution hardening in the bcc structure 2034
   2.7. Hardening in the NaCl and diamond structures 2038
   2.8. Creep of solid solutions 2039
      2.8.1. Steady-state creep through dislocation climb 2040
      2.8.2. Creep limited by dislocation drag (class I) and the Portevin–Le Chatelier effect .. 2041
      2.8.3. Steady-state creep controlled by cross-slip 2042
   2.9. Fatigue of solid solutions 2043

3. Precipitation-hardening 2043
   3.1. Interactions between dislocations and precipitate particles 2044
   3.2. Direct observation of precipitate-dislocation interactions 2047
   3.3. Mechanical properties of precipitation-hardened Al alloys 2049
      3.3.1. Overaged alloys 2050
      3.3.2. Zone-hardened alloys 2051
   3.4. Precipitation-hardening in other alloy systems 2051
      3.4.1. Copper–cobalt 2051
      3.4.2. Iron–carbon 2052
      3.4.3. Spinodally decomposed Cu–Ti alloys 2055

4. Order-hardening 2055
   4.1. The superdislocation 2056
   4.2. Theoretical dependence of the yield stress on the degree of order 2059
      4.2.1. Distortion of a partially ordered structure 2060
      4.2.2. Change of lattice parameter with order 2060
      4.2.3. Anti-phase domains of finite size 2061
      4.2.4. Thickness of anti-phase boundary 2061
      4.2.5. Cross-slip and climb of superdislocations 2061
      4.2.6. Short-range order hardening 2061
      4.2.7. Quench-hardening 2062
   4.3. Temperature dependence of the flow stress of ordered alloys 2063
   4.4. Creep in ordered alloys 2064
   4.5. Twinning of ordered alloys 2065

References 2066

Further reading 2072

Chapter 24. Mechanical properties of intermetallic compounds, by David P. Pope 2075

1. Introduction 2076
2. The superdislocation and planar faults 2081
3. Plastic deformation of $L1_2$ materials: Ni_3Al 2085
   3.1. APBs, faults and dislocation cores in $L1_2$ materials 2086
4. The yield anomaly: models 2089
5. Plasticity of NiAl 2091
6. TiAl 2093
   6.1. Two-phase $L1_0/DO_{19}$ material: Ti-rich TiAl 2094
   6.2. Crystal structure and phase equilibria 2095
   6.3. Ti-rich single crystals 2096
7. Atomistic studies of dislocation cores in TiAl 2099
8. Closing remarks 2101

References 2102

Further reading 2104

Chapter 25. Mechanical properties of multiphase alloys, by Jean-Loup Strudel 2105

1. Introduction 2106
2. Description and microstructure of dispersed-phase alloys 2107
3. Tensile properties of two-phase alloys 2111
   3.1. Experimental results in macroscopic tests 2111
      3.1.1. Initial yield stress 2111
      3.1.2. Stress–strain curves 2113
      3.1.3. Bauschinger effect 2113
   3.2. Microscopic mechanisms and models 2114
      3.2.1. Initial yield stress 2114
      3.2.2. Work-hardening at low temperature in alloys with small particles 2115
      3.2.3. Heterogeneous deformation of alloys containing large particles 2124
   3.3. Stress relaxation and recovery effects 2126
   3.4. A continuum-mechanics approach to the internal stress 2128
4. High-temperature behavior of dispersed-phase alloys 2133
   4.1. High-temperature subgrains in polycrystalline oxide-dispersion-strengthened alloys 2134
   4.2. Apparent and effective creep parameters 2135
   4.3. Average internal stresses in dispersed-phase alloys 2138
5. Composition and microstructure of precipitation-hardened alloys 2141
6. Tensile properties of precipitation-hardened alloys — behavior under high stress 2144
   6.1. Macroscopic properties 2145
   6.2. Deformation modes and hardening mechanisms 2147
      6.2.1. Superlattice stacking faults 2149
      6.2.2. Mechanical twinning of the ordered phase 2151
7. High-temperature creep of precipitation-hardened alloys 2152
   7.1. Creep curves 2154
   7.2. Deformation modes 2155
   7.3. Internal stress 2155
   7.4. Oriented coalescence of the hardening phase under strain 2157

8. Recrystallization . . . 2158
8.1. Particle size and amount of strain . . . 2159
8.2. Interparticle spacing . . . 2161
8.3. Effect of temperature . . . 2162
8.4. Micromechanisms . . . 2163

9. Duplex structures and multiphase alloys . . . 2165
9.1. Duplex structures . . . 2165
9.2. Multiphase precipitation-hardening . . . 2165
9.3. Mechanical alloying of complex alloys . . . 2167
9.4. Grain-size effects in multiphase alloys . . . 2168

References . . . 2174

Further reading . . . 2178

Addendum . . . 2179
A.1. Introduction . . . 2179
A.2. Stress relaxation and the measurement of activation parameters . . . 2179
A.3. Continuum mechanics approach to multiphase materials . . . 2182
A.3.1. Local micromechanical models . . . 2182
A.3.2. Macroscopic behavior of particle-hardened materials . . . 2182
A.3.3. Phenomenological approach . . . 2183
A.4. Oxide-dispersion-strengthened (ODS) materials and their resistance to high-temperature viscoplastic flow . . . 2184
A.4.1. The threshold stress . . . 2185
A.4.2. Dislocation climb models . . . 2186
A.4.3. High-temperature fatigue properties of ODS alloys . . . 2189
A.5. Micromechanisms of plasticity in nickel-base alloys . . . 2190
A.5.1. Single crystals hardened by a shearable phase . . . 2194
A.5.1.1. Plasticity of the γ' phase . . . 2195
A.5.1.2. Plasticity of the γ matrix . . . 2196
A.5.1.3. Plasticity of oriented nickel-base single crystals at intermediate temperatures . . . 2198
A.5.1.4. Rafting phenomena at high temperature . . . 2201
A.6. Recrystallization of ODS alloys . . . 2203

Addendum References . . . 2204

Addendum Further reading . . . 2206

Chapter 26. Fracture, by R. M. Thomson . . . 2207

1. Introduction and fracture overview . . . 2208

2. Qualitative and observational aspects of fracture . . . 2212
2.1. Fracture modes . . . 2212
2.2. Fractographic observations . . . 2213
2.3. The basis for fracture science . . . 2219

3. Elastic analysis of cracks . . . 2220
3.1. Stress analysis . . . 2220
3.2. Eshelby's theorem and the J-integral . . . 2225

4. Elastic dislocation–crack interactions . . . 2231

5. Equilibrium configurations . . . 2235
5.1. The Griffith crack . . . 2236
5.2. Shielding by one dislocation . . . 2237

5.3.	General shielding and the extrinsic toughness of materials	2238
5.4.	The HRR crack tip field	2242
5.5.	Summary	2243
6.	Atomic structure of cracks: theory	2245
6.1.	Methodology	2245
6.2.	Lattice trapping and slow crack growth	2248
6.3.	The Griffith condition	2252
7.	Atomic structure of cracks: dislocation emission	2254
7.1.	Dislocation emission criteria	2255
7.2.	Summary of ductility criteria	2260
7.3.	Crack stability and mixed mode effects	2262
8.	Interfacial cracks and chemical effects	2265
8.1.	Elasticity of interfacial cracks	2265
8.2.	Lattice description of the interfacial crack	2268
8.3.	Ductility at interfaces	2269
9.	Summary of basic ideas	2272
10.	Some practical implications and problems	2274
10.1.	Implications for final materials reliability	2275
10.2.	Brittle crack initiation	2277
10.3.	Ductile fracture, hole growth and the R curve	2277
10.4.	Ductile-brittle transitions — temperature and rate effects	2280
10.5.	Chemical effects — hydrogen embrittlement	2282
10.6.	Temper embrittlement and intergranular segregation	2285
10.7.	Liquid–metal embrittlement	2286
10.8.	Transformation-toughening	2286
	References	2287
	Further reading	2290

Chapter 27. Fatigue, by Campbell Laird 2293

1.	Introduction — History, fatigue design and nomenclature	2294
2.	Fatigue testing	2297
2.1.	Constant amplitude stress tests	2297
2.2.	Increasing stress amplitude tests	2298
2.3.	Constant plastic strain amplitude tests	2298
2.4.	Variable amplitude tests	2299
3.	Performance parameters of fatigue	2300
3.1.	Cyclic stress–strain behavior	2300
3.2.	Fatigue life behavior	2303
4.	Cyclic deformation	2304
4.1.	Phenomenological behavior and dislocation structures	2305
4.2.	Models of rapid hardening behavior: loop patches, persistent slip bands and channels	2313
4.3.	Saturation behavior and strain localization	2321
4.4.	Models of dislocation behavior in persistent slip bands	2326
4.5.	Cyclic hardening in metals other than fcc	2333
4.6.	Differences and similarities between monotonic and cyclic deformation	2336
4.7.	Cyclic deformation of polycrystalline metals	2338
4.8.	Cyclic deformation in alloys	2346
4.9.	Dislocation patterning in cyclic deformation	2361

5. Fatigue crack initiation in ductile metals 2362
5.1. Fatigue crack initiation and surface roughness: the phenomena 2362
5.2. Fatigue crack initiation in persistent slip bands — mechanisms 2369
5.3. Grain-boundary crack initiation 2372
5.4. Environmental effects on crack initiation 2374
6. Fatigue crack propagation 2376
6.1. Macroscopic behavior of fatigue crack propagation 2376
6.2. Short crack growth — Stage I growth 2381
6.3. Long crack growth — Stage II 2385
References 2391
Further reading 2397

Chapter 28. Recovery and recrystallization, by R. W. Cahn 2399
1. Classification of phenomena and terminology 2400
2. Recovery 2401
2.1. Recovery of electrical properties 2401
2.2. Recovery of stored internal energy 2401
2.3. Recovery of mechanical properties 2405
2.4. Recovery of microstructure 2410
2.4.1. Polygonization and subgrains 2410
2.4.2. Cell formation 2412
2.4.3. Quantitative theories of the recovery kinetics of yield strength 2417
2.4.4. Effect of prior recovery on textures 2418
3. Primary recrystallization 2419
3.1. Laws of recrystallization 2419
3.2. Kinetics of primary recrystallization 2421
3.3. Nucleation of primary grains 2425
3.4. Growth of primary grains and the role of impurities 2440
3.4.1. Impurity drag 2440
3.4.2. Special orientations 2448
3.4.3. Vacancies in grain boundaries 2450
3.5. Recrystallization during hot-working: dynamic recrystallization 2453
3.6. Annealing textures 2455
3.7. Mesotextures 2460
3.8. Primary recrystallization of two-phase alloys 2463
3.9. Recrystallization of ordered alloys (intermetallics) 2471
4. Grain growth and secondary recrystallization 2474
4.1. Mechanism and kinetics of grain growth 2474
4.2. Formation of annealing twins 2477
4.3. Grain growth in nanostructured materials 2479
4.4. Secondary recrystallization 2482
4.4.1. General features 2482
4.4.2. Surface-controlled secondary recrystallization 2487
4.4.3. Thin films 2489
4.4.4. Secondary recrystallization and sintering 2492
References 2492
Further reading 2500

Chapter 29. Magnetic properties of metals and alloys, by F. E. Luborsky, J. D. Livingston and G. Y. Chin† ... 2501

1. Origins of fundamental magnetic properties ... 2502

2. Magnetic measurements ... 2507
 2.1. Magnetization ... 2507
 2.2. Magnetic field ... 2508
 2.3. Demagnetizing field ... 2509
 2.4. Curie temperature ... 2509
 2.5. Magnetic anisotropy ... 2509
 2.6. Magnetostriction ... 2510
 2.7. Core loss ... 2510

3. Permanent-magnet materials ... 2510
 3.1. Reversal mechanisms and coercivity ... 2510
 3.2. Microstructure and properties ... 2513
 3.3. Shape-anisotropy materials ... 2515
  3.3.1. ESD magnets ... 2516
  3.3.2. Spinodal alloys ... 2516
 3.4. Crystal-anisotropy materials ... 2519
  3.4.1. Cobalt–rare earths ... 2519
  3.4.2. Iron-rare earths ... 2521
  3.4.3. Hard ferrites ... 2522
  3.4.4. Mn–Al–C ... 2523
  3.4.5. Co–Pt and related alloys ... 2523

4. Soft magnetic materials ... 2524
 4.1. Iron and low-carbon steels ... 2525
 4.2. Iron–silicon alloys ... 2526
  4.2.1. Phase diagram and intrinsic magnetic properties ... 2526
  4.2.2. Magnetic permeability ... 2527
  4.2.3. Core loss ... 2528
   4.2.3.1. Composition ... 2528
   4.2.3.2. Impurities ... 2528
   4.2.3.3. Grain orientation ... 2528
   4.2.3.4. Stress ... 2528
   4.2.3.5. Grain size ... 2530
   4.2.3.6. Thickness ... 2531
   4.2.3.7. Surface morphology ... 2531
  4.2.4. Metallurgy of silicon steels ... 2531
 4.3. Iron–aluminium and iron–aluminium–silicon alloys ... 2533
 4.4. Nickel–iron alloys ... 2534
  4.4.1. Phase diagram and intrinsic magnetic properties ... 2534
  4.4.2. Metallurgy of nickel-iron alloys ... 2536
   4.4.2.1. High-permeability alloys ... 2536
   4.4.2.2. Square-loop alloys ... 2539
   4.4.2.3. Skewed-loop alloys ... 2540
   4.4.2.4. Wear-resistant alloys ... 2540
   4.4.2.5. Invar alloys ... 2540
 4.5. Iron–cobalt alloys ... 2541
  4.5.1. Metallurgy of equiatomic Fe–Co alloys ... 2541
 4.6. Nanocrystalline alloys ... 2542
 4.7. Materials for recording heads ... 2543

5. Amorphous magnetic materials ... 2543
 5.1. Introduction ... 2543

5.2. Preparation ... 2544
5.3. Properties ... 2546
5.3.1. Curie temperature ... 2546
5.3.2. Saturation magnetization ... 2546
5.3.2.1. Dependence of magnetization on alloy composition ... 2546
5.3.2.2. Temperature-dependence of magnetization and spin waves ... 2549
5.3.3. Anisotropy ... 2551
5.3.3.1. Structural and compositional anisotropy ... 2553
5.3.3.2. Strain-magnetostriction anisotropy ... 2553
5.3.3.3. Directional-order anisotropy ... 2553
5.3.4. Magnetostriction ... 2555
5.3.5. Low-field properties ... 2555

6. Magnetic measurements in metallurgy ... 2558

References ... 2560

Further reading ... 2564

Chapter 30. Metallic composite materials, by T. W. Clyne ... 2567

1. Introduction ... 2568

2. Material production ... 2569
2.1. Liquid-phase processing ... 2569
2.1.1. Squeeze infiltration ... 2569
2.1.2. Stir casting ... 2571
2.1.3. Spray deposition ... 2574
2.1.4. Reactive processing ... 2576
2.2. Solid-state processing ... 2577
2.2.1. Powder blending and consolidation ... 2577
2.2.2. Diffusion bonding of foils ... 2579
2.2.3. Physical vapour deposition (PVD) ... 2581

3. Deformation behaviour ... 2581
3.1. Elastic properties ... 2581
3.2. Yielding and work hardening ... 2584
3.2.1. Matrix flow ... 2584
3.2.2. Thermal stresses ... 2589
3.2.3. Work hardening and stress relaxation ... 2592
3.3. Wear ... 2595

4. Fracture ... 2596
4.1. Damage development and ductility ... 2598
4.1.1. Damage mechanisms ... 2598
4.1.2. Ductility ... 2601
4.2. Fracture toughness and fatigue ... 2604
4.2.1. Fracture toughness ... 2604
4.2.2. Fatigue of discontinuous composites ... 2606
4.2.3. Fatigue of long fibre and layered composites ... 2607

5. High temperature behaviour ... 2609
5.1. Thermal expansion and thermal stresses ... 2609
5.2. Creep and thermal cycling effects ... 2611

References ... 2616

Chapter 31. Sintering processes, H. E. Exner and E. Arzt 2627

1. Solid-state sintering 2628
   1.1. Driving energy 2630
   1.2. Material sinks and sources 2632
   1.3. Neck growth and center approach in two-particle models 2634
   1.4. Shrinkage of particle arrays and powder compacts 2637
   1.5. Factors accelerating or retarding shrinkage 2640
   1.6. Development of microstructure and grain growth 2643
2. Hot pressing (pressure-sintering) 2645
   2.1. Stresses and mechanisms 2645
   2.2. Densification models 2646
   2.3. HIP (hot isostatic pressing) maps 2648
   2.4. Technological considerations 2649
3. Sintering with a liquid phase 2651
4. Outlook 2654

References 2654

Further reading 2660

Chapter 32. A metallurgist's guide to polymers, by A. H. Windle 2663

Preface 2664

1. Introduction to synthetic polymers 2665
   1.1. Thermosets (network polymers) 2665
   1.2. Thermoplastics: (a) Non-crystalline polymers 2665
   1.3. Thermoplastics: (b) Semi-crystalline polymers 2666
   1.4. Thermoplastics: (c) Liquid crystalline polymers 2667
   1.5. Naming of plastics 2668
2. Crystal morphology of polymers and the concept of crystallinity 2668
   2.1. Crystalline or non-crystalline? 2668
   2.2. Crystallinity 2670
   2.3. Chain folding 2670
   2.4. Annealing 2671
   2.5. Special cases 2672
   2.6. Spherulites 2673
3. Textures 2675
   3.1. Wire textures in metals — an overview 2675
   3.2. Fiber textures in polymers 2676
   3.3. Alignment of non-crystalline polymers 2677
   3.4. A parameter to describe the quality of fiber texture 2679
   3.5. Rolling textures 2680
4. Polymer alloys: phase diagrams in macromolecular systems 2682
   4.1. General 2682
   4.2. Entropy and enthalpy of mixing 2683
   4.3. The Flory–Huggins equation 2684
   4.4. Polymer–polymer miscibility 2684
   4.5. Copolymers 2689
5. Plastic deformation and yielding 2692
   5.1. Metals and polymers 2692
   5.2. True stress–strain relations 2694

5.3. Considère's criterion 2694
5.4. Yield drops and Lüders bands 2695
5.5. Drawing of polymers 2697
5.6. Structural control of the natural draw ratio 2698
5.7. Yield criteria 2698

6. High-performance polymer fibers 2700
6.1. Diamond — the ultimate polymer? 2700
6.2. Theoretical axial modulus of polymer crystals 2700
6.3. Axial properties of conventionally drawn fibers 2703
6.4. Making high-performance fibers 2705
6.5. The Achilles' heel and the diamond challenge 2706

7. Crazing 2707
7.1. Introduction to a craze 2707
7.2. Craze criteria 2707
7.3. Materials factors 2710
7.4. Microstructure and micromechanisms 2710
7.5. Multiply induced crazing 2713

8. Electrically conducting polymers 2713
8.1. Conjugated polymers 2713
8.2. Band structure 2714
8.3. Solitons 2715
8.4. Polarons 2717
8.5. Materials 2718
8.6. Applications 2718

9. The glass transition: to melt and rubber 2720
9.1. Formation of a polymer glass 2720
9.2. Rate effects 2721
9.3. Observation of the glass transition using differential scanning calorimetry (DSC) 2722
9.4. Control of the glass transition temperature (T_g) 2724
9.5. Melt or rubber? 2725
9.6. Viscoelasticity 2726
9.7. Model description of non-crystalline polymers 2729
10. Amorphous chain structures 2730
10.1. Simple statistical chains 2730
10.2. Real chains 2731
10.3. The Gaussian approximation 2732
10.4. The chain environment 2733
10.5. The condensed phase 2734
11. Rubber elasticity 2735
11.1. The network 2735
11.2. The entropy spring 2736
11.3. Thermodynamics 2736
11.4. Dependence of entropy on strain 2737
11.5. The stress–strain curve 2738
11.6. The high-strain discrepancy 2739
11.7. Summary 2740

References 2740

Author index A1

Subject index S1

CHAPTER 1

CRYSTAL STRUCTURE OF THE METALLIC ELEMENTS

W. STEUERER

Institute of Crystallography
ETH-Zentrum
CH-8092 Zürich, Switzerland

R. W. Cahn and P. Haasen†, eds.
Physical Metallurgy; fourth, revised and enhanced edition

1. Introduction

In the very beginning of materials "science", when men began to produce artificial materials, it was the time of trial and error, of pure empiricism. Today, we are a little closer to the realization of the old dream of designing any material with given properties owing to our improved understanding of the relationships between chemical composition, crystal structure and material properties. Though only a very few commercially and technologically important materials consist of metallic elements in their pure form (Si, Ge, Cu, Au, Ag, Pd, etc.), their crystal structures are of more than academic interest. Thus, to give an example, the crystal structure of a pure metal remains unchanged in the case of a solid solution, when one or several other components are added to tune the properties of a material. This technique has been used since time immemorial by alloying gold with copper or silver, for instance, to make jewelry or coins more resistant to wear. Especially the close packed structures and their derivatives, which are typical for pure metals, are also characteristic for numerous materials consisting of multi-component solid solutions or intermetallic alloys. Another reason for the study of "simple" element structures is that they are extremely helpful for the development and improvement of methods to understand why a given phase is adopting a particular crystal structure under certain conditions (temperature, pressure, etc.). The aim is, of course, to learn to predict the crystal structure of any given chemical compound under any ambient conditions and to model its possible phase transformations.

It is remarkable that even pure elements can have rather complicated crystal structures resulting from complex electronic interactions. Most elements are polymorphous, i.e., they occur in up to ten different crystal structures as a function of ambient conditions (temperature, pressure). The understanding of the phase transformations in these homo-atomic cases is also very helpful for understanding the more complicated phase transformations of complex intermetallic phases. Indeed, it is possible today to predict correctly most of the element structures and phase transformations by one-electron theory (SKRIVER [1985]).

2. Factors governing a crystal structure

Crystalline order, i.e., the three-dimensional (or in the case of quasicrystals or incommensurate phases, higher-dimensional) translationally periodic repetition of a particular atomic configuration, is the outstanding characteristic of condensed matter in thermodynamic equilibrium. Which crystal structure for a given chemical composition corresponds to the lowest Gibbs free energy, $G = H - TS$, depends on chemical bonding, electronic band structure and geometrical factors. Since it is not possible to solve the Schrödinger equation for a crystal and thus deduce the correct crystal structure, many approximations have been developed. Indeed, today there exist quite successful attempts to predict simpler crystal structures using one-electron approximations: the many-electron problem is reduced to a one-electron problem by the assumption that the electrons, surrounded by a mutual exclusion zone, are moving independently of each other in the average field of all the others (local density functional theory).

Beside this rather complicated and lengthy approach to understand and predict crystal structures, there exist a number of rules based on two factors: the chemical bond factor, which also takes into account the directionality of chemical bonds, and the geometrical factor, which considers optimum space filling, symmetry and connectivity. Especially in the case of the typical metallic elements, these structural principles work very well for predicting structures. (For electron theory of structural stability, see ch. 2, § 6.1).

2.1. Chemical bond factor

The concept of chemical bonding was originally developed to understand the formation of molecules. In a crystal, a collective interaction of all atoms always exists which may approximately be considered as the sum of nearest-neighbor interactions. A further simplification comes in by the fact that only the electrons of the outer shells contribute to the chemical bonding. Traditionally, several limiting types of the chemical bond are defined: strong ionic (heteropolar), covalent (homopolar), metallic bonds, and weak van der Waals and hydrogen bonds. The strong bonds have in common that the outer atomic orbitals contribute to new collective electron states in the crystal, the electron bands. They differ mainly in the degree of localization of the valence electrons: when these are transferred from one atom to another atom, Coulomb attraction between the cation and the anion results and the bond is called *ionic*; when they remain localized between two atoms the so-called exchange interaction results from overlapping orbitals and *covalent* bonds are formed; when the valence electrons are delocalized over the whole crystal *metallic bonding* is obtained. Thus, contrary to the other bond types which also occur within molecules, the metallic bond can only exist in large arrays of atoms. Since the interaction of electron orbitals depends on their separation and mutual orientation, the bond type may change during phase transformations. Sometimes, a slight change in temperature can be sufficient, as in the transition from metallic white tin to non-metallic grey tin below 291K ("tin pest"); sometimes very high pressures are necessary, as for the transformation from molecular hydrogen to metallic hydrogen, for instance.

The type of bonding occurring in crystals of the metallic elements ranges from pure metallic in the alkali metals to increasingly covalent for zinc or cadmium, for instance. The structural implications of these two bond types, which are just two contrary limiting manifestations of electronic interactions with a continuously changing degree of electron localization, will be characterized in the following in greater detail.

2.1.1. The covalent bond

The covalent bond may be described in terms of the more qualitative VB (valence bond) theory by overlapping atomic orbitals occupied by unpaired valence electrons (fig. 1). Its strength depends on the degree of overlapping and is given by the exchange integral. In terms of the more quantitative LCAO–MO (linear combination of atomic orbitals – molecular orbitals) theory, molecular orbitals are constructed by linear combination of atomic orbitals (fig. 2). The resulting bonding, non-bonding and anti-

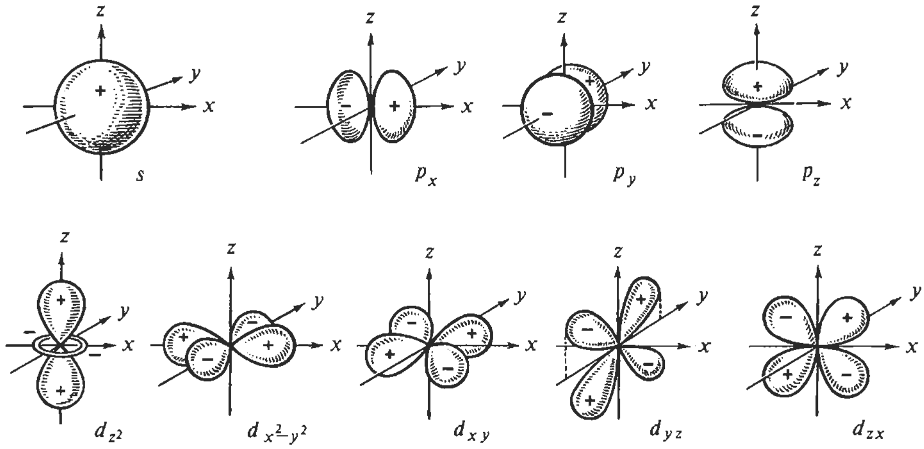

Fig. 1. Schematic structure of the atomic s-, p- and d-orbitals (from VAINSHTEIN *et al.* [1982]).

bonding molecular orbitals, filled up with valence electrons according to the Pauli exclusion principle, are localized between the bonding atoms with well defined geometry. Generally, covalent bonds can be characterized as strong, directional bonds. Increasing the number of atoms contributing to the bonds increases the number of molecular orbitals and their energy differences become smaller and smaller. Finally, the discrete energy levels of the molecular orbitals condense to quasicontinuous bands separated by energy gaps. Since in a covalent bond each atom reaches its particular stable noble gas configuration (filled shell) the energy bands are either completely filled or empty. Owing to the localization of the electrons, it needs much energy to lift them from the last filled valence band into the empty conduction band. The classic example of a crystal built from only covalently bonded atoms is diamond: all carbon atoms are bonded via tetrahedrally directed sp^3 hybrid orbitals (fig. 3). Thus the crystal structure of diamond results as a framework of tetrahedrally coordinated carbon atoms (fig. 4).

2.1.2. The metallic bond

The metallic bond can be described in a similar way as the covalent bond. The main difference between these two bond types is that the ionization energy for electrons occupying the outer orbitals of the metallic elements is much smaller. In typical metals, like the alkali metals, these outer orbitals are spherical *s*-orbitals allowing overlapping with up to 12 further *s*-orbitals of the surrounding atoms. Thus, the well-defined electron localization in bonds connecting pairs of atoms with each other loses its meaning. Quantum-mechanical calculations show that in large agglomerations of metal atoms the delocalized bonding electrons occupy lower energy levels than in the free atoms; this would not be true for isolated “metal molecules”. The metallic bond in typical metals is non-directional, favoring structures corresponding to closest packings of spheres. With increasing localization of valence electrons, covalent interactions cause deviations from spherically symmetric bonding, leading to more complicated structures.

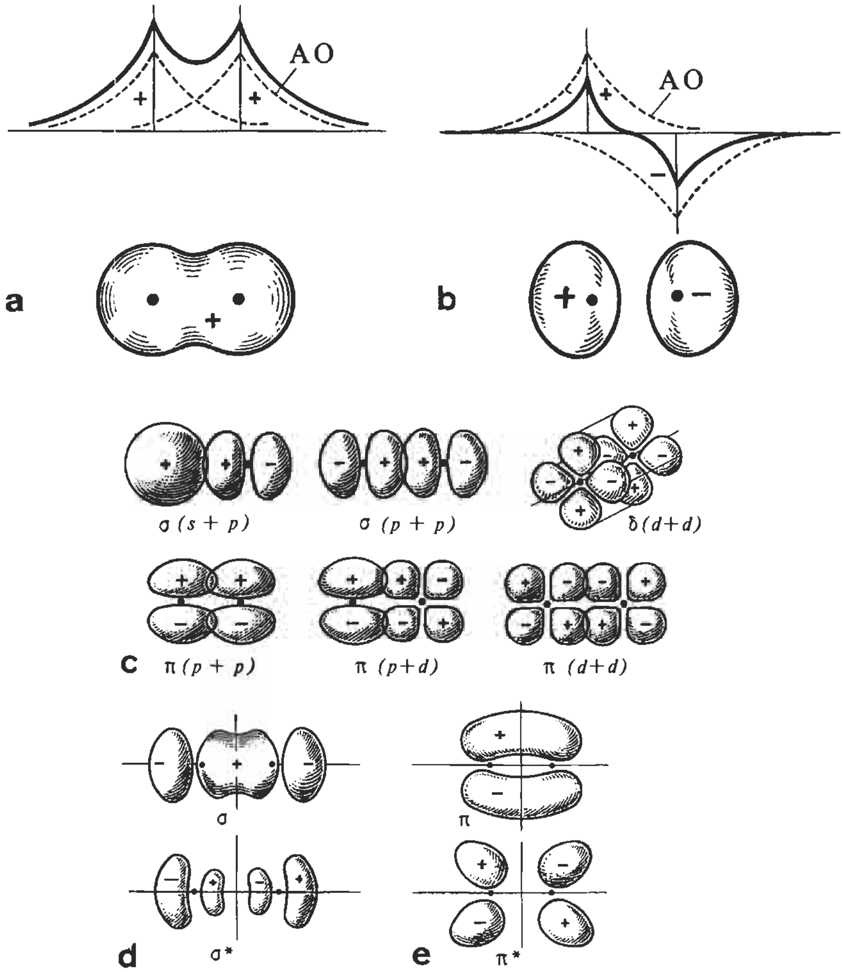

Fig. 2. (a) Bonding and (b) anti-bonding molecular orbitals of the H_2 molecule. (c) Schematic drawing of the building of the most important molecular orbitals from atomic orbitals and (d), (e) examples of molecular orbitals (bonding: σ, π and anti-bonding σ^*, π^*) (from VAINSHTEIN *et al.* [1982]).

2.2. Geometrical factors

A crystal structure type is fully defined by its general chemical composition, its space group symmetry, the equipoint (Wyckoff) positions occupied by the atoms and the coordinates of the atoms in the unit cell (fig. 5). The metrics, i.e., the dimension of the unit cell (lattice parameters), in general differ for all chemical compounds or phases occurring in one particular crystal structure type. Also, for general Wyckoff positions, the numerical values of the coordinates may vary in a range not destroying the characteris-

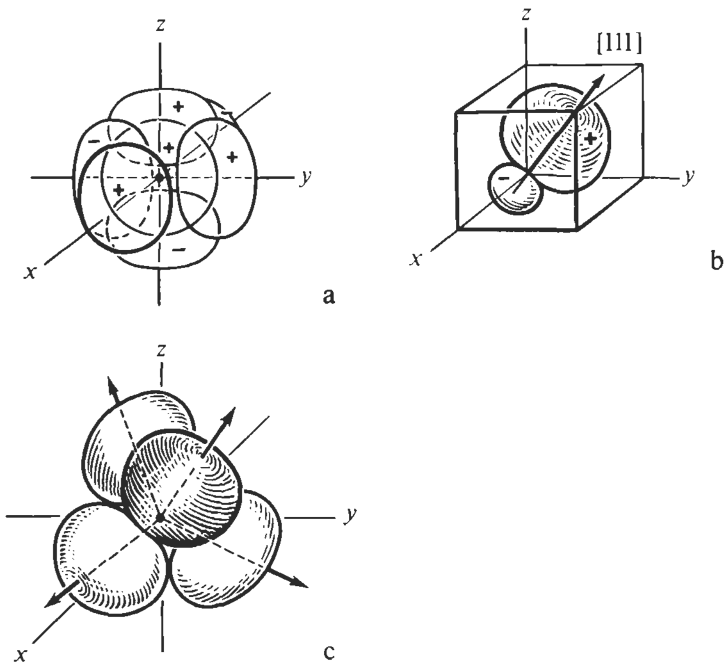

Fig. 3. Hybridization of (a) one s- and three p-orbitals to (b) sp^3–hybrid orbitals (c) which are directed along tetrahedron axes (from VAINSHTEIN *et al.* [1982]).

tics, i.e., coordination polyhedra and their linkings, of this crystal structure. With these data given it is easy to derive both the information about the global arrangement of structural units as well as the local environment of each atom (fig. 6). Besides this purely geometrical description of a structure, it is necessary to understand the characteristics of a crystal structure by identifying crystal-chemically meaningful structural units (coordination polyhedra) and their connecting principles (bonding).

For band-structure calculations, for instance, knowledge of the full crystal structure

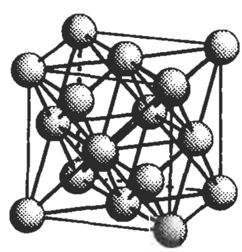

Fig. 4. The structure of diamond cF8–C, space group $Fd\bar{3}m$, No. 227, 8a: 0 0 0, ¾ ¼ ¾. All carbon atoms are tetrahedrally coordinated, they occupy the positions of a face-centered cubic lattice and one half of the centers of the eighth cubes.

is essential; for tensorial physical properties, however, the point symmetry group to which the space group belongs is the determining factor. Crystal-chemical properties are less sensitive to slight atomic shifts which may break the symmetry but do not change local environments of atoms. Thus the study of atomic coordinations may yield valuable tools in the analysis, description and comparison of crystal structures.

2.2.1. Coordination

A general technique to derive useful coordination polyhedra was suggested by BRUNNER and SCHWARZENBACH [1971]: all interatomic distances around a particular atom are calculated up to a certain limit, and all atoms within a distance defined by the first maximum gap in a histogram of distances belong to the coordination polyhedron (fig. 6). If there is no clear maximum gap observable, a second criterion may be the maximum-convex-volume rule: all coordinating atoms lying at the intersections of at least three faces should form a convex polyhedron (DAAMS *et al.* [1992]).

2.2.2. Space filling

Owing to the isotropic properties of the metallic bond the structure of typical metallic elements can often be described in terms of dense sphere packings. A sphere packing is an infinite set of non-interpenetrating spheres with the property that any pair of spheres is connected by a chain of spheres with mutual contact. A sphere packing is called homogenous if all spheres are symmetrically equivalent, otherwise it is called heterogenous (KOCH and FISCHER [1992]). In the last named case, the spheres of the different non-symmetrically equivalent subsets may have different radii and occupy the positions of different crystallographic orbits. The number of types of heterogenous sphere packings is infinite whereas it is finite for homogenous sphere packing types. There are, for instance, 199 different cubic and 394 different possible tetragonal homogenous sphere packings. The densities, i.e., the fractions of volumes occupied by the spheres, are with $q=0.7405$ highest for the well-known hexagonal closest packing (hcp) and cubic closest packing (ccp) (figs. 7 and 8, respectively). In both cases the coordination numbers (CN) are twelve and the distances to the nearest neighbors the same. The number k of contacts per sphere amounts to $3 \leq k \leq 12$. Table 1 gives some examples for sphere packings with the highest and lowest densities and contact numbers, and table 2 space filling values for a number of structure types. Very low packing densities, such as that for the cF8–C type, for instance, indicate that a hard sphere packing is no longer an adequate description of such a structure.

The crystal structures of the metallic elements adopt dense sphere packings as long as purely geometrical packing principles are dominant. Covalent bonding contributions and electronic effects give rise to more complicated structures.

2.2.3. Layer stackings, polytypism

Many crystal structures can be considered to consist of successive stackings of atomic layers. The above mentioned hexagonal closest packing (hcp) refers to a stacking of dense packed layers with periodic sequence ..AB.., the cubic closest packing (ccp) to a sequence ..ABC.. (figs. 7 and 8). The atomic layers are denoted by A, B or C depending

References: p. 45.

$Fd\bar{3}m$	O_h^7	$m\bar{3}m$	Cubic
No. 227	$F4_1/d\bar{3}2/m$		Patterson symmetry $Fm\bar{3}m$

ORIGIN CHOICE 1

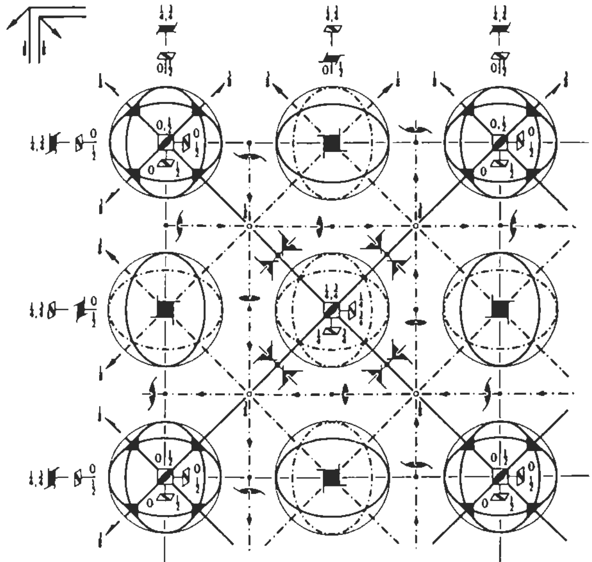

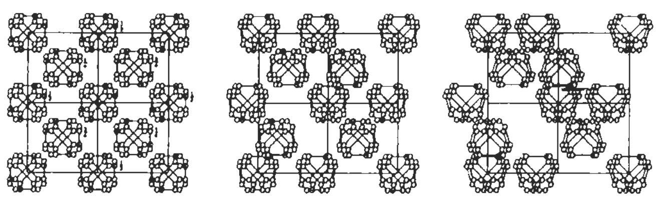

Origin at $\bar{4}3m$, at $-\frac{1}{8},-\frac{1}{8},-\frac{1}{8}$ from centre ($\bar{3}m$)

Asymmetric unit $0\leq x\leq\frac{1}{2}$; $0\leq y\leq\frac{1}{4}$; $-\frac{1}{8}\leq z\leq\frac{1}{8}$; $y\leq\min(\frac{1}{2}-x,x)$; $-y\leq z\leq y$

Vertices $0,0,0$ $\frac{1}{2},0,0$ $\frac{1}{4},\frac{1}{4},\frac{1}{8}$ $\frac{1}{8},\frac{1}{8},\frac{1}{8}$ $\frac{1}{4},\frac{1}{4},-\frac{1}{8}$ $\frac{1}{8},\frac{1}{8},-\frac{1}{8}$

Symmetry operations

Fig. 5. Information given in the *International Tables for Crystallography* (Hahn [1992]) on the example of the space group Fd$\bar{3}$m of the diamond structure. Left side, top line: space group symbol in short Hermann–Mauguin and Schoenflies notation, point group (crystal class), crystal system. Second line: consecutive space group number, full space group symbol, Patterson symmetry, short space group symbol. Upper drawing: framework of symmetry elements in a unique part of one unit cell. Lower drawings: point complexes generated by the action of symmetry operations. Below: choice of origin, definition of the asymmetric unit. Right side: the Wyckoff letters a, b, c ... i denote the equipoint positions with multiplicities 8, 8, 16 ... 192. The positions of the carbon atoms in the diamond structure are given in Wyckoff position 8a.

No. 227 $Fd\bar{3}m$

Generators selected (1); $t(1,0,0)$; $t(0,1,0)$; $t(0,0,1)$; $t(0,\frac{1}{2},\frac{1}{2})$; $t(\frac{1}{2},0,\frac{1}{2})$; (2); (3); (5); (13); (25)

Positions

Multiplicity, Wyckoff letter, Site symmetry — Coordinates — Reflection conditions

$(0,0,0)+$ $(0,\frac{1}{2},\frac{1}{2})+$ $(\frac{1}{2},0,\frac{1}{2})+$ $(\frac{1}{2},\frac{1}{2},0)+$ — h,k,l permutable

General:

192 i 1

(1) x,y,z	(2) $\bar{x},\bar{y}+\frac{1}{2},z+\frac{1}{2}$	(3) $\bar{x}+\frac{1}{2},y+\frac{1}{2},\bar{z}$	(4) $x+\frac{1}{2},\bar{y},\bar{z}+\frac{1}{2}$
(5) z,x,y	(6) $z+\frac{1}{2},\bar{x},\bar{y}+\frac{1}{2}$	(7) $\bar{z},\bar{x}+\frac{1}{2},y+\frac{1}{2}$	(8) $\bar{z}+\frac{1}{2},x+\frac{1}{2},\bar{y}$
(9) y,z,x	(10) $\bar{y}+\frac{1}{2},z+\frac{1}{2},\bar{x}$	(11) $y+\frac{1}{2},\bar{z},\bar{x}+\frac{1}{2}$	(12) $\bar{y},\bar{z}+\frac{1}{2},x+\frac{1}{2}$
(13) $y+\frac{3}{4},x+\frac{1}{4},\bar{z}+\frac{3}{4}$	(14) $\bar{y}+\frac{1}{4},\bar{x}+\frac{1}{4},\bar{z}+\frac{1}{4}$	(15) $y+\frac{1}{4},\bar{x}+\frac{3}{4},z+\frac{3}{4}$	(16) $\bar{y}+\frac{3}{4},x+\frac{3}{4},z+\frac{1}{4}$
(17) $x+\frac{3}{4},z+\frac{1}{4},\bar{y}+\frac{3}{4}$	(18) $\bar{x}+\frac{3}{4},z+\frac{3}{4},y+\frac{1}{4}$	(19) $\bar{x}+\frac{1}{4},\bar{z}+\frac{1}{4},\bar{y}+\frac{1}{4}$	(20) $x+\frac{1}{4},\bar{z}+\frac{3}{4},y+\frac{3}{4}$
(21) $z+\frac{3}{4},y+\frac{1}{4},\bar{x}+\frac{3}{4}$	(22) $z+\frac{1}{4},\bar{y}+\frac{3}{4},x+\frac{3}{4}$	(23) $\bar{z}+\frac{3}{4},y+\frac{3}{4},x+\frac{1}{4}$	(24) $\bar{z}+\frac{1}{4},\bar{y}+\frac{1}{4},\bar{x}+\frac{1}{4}$
(25) $\bar{x}+\frac{1}{4},\bar{y}+\frac{1}{4},\bar{z}+\frac{1}{4}$	(26) $x+\frac{1}{4},y+\frac{3}{4},\bar{z}+\frac{3}{4}$	(27) $x+\frac{3}{4},\bar{y}+\frac{3}{4},z+\frac{1}{4}$	(28) $\bar{x}+\frac{3}{4},y+\frac{1}{4},z+\frac{3}{4}$
(29) $\bar{z}+\frac{1}{4},\bar{x}+\frac{1}{4},\bar{y}+\frac{1}{4}$	(30) $\bar{z}+\frac{3}{4},x+\frac{3}{4},y+\frac{1}{4}$	(31) $z+\frac{3}{4},x+\frac{1}{4},\bar{y}+\frac{3}{4}$	(32) $z+\frac{1}{4},\bar{x}+\frac{3}{4},y+\frac{3}{4}$
(33) $\bar{y}+\frac{1}{4},\bar{z}+\frac{1}{4},\bar{x}+\frac{1}{4}$	(34) $y+\frac{3}{4},\bar{z}+\frac{3}{4},x+\frac{1}{4}$	(35) $\bar{y}+\frac{3}{4},z+\frac{1}{4},x+\frac{3}{4}$	(36) $y+\frac{1}{4},z+\frac{3}{4},\bar{x}+\frac{3}{4}$
(37) $\bar{y}+\frac{1}{2},\bar{x},z+\frac{1}{2}$	(38) y,x,z	(39) $\bar{y},x+\frac{1}{2},\bar{z}+\frac{1}{2}$	(40) $y+\frac{1}{2},\bar{x}+\frac{1}{2},\bar{z}$
(41) $\bar{x}+\frac{1}{2},\bar{z},y+\frac{1}{2}$	(42) $x+\frac{1}{2},\bar{z}+\frac{1}{2},\bar{y}$	(43) x,z,y	(44) $\bar{x},z+\frac{1}{2},\bar{y}+\frac{1}{2}$
(45) $\bar{z}+\frac{1}{2},\bar{y},x+\frac{1}{2}$	(46) $\bar{z},y+\frac{1}{2},\bar{x}+\frac{1}{2}$	(47) $z+\frac{1}{2},\bar{y}+\frac{1}{2},\bar{x}$	(48) z,y,x

Reflection conditions (General):
hkl : $h+k=2n$ and $h+l,k+l=2n$
$0kl$: $k+l=4n$ and $k,l=2n$
hhl : $h+l=2n$
$h00$: $h=4n$

Special: as above, plus

96 h ..2 — no extra conditions

$\frac{1}{8},y,\bar{y}+\frac{1}{4}$	$\frac{7}{8},\bar{y}+\frac{1}{2},\bar{y}+\frac{3}{4}$	$\frac{3}{8},y+\frac{1}{2},y+\frac{3}{4}$	$\frac{5}{8},\bar{y},y+\frac{1}{4}$
$\bar{y}+\frac{1}{4},\frac{1}{8},y$	$\bar{y}+\frac{3}{4},\frac{7}{8},\bar{y}+\frac{1}{2}$	$y+\frac{3}{4},\frac{3}{8},y+\frac{1}{2}$	$y+\frac{1}{4},\frac{5}{8},\bar{y}$
$y,\bar{y}+\frac{1}{4},\frac{1}{8}$	$\bar{y}+\frac{1}{2},\bar{y}+\frac{3}{4},\frac{7}{8}$	$y+\frac{1}{2},y+\frac{3}{4},\frac{3}{8}$	$\bar{y},y+\frac{1}{4},\frac{5}{8}$
$\frac{1}{8},\bar{y}+\frac{1}{4},y$	$\frac{3}{8},y+\frac{3}{4},y+\frac{1}{2}$	$\frac{7}{8},\bar{y}+\frac{3}{4},\bar{y}+\frac{1}{2}$	$\frac{5}{8},y+\frac{1}{4},\bar{y}$
$y,\frac{1}{8},\bar{y}+\frac{1}{4}$	$y+\frac{1}{2},\frac{3}{8},y+\frac{3}{4}$	$\bar{y}+\frac{1}{2},\frac{7}{8},\bar{y}+\frac{3}{4}$	$\bar{y},\frac{5}{8},y+\frac{1}{4}$
$\bar{y}+\frac{1}{4},y,\frac{1}{8}$	$y+\frac{3}{4},y+\frac{1}{2},\frac{3}{8}$	$\bar{y}+\frac{3}{4},\bar{y}+\frac{1}{2},\frac{7}{8}$	$y+\frac{1}{4},\bar{y},\frac{5}{8}$

96 g ..m — no extra conditions

x,x,z	$\bar{x},\bar{x}+\frac{1}{2},z+\frac{1}{2}$	$\bar{x}+\frac{1}{2},x+\frac{1}{2},\bar{z}$	$x+\frac{1}{2},\bar{x},\bar{z}+\frac{1}{2}$
z,x,x	$z+\frac{1}{2},\bar{x},\bar{x}+\frac{1}{2}$	$\bar{z},\bar{x}+\frac{1}{2},x+\frac{1}{2}$	$\bar{z}+\frac{1}{2},x+\frac{1}{2},\bar{x}$
x,z,x	$\bar{x}+\frac{1}{2},z+\frac{1}{2},\bar{x}$	$x+\frac{1}{2},\bar{z},\bar{x}+\frac{1}{2}$	$\bar{x},\bar{z}+\frac{1}{2},x+\frac{1}{2}$
$x+\frac{3}{4},x+\frac{1}{4},\bar{z}+\frac{3}{4}$	$\bar{x}+\frac{1}{4},\bar{x}+\frac{1}{4},\bar{z}+\frac{1}{4}$	$x+\frac{1}{4},\bar{x}+\frac{3}{4},z+\frac{3}{4}$	$\bar{x}+\frac{3}{4},x+\frac{3}{4},z+\frac{1}{4}$
$x+\frac{3}{4},z+\frac{1}{4},\bar{x}+\frac{3}{4}$	$\bar{x}+\frac{3}{4},z+\frac{3}{4},x+\frac{1}{4}$	$\bar{x}+\frac{1}{4},\bar{z}+\frac{1}{4},\bar{x}+\frac{1}{4}$	$x+\frac{1}{4},\bar{z}+\frac{3}{4},x+\frac{3}{4}$
$z+\frac{3}{4},x+\frac{1}{4},\bar{x}+\frac{3}{4}$	$z+\frac{1}{4},\bar{x}+\frac{3}{4},x+\frac{3}{4}$	$\bar{z}+\frac{3}{4},x+\frac{3}{4},x+\frac{1}{4}$	$\bar{z}+\frac{1}{4},\bar{x}+\frac{1}{4},\bar{x}+\frac{1}{4}$

48 f 2.mm — hkl : $h=2n+1$ or $h+k+l=4n$

$x,0,0$	$\bar{x},\frac{1}{2},\frac{1}{2}$	$0,x,0$	$\frac{1}{2},\bar{x},\frac{1}{2}$	$0,0,x$	$\frac{1}{2},\frac{1}{2},\bar{x}$
$\frac{3}{4},x+\frac{1}{4},\frac{3}{4}$	$\frac{1}{4},\bar{x}+\frac{1}{4},\frac{1}{4}$	$x+\frac{3}{4},\frac{1}{4},\frac{3}{4}$	$\bar{x}+\frac{3}{4},\frac{3}{4},\frac{1}{4}$	$\frac{3}{4},\frac{1}{4},\bar{x}+\frac{3}{4}$	$\frac{1}{4},\frac{3}{4},x+\frac{3}{4}$

32 e .3m — no extra conditions

x,x,x	$\bar{x},\bar{x}+\frac{1}{2},x+\frac{1}{2}$
$\bar{x}+\frac{1}{2},x+\frac{1}{2},\bar{x}$	$x+\frac{1}{2},\bar{x},\bar{x}+\frac{1}{2}$
$x+\frac{3}{4},x+\frac{1}{4},\bar{x}+\frac{3}{4}$	$\bar{x}+\frac{1}{4},\bar{x}+\frac{1}{4},\bar{x}+\frac{1}{4}$
$x+\frac{1}{4},\bar{x}+\frac{3}{4},x+\frac{3}{4}$	$\bar{x}+\frac{3}{4},x+\frac{3}{4},x+\frac{1}{4}$

16 d .$\bar{3}m$ — $\frac{5}{8},\frac{5}{8},\frac{5}{8}$ $\frac{3}{8},\frac{7}{8},\frac{1}{8}$ $\frac{7}{8},\frac{1}{8},\frac{3}{8}$ $\frac{1}{8},\frac{3}{8},\frac{7}{8}$

16 c .$\bar{3}m$ — $\frac{1}{8},\frac{1}{8},\frac{1}{8}$ $\frac{7}{8},\frac{3}{8},\frac{5}{8}$ $\frac{3}{8},\frac{5}{8},\frac{7}{8}$ $\frac{5}{8},\frac{7}{8},\frac{3}{8}$

(16 d, 16 c): hkl : $h=2n+1$ or $h,k,l=4n+2$ or $h,k,l=4n$

8 b $\bar{4}3m$ — $\frac{1}{2},\frac{1}{2},\frac{1}{2}$ $\frac{1}{4},\frac{3}{4},\frac{1}{4}$

8 a $\bar{4}3m$ — $0,0,0$ $\frac{3}{4},\frac{1}{4},\frac{3}{4}$

(8 b, 8 a): hkl : $h=2n+1$ or $h+k+l=4n$

Symmetry of special projections

Along [001] $p4mm$
$\mathbf{a}'=\frac{1}{2}(\mathbf{a}-\mathbf{b})$ $\mathbf{b}'=\frac{1}{2}(\mathbf{a}+\mathbf{b})$
Origin at $0,0,z$

Along [111] $p6mm$
$\mathbf{a}'=\frac{1}{3}(2\mathbf{a}-\mathbf{b}-\mathbf{c})$ $\mathbf{b}'=\frac{1}{3}(-\mathbf{a}+2\mathbf{b}-\mathbf{c})$
Origin at x,x,x

Along [110] $c2mm$
$\mathbf{a}'=\frac{1}{2}(-\mathbf{a}+\mathbf{b})$ $\mathbf{b}'=\mathbf{c}$
Origin at $x,x,\frac{1}{8}$

References: p. 45.

Table 1
Examples of homogeneous sphere packings with distance d between neighboring spheres, highest and lowest contact numbers, k, and fractional packing densities, q.

k	Space Group Wyckoff position	Parameters	Distance d	Density q
12	$P6_3/mmc$ 2c $\frac{1}{3}\,\frac{2}{3}\,\frac{1}{4}$	$c/a = \frac{2}{3}\sqrt{6} = 1.633$	a	0.7405
12	$Fm\bar{3}m$ 4a 0 0 0		$\frac{1}{2}\sqrt{2}\,a$	0.7405
11	C2/m 4i x 0 z	$x = \frac{1}{2}(\sqrt{2}-1)$ $z = 3\sqrt{2} - 4\; b/a = \frac{1}{3}\sqrt{3}$ $c/a = \frac{1}{6}\sqrt{6} + \frac{1}{3}\sqrt{3} = 0.986$ $\cos\beta = \frac{1}{6}\sqrt{6} - \frac{1}{3}\sqrt{3}$	b	0.7187
10	I4/mmm 2a 0 0 0	$c/a = \frac{1}{3}\sqrt{6} = 0.8165$	c	0.6981
3	$I4_132$ 24h $\frac{1}{8}$ y $\frac{1}{4}$-y	$y = \frac{1}{4}\sqrt{3} - \frac{3}{8}$	$(\frac{1}{2}\sqrt{6} - \frac{3}{4}\sqrt{2})a$	0.0555

on their relative position against each other. The packing fractions as well as the coordination numbers (CN = 12) are equal in both cases. The first shell atomic environment corresponds to a cuboctahedron for ccp and to a disheptahedron for hcp. The distribution of atomic distances becomes different not until the third and higher coordination shells (fig. 9).

These two types of layer stackings are not the only possible ones, there exist infinitely many with exactly the same coordination numbers and packing fractions. They are called *polytypes*. Examples for such layer structures occurring for metallic elements are cobalt (..ABABAB**ABC**BCBCBC..), with one ccp sequence **ABC** statistically occurring among about ten hcp sequences, ordered hP4–La (..ACAB..) or hR3–Sm (..ABABCBCAC..) (fig. 10).

2.2.4. Polymorphism

Most of the elements adopt several different (allotropic) crystal structures at different pressures, temperatures or external fields. The transitions from one modification to the other are called polymorphous transformations or phase transitions.

A phase transition is connected with a change in structural parameters and/or in the ordering of electron spins. There are two basically different types of phase transitions: first-order transitions which are correlated with a jumpwise change in the first-order

Pearson symbol	Structure type	Space group	Space group number
cF8	C	*Fd3m*	227

a – .3567 nm

origin choice 1

Number	Atom	Multiplicity Wyckoff letter	x	y	z	Occupancy
1	C	8 a	0	0	0	1

Reference
T. Hom et al. JOURNAL OF APPLIED CRYSTALLOGRAPHY 1975
8 *p457*

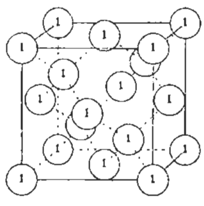

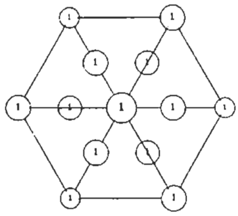

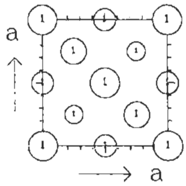

Cell content

(0,0,0) + (0,1/2,1/2) + (1/2,0,1/2) + (1/2,1/2,0) +

Number	Atom	Coordinates x	y	z
1	C	0	0	0
		1/4	1/4	1/4

1 C at 0 0 0

Distance	Number	Atom	x	y	z
.1545	1	C	1/4	1/4	1/4
.1545	1	C	1/4	-1/4	-1/4
.1545	1	C	-1/4	1/4	-1/4
.1545	1	C	-1/4	-1/4	1/4

CN = 4 polyhedron code = 4[illegible]

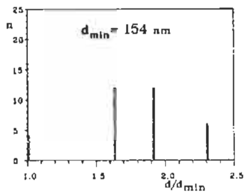

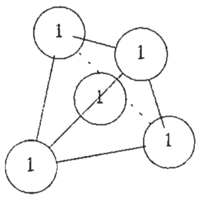

Fig. 6. Information given in the *Atlas of Crystal Structure Types for Intermetallic Phases* (DAAMS *et al.* [1991]) on the example of the diamond structure type. Beside numerical information and an atomic distances histogram, drawings of the crystal structure and characteristic coordination polyhedra in different projections are also shown.

derivatives of the Gibbs free energy G = H – TS (i.e., volume, entropy, ...), and second-order transitions which show a jump in the second derivatives of the Gibbs free energy (with respect to heat capacity, compressibility, etc.). In both types of phase transitions the crystal structure changes discontinuously at the transition point: in a first-order transition, in general no symmetry relationship exists between the two modifications; in a second-order transition, a group/subgroup relationship can always be found for the symmetry groups of the two polymorphous crystals structures.

With regard to structural changes resulting from a phase transformation of any order it is useful to distinguish between several different types: reconstructive phase transitions with essential changes in coordination numbers, atomic positions (α-Fe and γ-Fe, for instance, with coordination numbers CN = 8 and CN = 12, respectively, fig. 11) and sometimes also in chemical bonding (grey α-Sn and white β-Sn, for instance, with minimum distances changing from $d_{min}^{\alpha\text{-Sn}} = 1.54$ Å to $d_{min}^{\beta\text{-Sn}} = 3.02$ Å). These transformations are always of first order. Displacive phase transitions with small atomic shifts not changing the first coordination shells may change the lattice by small atomic displacements (martensitic diffusionless lattice rearrangement). Order/disorder transitions are related to the long-range ordered or disordered arrangement of structure elements (copper–gold system, for instance).

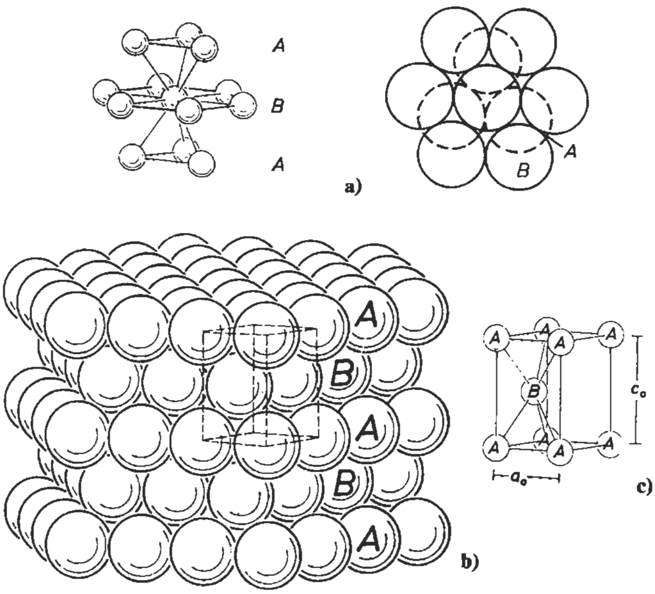

Fig. 7. Characteristics of the hexagonal closest-sphere packing. (a) The coordination polyhedron (disheptahedron) in perspective view and projected to show the packing principle, (b) the crystal structure and (c) one unit cell with atoms marked according to their belonging to layer A or B, are depicted (from BORCHARDT-OTT [1993]).

Table 2
Fractional packing densities q of elemental structures (PEARSON [1972]).

Element	Structure Type, *c*/*a*	Space filling value *q*	Element	Structure Type, *c*/*a*	Space filling value *q*
Cu	cF4	0.740	Po	cP1	0.523
Mg	hP2, 1.63	0.740	Bi	hR2, 2.60	0.446
Zn	hP2, 1.86	0.650	Sb	hR2, 2.62	0.410
Pa	tI2	0.696	As	hR2, 2.80	0.385
In	tI2	0.686	Ga	oC8	0.391
W	cI2	0.680	Te	hP3	0.364
Hg	hR1	0.609	C (diamond)	cF8	0.340
Sn	tI4	0.535	P (black)	oC8	0.285
α-U	oC4	0.534			

3. *Crystal structure of metallic elements*

In the following, the crystal structures of all metallic and semi-metallic elements (table 3) will be discussed. If it is not indicated specifically, the crystal structure data

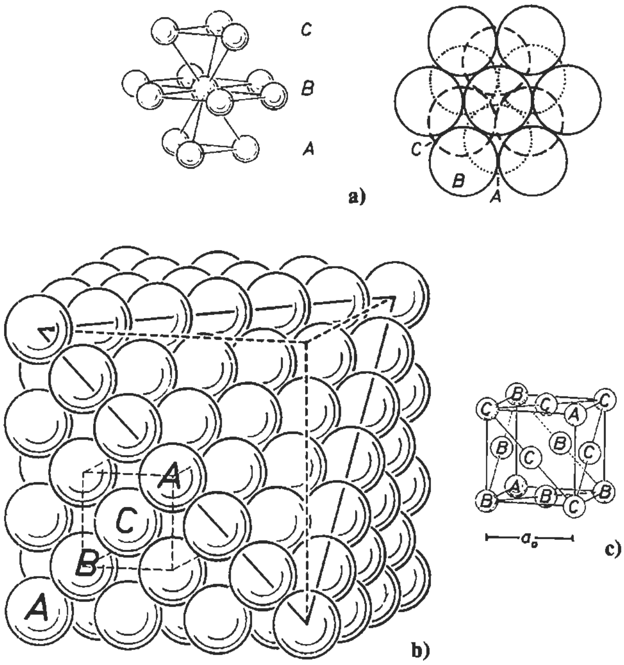

Fig. 8. Characteristics of the cubic closest-sphere packing. (a) The coordination polyhedron (cuboctahedron) in perspective view and projected to show the packing principle, (b) the crystal structure and (c) one unit cell with atoms marked according to their belonging to layer A, B or C, are depicted (from BORCHARDT–OTT [1993]).

have been taken from VILLARS and CALVERT [1991], YOUNG [1991] or MASSALSKI [1990]. In the (not so rare) cases of contradictory data, the most recent and reliable (?) ones have been used or the Pearson symbol has been replaced by a question mark. Particularly the structural information given for the high-pressure phases, which in most cases are derived from very small data sets, may be revised in future once better diffraction data become available.

3.1. Nomenclature

For the short-hand characterization of crystal structures, the Pearson notation in combination with the prototype formula defining the structure type is used throughout the paper. In accordance with the IUPAC recommendations (LEIGH [1990]) the old *Strukturbericht* designation (A3 for hP2–Mg, for instance) should not be used any longer. A comparison of the Pearson notation, prototype formula, space group and Strukturbericht designation for a large number of crystal structure types is given in MASSALSKI [1990].

The Pearson symbol consists of two letters and a number. The first (lower case letter) denotes the crystal family, the second (upper case) letter the Bravais lattice type (table 4). The symbol is completed by the number of atoms in the unit cell. The symbol cF4, for instance, classifies a structure type to be cubic (c), all-face centered (F), with 4 atoms per unit cell. In

Table 3

Periodic table of the elements. In accordance with the recommendations of the IUPAC 1988, the columns are numbered consecutively from 1 to 18. The elements whose structures are discussed in this chapter are shadowed.

1	2	3	4	5	6	7	8	9	10	11	12	13	14	15	16	17	18
1 H																	2 He
3 Li	4 Be											5 B	6 C	7 N	8 O	9 F	10 Ne
11 Na	12 Mg											13 Al	14 Si	15 P	16 S	17 Cl	18 Ar
19 K	20 Ca	21 Sc	22 Ti	23 V	24 Cr	25 Mn	26 Fe	27 Co	28 Ni	29 Cu	30 Zn	31 Ga	32 Ge	33 As	34 Se	35 Br	36 Kr
37 Rb	38 Sr	39 Y	40 Zr	41 Nb	42 Mo	43 Tc	44 Ru	45 Rh	46 Pd	47 Ag	48 Cd	49 In	50 Sn	51 Sb	52 Te	53 I	54 Xe
55 Cs	56 Ba	57* La	72 Hf	73 Ta	74 W	75 Re	76 Os	77 Ir	78 Pt	79 Au	80 Hg	81 Tl	82 Pb	83 Bi	84 Po	85 At	86 Rn
87 Fr	88 Ra	89+ Ac															

* Lanthanide metals	58 Ce	59 Pr	60 Nd	61 Pm	62 Sm	63 Eu	64 Gd	65 Tb	66 Dy	67 Ho	68 Er	69 Tm	70 Yb	71 Lu
+Actinide metals	90 Th	91 Pa	92 U	93 Np	94 Pu	95 Am	96 Cm	97 Bk	98 Cf	99 Es	100 Fm	101 Md	102 No	103 Lr

the case of rhombohedral structures, like the hR3–Sm type, the number of atoms in the unit cell in the rhombohedral setting ($a=b=c$, $\alpha=\beta=\gamma\neq 90°$) is given. The number of atoms in the corresponding hexagonal setting ($a=b\neq c$, $\alpha=\beta=90°$, $\gamma=120°$) would be three times as much.

Table 4

Meaning of the letters included in the Pearson Symbol.

Crystal family		Bravais lattice type	
a	triclinic (anorthic)	P	primitive
m	monoclinic	I	body centered
o	orthorhombic	F	all-face centered
t	tetragonal	C	side- or base-face centered
h	hexagonal, trigonal (rhombohedral)	R	rhombohedral
c	cubic		

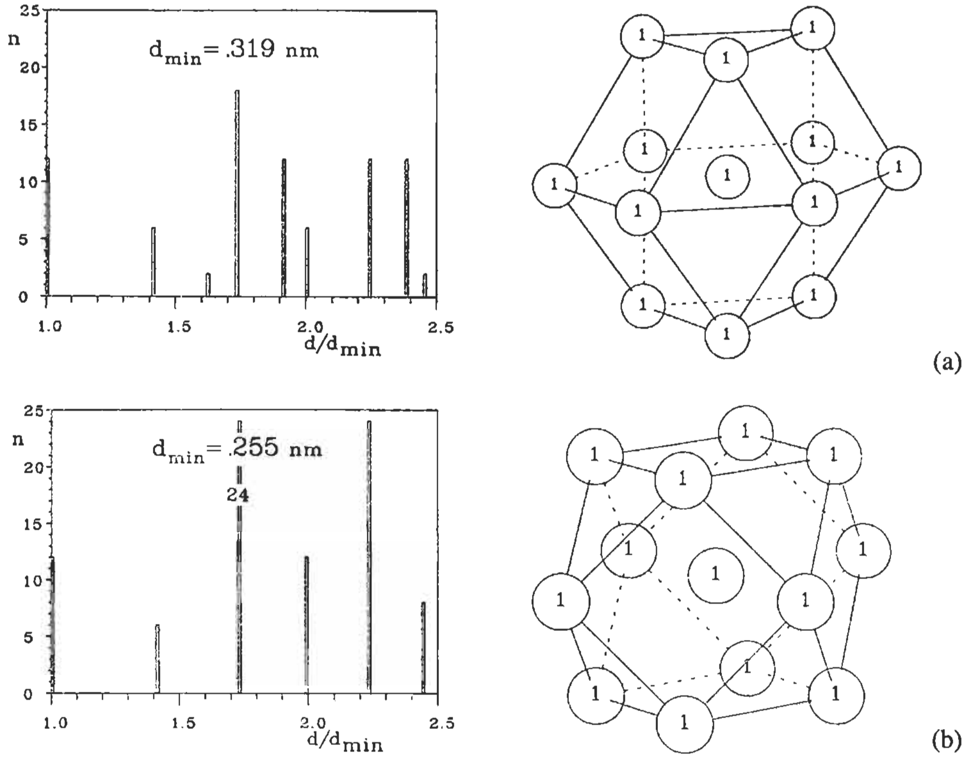

Fig. 9. Histograms of distances and coordination polyhedra of (a) hexagonal and (b) cubic closest packing (from DAAMS *et al.* [1991]).

3.2. Group 1 and 2, alkali and alkaline earth metals

The alkali and alkaline earth metals (table 5) belong to the typical metals. The outer electrons occupy the ns-orbitals, ionization removes the electrons of a whole shell, thus drastically reducing the atomic radius (Li: atomic radius 1.56 Å, ionic radius 0.60 Å, for instance). The absence of directional bonds forces close atomic (sphere) packings; the alkali metals conform most closely to the free electron gas model of metals. Under ambient conditions the alkali metals all crystallize in the simple body-centered cubic (bcc) structure cI2–W (fig. 12). The bcc structure is assumed to be more stable at higher temperature than the ccp or hcp one owing to its higher vibrational entropy. At lower temperature or higher pressure, the bcc structure is transformed martensitically to the closest-packed lattice types, hR3–Sm or cF4–Cu, respectively. Contrary to earlier studies, the hexagonal closest-packed phases are not of the hP2–Mg but of the hR3–Sm type (fig. 10) with stacking sequence ...ABABCBCAC.. (YOUNG [1991]).

The extremely strong dependence of the atomic volume on pressure, which increases with increasing atomic number due to the shielding of the outer electrons by the

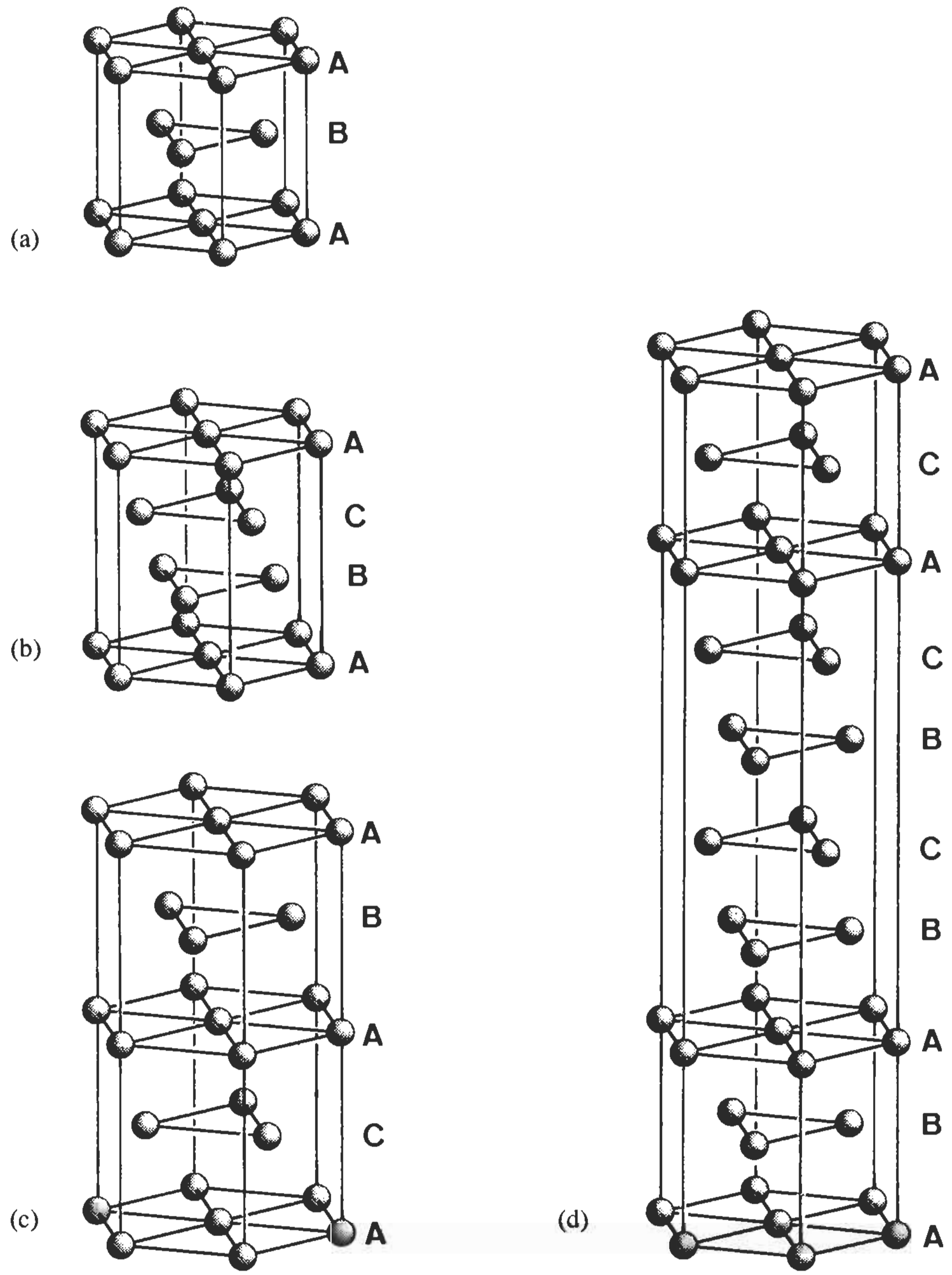

Fig. 10. Schematical representation of the stacking sequences of the closest-packed structures (a) hP2–Mg, (b) cF4–Cu, (c) hP4–La and (d) hR3–Sm.

Table 5

Structure information for the elements of group 1, alkali metals, and of group 2, alkaline earth metals. In the first line of each box the chemical symbol, atomic number Z, and the atomic volume V_{at} under ambient conditions is listed. In the second line the electronic ground state configuration is given. For each phase there is tabulated: limiting temperature T[K] and pressure P[GPa], Pearson symbol PS, prototype structure PT, and, if applicable, the lattice parameter ratio *c/a*.

	T[K]	P[GPa]	PS	PT	*c/a*		T[K]	P[GPa]	PS	PT	*c/a*
Li 3 $V_{at}=21.60\,Å^3$						**Be** 4 $V_{at}=8.11\,Å^3$					
$1s^22s^1$						$1s^22s^22$					
α	<70		hR3	Sm		α			hP2	Mg	1.568
β			cI2	W		β	>1543		cI2	W	
γ		>6.9	cF4	Cu		γ		>28.3	hP8?		0.789
Na 11 $V_{at}=39.50\,Å^3$						**Mg** 12 $V_{at}=23.24\,Å^3$					
$1s^22s^2p^63s^1$						$1s^22s^2p^63s^2$					
α	<40		hR3	Sm		α			hP2	Mg	1.624
β			cI2	W		β		>50	cI2	W	
K 19 $V_{at}=75.33\,Å^3$						**Ca** 20 $V_{at}=43.62\,Å^3$					
$1s^22s^2p^63s^2p^64s^1$						$1s^22s^2p^63s^2p^64s^2$					
α			cI2	W		α			cF4	Cu	
β		>12	cF4	Cu		β	>728 or	>19.5	cI2	W	
						γ		>32	cP1	α-Po	
Rb 37 $V_{at}=92.59\,Å^3$						**Sr** 38 $V_{at}=56.35\,Å^3$					
$1s^22s^2p^63s^2p^6d^{10}4s^2p^65s^1$						$1s^22s^2p^63s^2p^6d^{10}4s^2p^65s^2$					
α			cI2	W		α			cF4	Cu	
β		>7.0	cF4	Cu		β	>504		hP2	Mg	1.636
γ		>14				γ	>896 or	>3.5	cI2	W	
δ		>17				δ		>26			
ε		>20	tI4			ε		>35			
Cs 55 $V_{at}=117.79\,Å^3$						**Ba** 56 $V_{at}=63.36\,Å^3$					
$1s^22s^2p^63s^2p^6d^{10}4s^2p^6d^{10}5s^2p^66s^1$						$1s^22s^2p^63s^2p^6d^{10}4s^2p^6d^{10}5s^2p^66s^2$					
α			cI2	W		α			cI2	W	
β		>2.37	cF4	Cu		β		>5.33	hP2	Mg	1.581
β'		>4.22	cF4	Cu		γ		>7.5			
γ		>4.27	tI4			δ		>12.6			
δ		>10									
ε		>72	cF4?								
Fr 87						**Ra** 88 $V_{at}=68.22\,Å^3$					
$1s^22s^2p^63s^2p^6d^{10}4s^2p^6d^{10}f^{14}5s^2p^6d^{10}6s^2p^67s^1$						$1s^22s^2p^63s^2p^6d^{10}4s^2p^6d^{10}f^{14}5s^2p^6d^{10}6s^2p^67s^2$					
						α			cI2	W	

increasing number of inner electron shells, is shown by the example of Cs (fig. 13). With increasing pressure, the valence electrons change from s to d character, giving rise to a large number of pressure-induced phase transitions at ambient temperature (YOUNG [1991]):

$$\alpha\text{-Cs} \overset{2.37\text{ GPa}}{\Leftrightarrow} \beta\text{-Cs} \overset{4.22\text{ GPa}}{\Leftrightarrow} \beta'\text{-Cs} \overset{4.27\text{ GPa}}{\Leftrightarrow} \gamma\text{-Cs} \overset{10\text{ GPa}}{\Leftrightarrow} \delta\text{-Cs} \overset{72\text{ GPa}}{\Leftrightarrow} \varepsilon\text{-Cs}$$

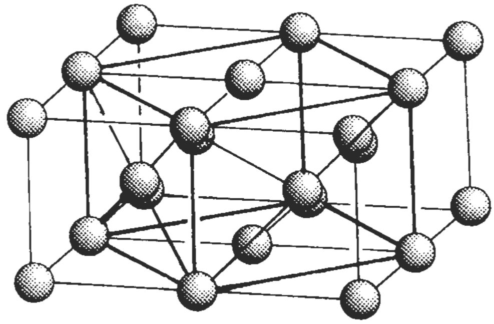

Fig. 11. Relationship between body-centered cubic (bcc) α-Fe, cI2–W type, space group Im$\bar{3}$m, No. 229, 1a: 0 0 0, and face-centered cubic (fcc) γ-Fe, cF4–Cu type, space group Fm$\bar{3}$m, No. 225, 4a: 0 0 0. The face-centered tetragonal unit cell drawn into an array of four bcc unit cells transforms by shrinking its faces to fcc.

The alkaline earth metals behave quite similarly to the alkali metals. They crystallize under ambient conditions in one of the two closest-packed structures (ccp or hcp) or in the body-centered cubic (bcc) structure type and also show several allotropic forms (fig. 14). The large deviation $c/a = 1.56$ from the ideal value of 1.633 for beryllium indicates covalent bonding contributions.

For alkali and alkaline earth metals, the pressure-induced phase transitions from cI2–W to cF4–Cu occur with increasing atomic number at decreasing pressures.

3.3. Groups 3 to 10, transition metals

The elements of groups 3 to 10 are typical metals which have in common that their d-orbitals are partially occupied. These orbitals are only slightly screened by the outer s-electrons, leading to significantly different chemical properties of the transition elements going from left to right in the periodic system. The atomic volumes decrease rapidly with increasing number of electrons in bonding d-orbitals, because of cohesion, and increase as the anti-bonding d-orbitals become filled (fig. 15). The anomalous behavior of the 3d-transition metals, Mn, Fe and Co, may be explained by the existence of non-bonding d-electrons (Pearson [1972]).

Scandium, yttrium, lanthanum and actinium (table 6) are expected to behave quite

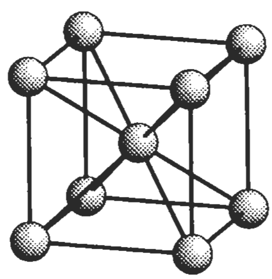

Fig. 12. Unit cell of the body-centered cubic structure type cI2–W, space group Im$\bar{3}$m, No. 229, 1a: 0 0 0.

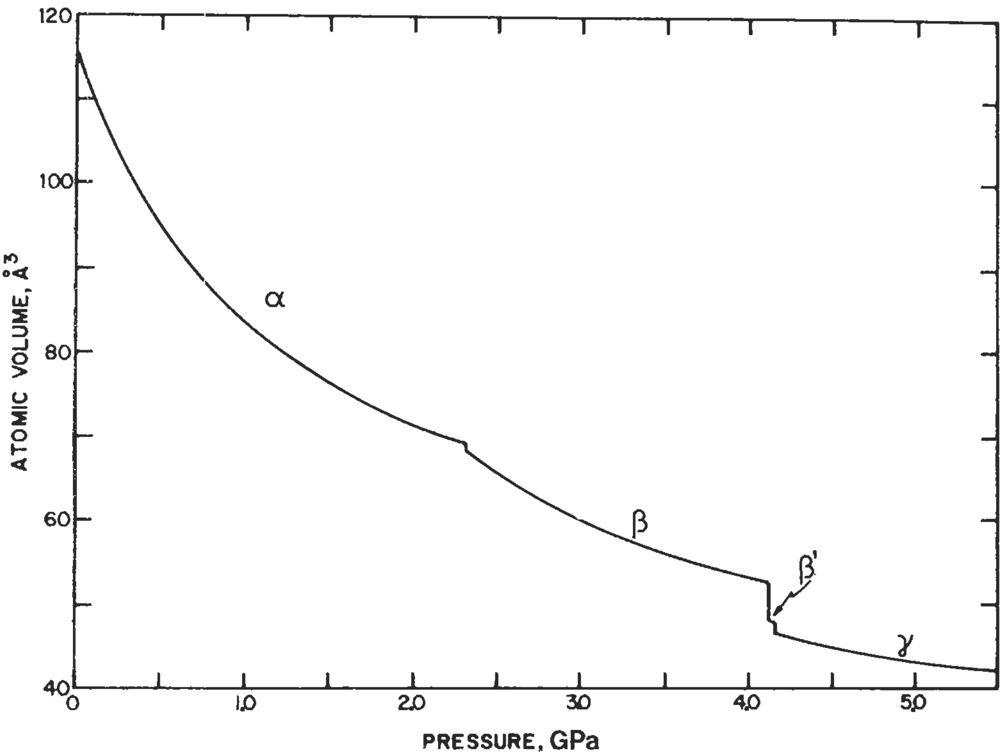

Fig. 13. The variation of the atomic volume of cesium with pressure (after DONOHUE [1974]).

similarly. Indeed they show similar phase sequences: the high-pressure phases of light elements occur as the ambient-pressure phases of the heavy homologues. The hP4 phase of lanthanum, with the sequence ..ACAB.., is one of the simpler closest-packed polytypic structures common for the lanthanides (fig. 16 and fig. 10). Another typical polytype for lanthanides is the hR3 phase of yttrium with stacking sequence ..ABABCBCAC.. (fig. 17 and fig. 10).

Titanium, zirconium and hafnium (table 6) crystallize in a slightly compressed hcp structure type and transform to bcc at higher temperatures. At higher pressures the ω-Ti phase is obtained (fig. 18). The packing density of the hP3–Ti structure with ~0.57 is slightly larger than that of the simple cubic α-Po structure (~0.52) but substantially lower than for bcc (~0.68) or ccp and hcp (~0.74) type structures. Calculations have shown that the ω-Ti phase is stable owing to covalent bonding contributions from s–d electron transfer. At even higher pressures, zirconium and hafnium transform to the cI2–W type, while titanium remains in the ~~hp3~~–Ti phase up to at least 87 GPa. By theoretical considerations it is also expected that titanium performs this transformation at sufficiently high pressures (AHUJA *et al.* [1993]). A general theoretical phase diagram for Ti, Zr and Hf is shown in fig. 19.

Vanadium, niobium, tantalum, molybdenum and tungsten have only simple bcc

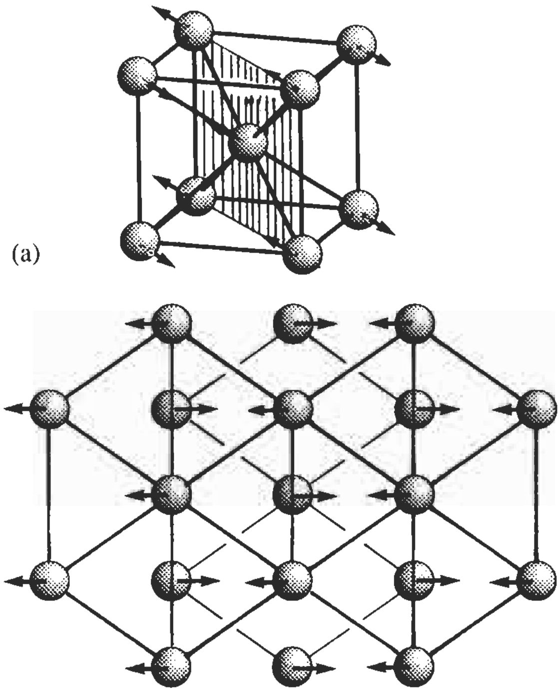

(a)

(b)

Fig. 14. Illustration of the bcc-to-hcp phase transition of Ba. (a) bcc unit cell with (110) plane marked. (b) Projection of the bcc structure upon the (110) plane. Atomic displacements necessary for the transformation are indicated by arrows.

structures (table 7). Up to pressures of 170 to 364 GPa no further allotropes could be found, in agreement with theoretical calculations. Chromium shows two antiferromagnetic phase transitions, which modify the structure only very slightly (YOUNG [1991]).

The high-temperature phases of manganese (table 8), γ-Mn, cF4–Cu type, and δ-Mn, cI2–W type, are typical metal structures, whereas α-Mn and β-Mn form very complicated structures, possibly caused by their antiferromagnetism. Thus, the α-Mn structure can be described as a $3\times3\times3$ superstructure of bcc unit cells, with 20 atoms slightly shifted and 4 atoms added resulting in 58 atoms over all (fig. 20). The structure of β-Mn (fig. 21) is also governed by the valence electron concentration ("electron compound" or Hume–Rothery-type phase). The variation of the atomic volume of manganese with temperature is illustrated in fig. 22. For technetium, rhenium, ruthenium and osmium, only simple hcp structures are known.

The technically most important element and the main constituent of the Earth's core, iron (table 8) shows five allotropic forms (fig. 23): ferromagnetic bcc α-Fe transforms to paramagnetic isostructural β-Fe with a Curie temperature of 1043 K; at 1185 K fcc γ-Fe forms while at 1667 K a bcc phase, now called δ-Fe, appears again. For the variation of

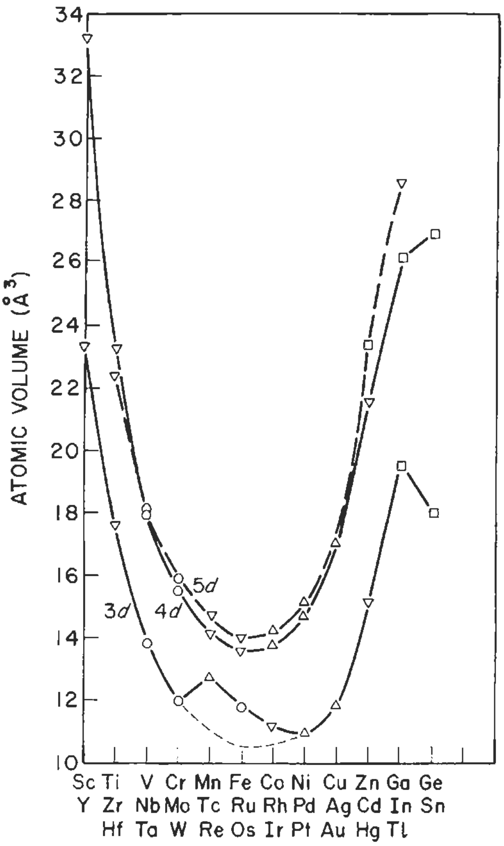

Fig. 15. Atomic volumes of the transition metals. △ means cF4–Cu type, ▽ hP2–Mg, ○ cI2–W, □ other types (after PEARSON [1972]).

the atomic volume with temperature see fig. 24. High-pressure nonmagnetic ε-Fe, existing above 13 GPa, has a slightly compressed hcp structure.

Cobalt (table 9) is dimorphous, hcp at ambient conditions and ccp at higher temperatures. By annealing it in a special way, stacking disorder can be generated: the hcp sequence ..ABAB.. is statistically disturbed by a ccp sequence ..ABCABC.. like ..ABABABABCBCBCBC.. with a frequency of about one ..ABC.. among ten ..AB... Rhodium, iridium, nickel, palladium and platinum all crystallize in simple cubic closest-packed structures.

3.4. Groups 11 and 12, copper and zinc group metals

The "mint metals", copper, silver and gold (table 10) are typical metals with ccp structure type (fig. 25). Their single ns electron is less shielded by the filled d-orbitals than the ns electron of the alkali metals by the filled noble gas shell. The d-electrons also contribute to the metallic bond. These factors are responsible for the more noble

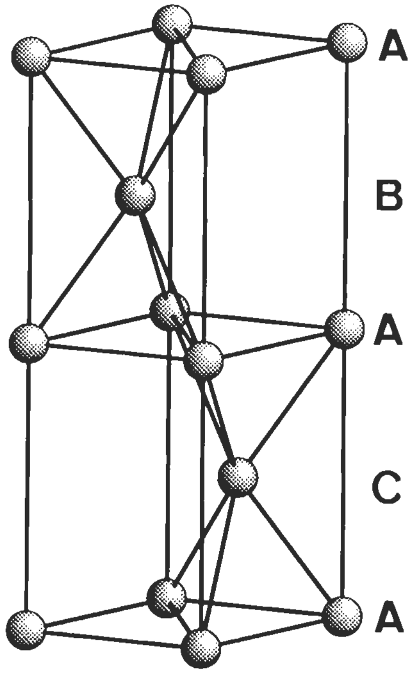

Fig. 16. One unit cell of the hP4–La structure type, space group $P6_3/mmc$, No. 194, 2a: 0 0 0, 2c: ⅓ ⅔ ¼.

character of these metals than of the alkali metals and that these elements sometimes are grouped to the transition elements.

For zinc, cadmium and mercury (table 10) covalent bonding contributions (filled d-band) lead to deviations from hexagonal closest packing (hcp), with its ideal axial ratio $c/a = 1.633$, to values of 1.856 (Zn) and 1.886 (Cd), respectively. The bonds in the hcp layers are shorter and stronger, consequently, than between the layers. With increasing pressure, c/a approximates the ideal value 1.633: for Cd $c/a = 1.68$ was observed at 30 GPa (Donohue [1974]), and for Hg, $c/a = 1.76$ at 46.8 GPa (Schulte and Holzapfel [1993]).

The rhombohedral structure of α-Hg may be derived from a ccp structure by compression along the threefold axis (fig. 26). In contrast to zinc and cadmium, the ratio $c/a = 1.457$ for a hypothetical distorted hcp structure is smaller than the ideal value. There also exist several high-pressure allotropes (fig. 27).

3.5. Groups 13 to 16, metallic and semi-metallic elements

Only aluminum, thallium and lead crystallize in the closest-packed structures characteristic for typical metals (table 11). The s–d transfer effects, important for alkali- and alkaline-earth metals, do not appear for the heavier group 13 elements owing to their filled d-bands. Orthorhombic gallium forms a 6^3 network of distorted hexagons parallel to (100) at heights $x = 0$ and 1/2 (fig. 28). The bonds between the layers are considerably

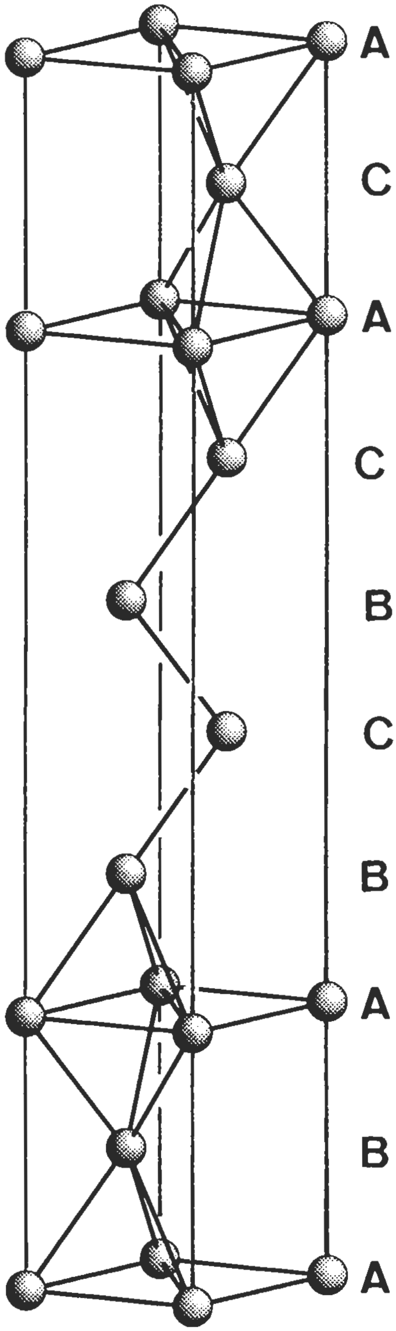

Fig. 17. One unit cell of the hR3–Sm structure type, space group R$\bar{3}$m, No. 166, 3a: 0 0 0, 6c: 0 0 0.22.

References: p. 45.

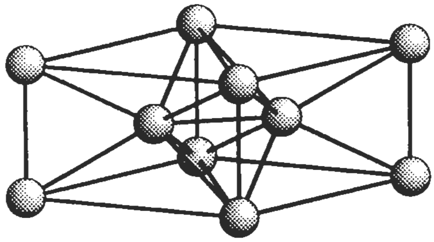

Fig. 18. The hP3–Ti structure type, space group P6/mmm, No. 191, 1a: 0 0 0, 2d: ⅓ ⅔ ½.

weaker than within. At higher pressure gallium transforms to a bcc phase, cI12–Ga, and additionally increasing the temperature leads to the tetragonal indium structure type tI2–In (fig. 29). In an alternative description based on a face-centered tetragonal unit cell with $a' = \sqrt{2}\,a$, the resemblance to a slightly distorted cubic close-packed structure with $c/a = 1.08$ becomes clear.

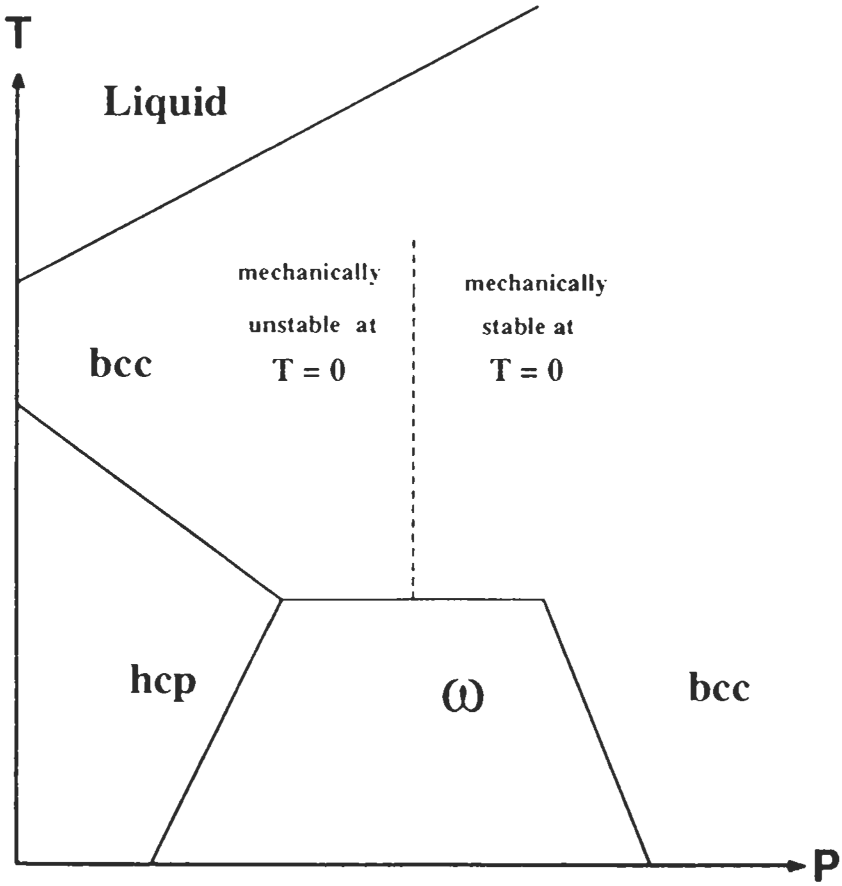

Fig. 19. Schematic calculated phase diagram for Ti, Zr and Hf (from AHUJA *et al.* [1993]).

Table 6

Structure information for the elements of groups 3 and 4. In the first line of each box the chemical symbol, atomic number Z, and the atomic volume V_{at} under ambient conditions is listed. In the second line the electronic ground state configuration is given. For each phase there is tabulated: limiting temperature T[K] and pressure P[GPa], Pearson symbol PS, prototype structure PT, and, if applicable, the lattice parameter ratio *c/a*.

	T[K]	P[GPa]	PS	PT	*c/a*		T[K]	P[GPa]	PS	PT	*c/a*
Sc 21 $V_{at}=24.97$ Å^3						**Ti** 22 $V_{at}=17.65$ Å^3					
$1s^22s^2p^63s^2p^6d^14s^2$						$1s^22s^2p^63s^2p^6d^24s^2$					
α			hP2	Mg	1.592	α			hP2	Mg	1.587
β	> 1610		cI2	W		β	> 1155		cI2	W	
γ		> 19	tP4?			ω		> 2	hP3	ω-Ti	
Y 39 $V_{at}=33.01$ Å^3						**Zr** 40 $V_{at}=23.28$ Å^3					
$1s^22s^2p^63s^2p^6d^{10}4s^2p^6d^15s^2$						$1s^22s^2p^63s^2p^6d^{10}4s^2p^6d^25s^2$					
α			hP2	Mg	1.571	α			hP2	Mg	1.593
β	> 1751		cI2	W		β	> 1136		cI2	W	
γ		> 10	hR3	Sm		ω		> 2	hP3	ω-Ti	
δ		> 26	hP4?			ω′		> 30	cI2	W	
ε		> 39	cF4	Cu							
La 57 $V_{at}=37.17$ Å^3						**Hf** 72 $V_{at}=22.31$ Å^3					
$1s^22s^2p^63s^2p^6d^{10}4s^2p^6d^{10}5s^2p^6d^16s^2$						$1s^22s^2p^63s^2p^6d^{10}4s^2p^6d^{10}f^{14}5s^2p^6d^26s^2$					
α			hP4	α-La	2×1.613	α			hP2	Mg	1.581
β	> 583 or > 2.3		cF4	Cu		β	> 2016		cI2	W	
γ	> 1138		cI2	W		ω		> 38	hP3	ω-Ti	
δ		> 7.0	hP6			ω′		> 71	cI2	W	
Ac 89 $V_{at}=37.45$ Å^3 at 293 K						**Ku** 104					
$...3s^2p^6d^{10}4s^2p^6d^{10}f^{14}5s^2p^6d^{10}6s^2p^6d^17s^2$						$...3s^2p^6d^{10}4s^2p^6d^{10}f^{14}5s^2p^6d^{10}f^{14}6s^2p^6d^27s^2$					
α			cF4	Cu							

Silicon and germanium (table 11) under ambient conditions crystallize in the diamond structure, owing to strong covalent bonding. At higher pressures they transform to the metallic white-tin (tI4–Sn) structure. This structure type consists of a body-centered tetragonal lattice which can be regarded as being intermediate between the diamond structure of semiconducting α-Sn and ccp lead (fig. 30). For an ideal ratio of $c/a=0.528$ one atom is sixfold coordinated. The high-pressure phase hP1–BiIn has a quasi-eightfold coordination, the ideal ratio for CN = 8 would be $c/a=1$. At higher pressures, closest-packed structures with twelvefold coordinations are obtained. Thus with increasing pressure silicon runs through phases with coordination numbers 4, 6, 8 and 12.

The effective radius of tin in β-Sn and of lead in α-Pb is large compared with that of other typical metals with large atomic number due to uncomplete ionization of the single ns electron. This means that in α-Sn, for instance, the electron configuration is $...5s^15p^3$, allowing sp^3–hybridization and covalent tetrahedrally coordinated bonding, whereas in β-Sn with $...5s^25p^2$ only two p-orbitals are available for covalent and one further p-orbital for metallic bonding.

The structure of arsenic, antimony and bismuth (isotypic under ambient conditions)

Table 7

Structure information for the elements of groups 5 and 6. In the first line of each box the chemical symbol, atomic number Z, and the atomic volume V_{at} under ambient conditions is listed. In the second line the electronic ground state configuration is given. For each phase there is tabulated: limiting temperature T[K] and pressure P[GPa], Pearson symbol PS, prototype structure PT, and, if applicable, the lattice parameter ratio *c/a*.

	T[K]	P[GPa]	PS	PT	*c/a*		T[K]	P[GPa]	PS	PT	*c/a*
V 23 $V_{at} = 13.82\,Å^3$						**Cr** 24 $V_{at} = 12.00\,Å^3$					
$1s^22s^2p^63s^2p^6d^34s^2$						$1s^22s^2p^63s^2p^6d^54s^1$					
			cI2	W					cI2	W	
Nb 41 $V_{at} = 17.98\,Å^3$						**Mo** 42 $V_{at} = 15.58\,Å^3$					
$1s^22s^2p^63s^2p^6d^{10}4s^2p^6d^45s^1$						$1s^22s^2p^63s^2p^6d^{10}4s^2p^6d^55s^1$					
			cI2	W					cI2	W	
Ta 73 $V_{at} = 18.02\,Å^3$						**W** 74 $V_{at} = 15.85\,Å^3$					
$1s^22s^2p^63s^2p^6d^{10}4s^2p^6d^{10}f^{14}5s^2p^6d^36s^2$						$1s^22s^2p^63s^2p^6d^{10}4s^2p^6d^{10}f^{14}5s^2p^6d^46s^2$					
			cI2	W					cI2	W	

(table 12) consists of puckered layers of covalently bonded atoms stacked along the hexagonal axis (fig. 31). The structure can be regarded as a distorted primitive cubic structure (α-Po) in which the atomic distance d_1 in the layer equals that between the layers d_2. The metallic character of these elements increases for d_2/d_1 approximating to 1 (table 13).

The helical structures of isotypic α-Se and α-Te may also be derived from the

Table 8

Structure information for the elements of groups 7 and 8. In the first line of each box the chemical symbol, atomic number Z, and the atomic volume V_{at} under ambient conditions is listed. In the second line the electronic ground state configuration is given. For each phase there is tabulated: limiting temperature T[K] and pressure P[GPa], Pearson symbol PS, prototype structure PT, and, if applicable, the lattice parameter ratio *c/a*.

	T[K]	P[GPa]	PS	PT	*c/a*		T[K]	P[GPa]	PS	PT	*c/a*
Mn 25 $V_{at} = 12.21\,Å^3$						**Fe** 26 $V_{at} = 11.78\,Å^3$					
$1s^22s^2p^63s^2p^6d^54s^2$						$1s^22s^2p^63s^2p^6d^64s^2$					
α			cI58	α-Mn		α			cI2	W	
β	>1000		cP20	β-Mn		γ	>1185		cF4	Cu	
γ	>1373		cF4	Cu		δ	>1667		cI2	W	
δ	>1411		cI2	W		ε		>13	hP2	Mg	1.603
Tc 43 $V_{at} = 14.26\,Å^3$						**Ru** 44 $V_{at} = 13.57\,Å^3$					
$1s^22s^2p^63s^2p^6d^{10}4s^2p^6d^65s^1$						$1s^22s^2p^63s^2p^6d^{10}4s^2p^6d^75s^1$					
			hP2	Mg	1.604				hP2	Mg	1.582
Re 75 $V_{at} = 14.71\,Å^3$						**Os** 76 $V_{at} = 13.99\,Å^3$					
$1s^22s^2p^63s^2p^6d^{10}4s^2p^6d^{10}f^{14}5s^2p^6d^56s^2$						$1s^22s^2p^63s^2p^6d^{10}4s^2p^6d^{10}f^{14}5s^2p^6d^66s^2$					
			hP2	Mg	1.615				hP2	Mg	1.580

(a)

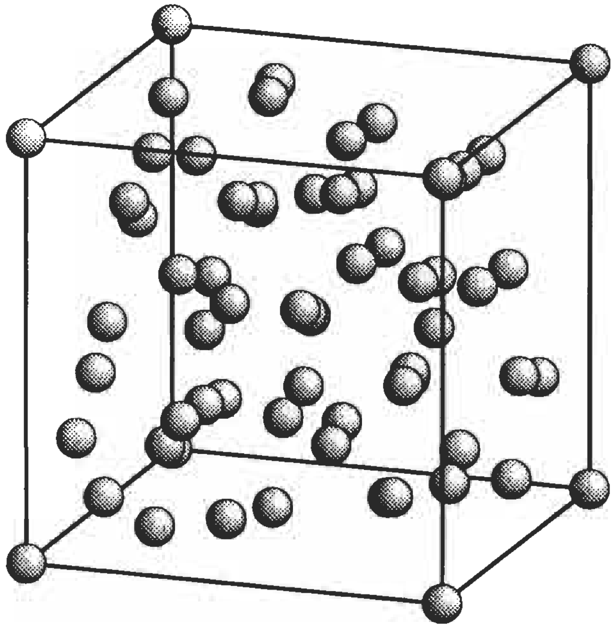

(b)

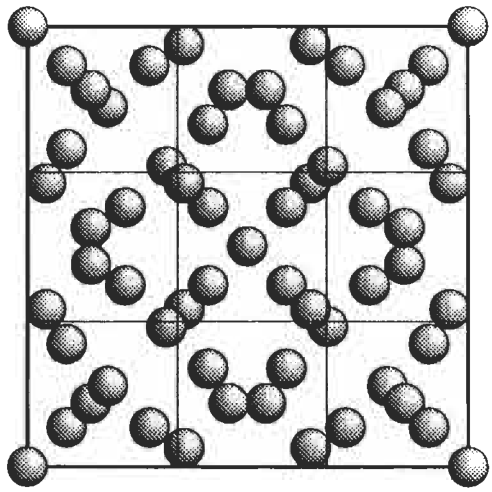

Fig. 20. One unit cell of cI58–Mn, space group $I\bar{4}3m$, No. 217, with four different types of Mn atoms in 2a: 0 0 0, 8c: 0.316 0.316 0.316, 24g: 0.356 0.356 0.034, 24g: 0.089 0.089 0.282, shown (a) in perspective view and (b) in projection. Two types of Mn atoms are coordinated by CN 16 Friauf polyhedra, one by a CN 14 Frank-Kasper polyhedron and one by an icosahedron.

primitive cubic α-Po structure (fig. 32). The infinite helices run along the trigonal axes, and have three atoms per turn. The interhelix bonding distance d_2 plays a comparable

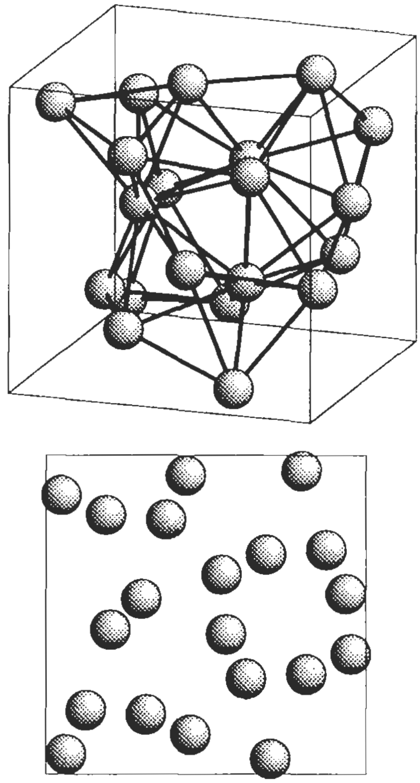

Fig. 21. One unit cell of cP20–Mn, space group $P4_132$, No 213, with two types of Mn atoms: 8c: 0.063 0.063 0.063, 12d: 0.125 0.202 0.452, shown (a) in perspective view and (b) in projection. The atoms in 8c are coordinated by 12 atoms in a distorted icosahedron, the Mn atoms in 12d by 14 atoms in a distorted Frank-Kasper CN 14 type polyhedron.

role for the metallic character of these elements as does the interlayer distance in the case of the group 15 elements. Wih increasing pressure, the transition to the metallic β–Te phase takes place.

3.6. Lanthanides and actinides

Lanthanides and actinides (table 14) are characterized by the fact that their valence electrons occupying the f-orbitals are shielded by filled outer s- and p-orbitals. The chemical properties of the lanthanides are rather uniform since the 4f-orbitals are largely screened by the 5s- and 5p-electrons. The chemical behavior of the actinides, however, is somelike in between that of the 3d transition metals and the lanthanides since the 5f-orbitals are screened to a much smaller amount by the 6s- and 6p-electrons. With the exception of Sm and Eu, all lanthanides under ambient conditions show either a simple hcp structure with the standard stacking sequence ..AB.. or a twofold superstructure with a stacking sequence ..ACAB... Samarium has, with ..ABABCBCAC.., an even more

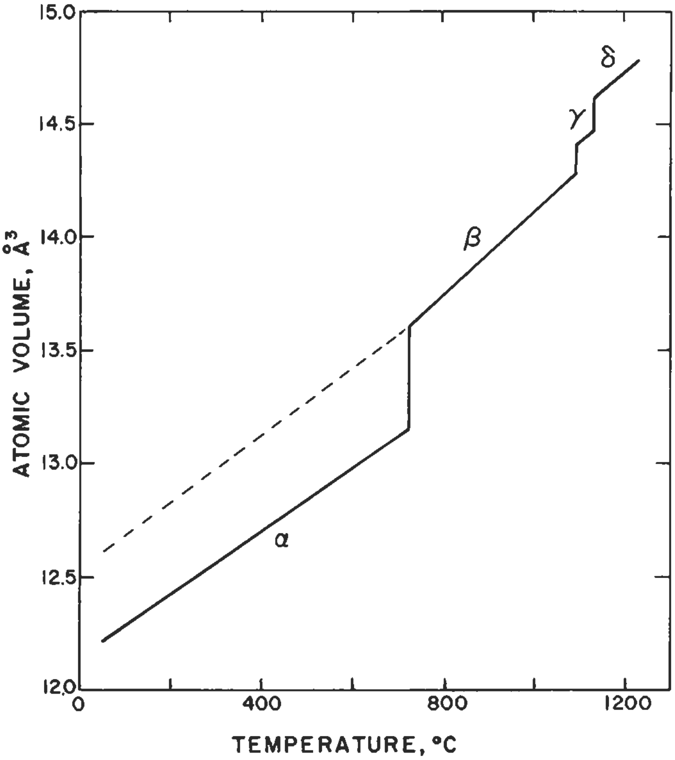

Fig. 22. The variation of the atomic volume of manganese with temperature (from DONOHUE [1974]).

Table 9

Structure information for the elements of groups 9 and 10. In the first line of each box the chemical symbol, atomic number Z, and the atomic volume V_{at} under ambient conditions is listed. In the second line the electronic ground state configuration is given. For each phase there is tabulated: limiting temperature T[K] and pressure P[GPa], Pearson symbol PS, prototype structure PT, and, if applicable, the lattice parameter ratio *c/a*.

	T[K]	P[GPa]	PS	PT	*c/a*		T[K]	P[GPa]	PS	PT	*c/a*
Co 27 V_{at} = 11.08 Å^3						**Ni** 28 V_{at} = 10.94 Å^3					
$1s^22s^2p^63s^2p^6d^74s^2$						$1s^22s^2p^63s^2p^6d^84s^2$					
ε			hP2	Mg	1.623				cF4	Cu	
α	>695		cF4	Cu							
Rh 45 V_{at} = 13.75 Å^3						**Pd** 46 V_{at} = 14.72 Å^3					
$1s^22s^2p^63s^2p^6d^{10}4s^2p^6d^85s^1$						$1s^22s^2p^63s^2p^6d^{10}4s^2p^6d^{10}$					
			cF4	Cu					cF4	Cu	
Ir 77 V_{at} = 14.15 Å^3						**Pt** 78 V_{at} = 15.10 Å^3					
$1s^22s^2p^63s^2p^6d^{10}4s^2p^6d^{10}f^{14}5s^2p^6d^76s^2$						$1s^22s^2p^63s^2p^6d^{10}4s^2p^6d^{10}f^{14}5s^2p^6d^96s^1$					
			cF4	Cu					cF4	Cu	

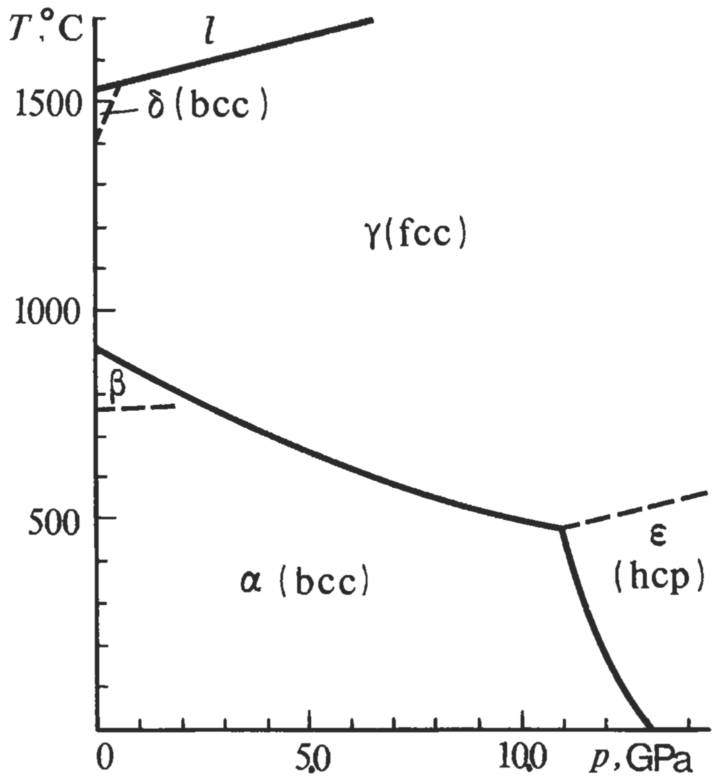

Fig. 23. Phase diagram of iron (from VAINSHTEIN *et al.* [1982]).

Table 10

Structure information for the elements of groups 11 and 12. In the first line of each box the chemical symbol, atomic number Z, and the atomic volume V_{at} under ambient conditions is listed. In the second line the electronic ground state configuration is given. For each phase there is tabulated: limiting temperature T[K] and pressure P[GPa], Pearson symbol PS, prototype structure PT, and, if applicable, the lattice parameter ratio *c/a*.

	T[K]	P[GPa]	PS	PT	*c/a*		T[K]	P[GPa]	PS	PT	*c/a*
Cu 29 $V_{at}=11.81$ Å^3						**Zn** 30 $V_{at}=15.20$ Å^3					
$1s^22s^2p^63s^2p^6d^{10}4s^1$						$1s^22s^2p^63s^2p^6d^{10}4s^2$					
			cF4	Cu					hP2	Mg	1.856
Ag 47 $V_{at}=17.05$ Å^3						**Cd** 48 $V_{at}=21.60$ Å^3					
$1s^22s^2p^63s^2p^6d^{10}4s^2p^6d^{10}5s^1$						$1s^22s^2p^63s^2p^6d^{10}4s^2p^6d^{10}5s^2$					
			cF4	Cu					hP2	Mg	1.886
Au 79 $V_{at}=16.96$ Å^3						**Hg** 80 $V_{at}=23.13$ Å^3 at 80 K					
$1s^22s^2p^63s^2p^6d^{10}4s^2p^6d^{10}f^{14}5s^2p^6d^{10}6s^1$						$1s^22s^2p^63s^2p^6d^{10}4s^2p^6d^{10}f^{14}5s^2p^6d^{10}6s^2$					
			cF4	Cu		α	<234.3		hR1	α-Hg	
						β		>3.7	tI2	α-Pa	
						γ		>12	oP4		
						δ		>37	hP2	Mg	1.76

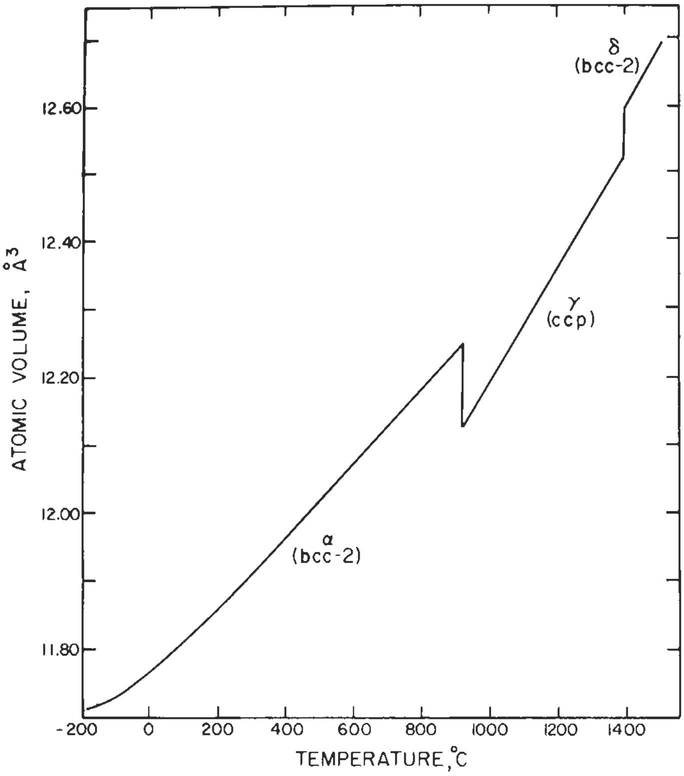

Fig. 24. The variation of atomic volume of iron with temperature (from DONOHUE [1974]).

complicated stacking order with 4.5–fold superperiod. For all lanthanides the ratio c/a is near the ideal value of $n \times 1.633$. It is interesting that with increasing pressure and decreasing atomic number the sequence of closest-packed phases hP2–Mg (..AB..) ⇒ hR3–Sm (..ABABCBCAC..) ⇒ hP4–La (..ACAB..) ⇒ cF4–Cu (..ABC..) ⇒ hP6–Pr appears (cf. figs. 10, 17 and 33).

Cerium undergoes a transformation from the γ to the α-phase at pressures >0.7 GPa:

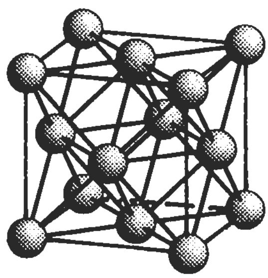

Fig. 25. The structure of cF4–Cu, space group Fm$\bar{3}$m, No. 225, 4a 0 0 0.

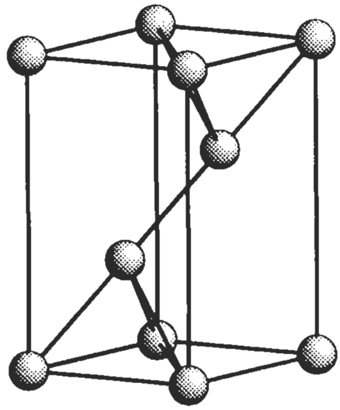

Fig. 26. The structure of hR1–Hg, space group R$\bar{3}$m, No. 166, 3a 0 0 0.

the ccp structure is preserved but the lattice constant decreases drastically from 5.14 to 4.84 Å owing to a transition of one 4f-electron to the 5d-level (fig. 34). This isostructural transition is terminated in a critical point near 550 K and 1.75 GPa (YOUNG [1991]). Further compression gives the transformation at 5.1 GPa to the α'-phase, and finally at 12.2 GPa to the ε-phase. Europium shows a completely different behavior, as do the other lanthanides, owing to the stability of its half filled 4f-orbitals. Thus, it has more similarities to the alkaline earth metals; its phase diagram is comparable to that of barium

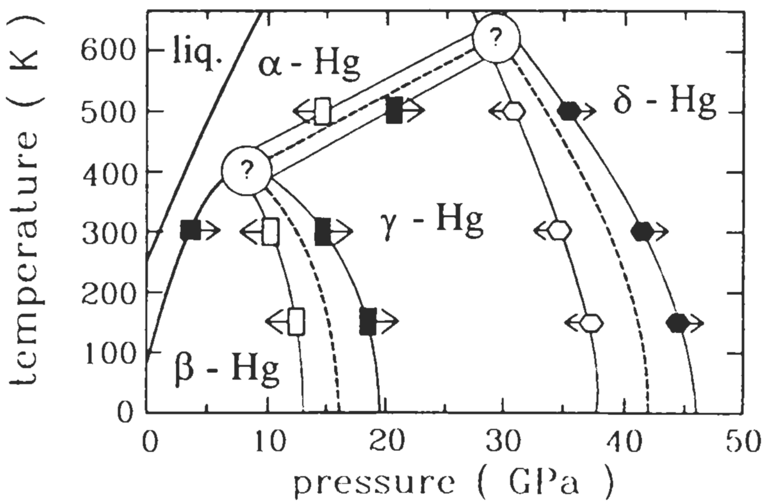

Fig. 27. Schematical phase diagram of mercury (from SCHULTE and HOLZAPFEL [1993]).

Table 11

Structure information for the elements of groups 13 and 14. In the first line of each box the chemical symbol, atomic number Z, and the atomic volume V_{at} under ambient conditions is listed. In the second line the electronic ground state configuration is given. For each phase there is tabulated: limiting temperature T[K] and pressure P[GPa], Pearson symbol PS, prototype structure PT, and, if applicable, the lattice parameter ratio *c/a*.

	T[K]	P[GPa]	PS	PT	*c/a*		T[K]	P[GPa]	PS	PT	*c/a*
Al 13 $V_{at}=16.60$ Å^3						**Si** 14 $V_{at}=20.02$ Å^3					
$1s^2 2s^2 p^6 3s^2 p^1$						$1s^2 2s^2 p^6 3s^2 p^2$					
			cF4	Cu		α			cF8	Cd	
						β		>12	tI4	β-Sn	0.552
						γ		>13.2	hP1	BiIn	0.92
						δ		>36	o?		
						ε		>43	hP2	Mg	1.699
						ζ		>78	cF4	Cu	
Ga 31 $V_{at}=19.58$ Å^3						**Ge** 32 $V_{at}=22.63$ Å^3					
$1s^2 2s^2 p^6 3s^2 p^6 d^{10} 4s^2 p^1$						$1s^2 2s^2 p^6 3s^2 p^6 d^{10} 4s^2 p^2$					
α			oC8	α-Ga		α			cF8	C	
β	<330	>1.2	cI12			β		>11	tI4	β-Sn	0.551
γ	>330	>3.0	tI2	In	1.588	γ		>75	hP1	BiIn	0.92
						δ		>106	hP4		
In 49 $V_{at}=26.16$ Å^3						**Sn** 50 $V_{at}=34.16$ Å^3 at 285 K					
$1s^2 2s^2 p^6 3s^2 p^6 d^{10} 4s^2 p^6 d^{10} 5s^2 p^1$						$1s^2 2s^2 p^6 3s^2 p^6 d^{10} 4s^2 p^6 d^{10} 5s^2 p^2$					
			tI2	In	1.521	α	<291		cF8	C	
						β	>291		tI4	β-Sn	0.546
						γ		>9.2	tI2	Pa	0.91
						δ		>40	cI2	W	
Tl 81 $V_{at}=28.59$ Å^3						**Pb** 82 $V_{at}=30.32$ Å^3					
$1s^2 2s^2 p^6 3s^2 p^6 d^{10} 4s^2 p^6 d^{10} f^{14} 5s^2 p^6 d^{10} 6s^2 p^1$						$1s^2 2s^2 p^6 3s^2 p^6 d^{10} 4s^2 p^6 d^{10} f^{14} 5s^2 p^6 d^{10} 6s^2 p^2$					
α			hP2	Mg	1.598	α			cF4	Cu	
β	>503		cI2	W		β		>13.7	hP2	Mg	1.650
γ		>3.7	cF4	Cu		γ		>109	cI2	W	

rather than to the other lanthanides. A similar behavior is observed for ytterbium which is divalent owing to the stability of the completely filled 4f-orbitals; its phase diagram resembles that of strontium.

The *c*-lattice parameter of gadolinium exhibits an anomalous expansion when cooled below 298 K (fig. 35) due to a change in the magnetic properties of the metal. Several other lanthanides show a similar behavior.

According to their electronic properties, the actinides (table 14) can be divided into two subgroups: the elements from thorium to plutonium have itinerant 5f-electrons contributing to the metallic bond, whereas the elements from americium onwards have more localized 5f-electrons. This situation leads to superconductivity for thorium, protactinium and uranium, for instance, and to magnetic ordering for curium, berkelium and californium (Dabos-Seignon *et al.* [1993]). The contribution of 5f-electrons to

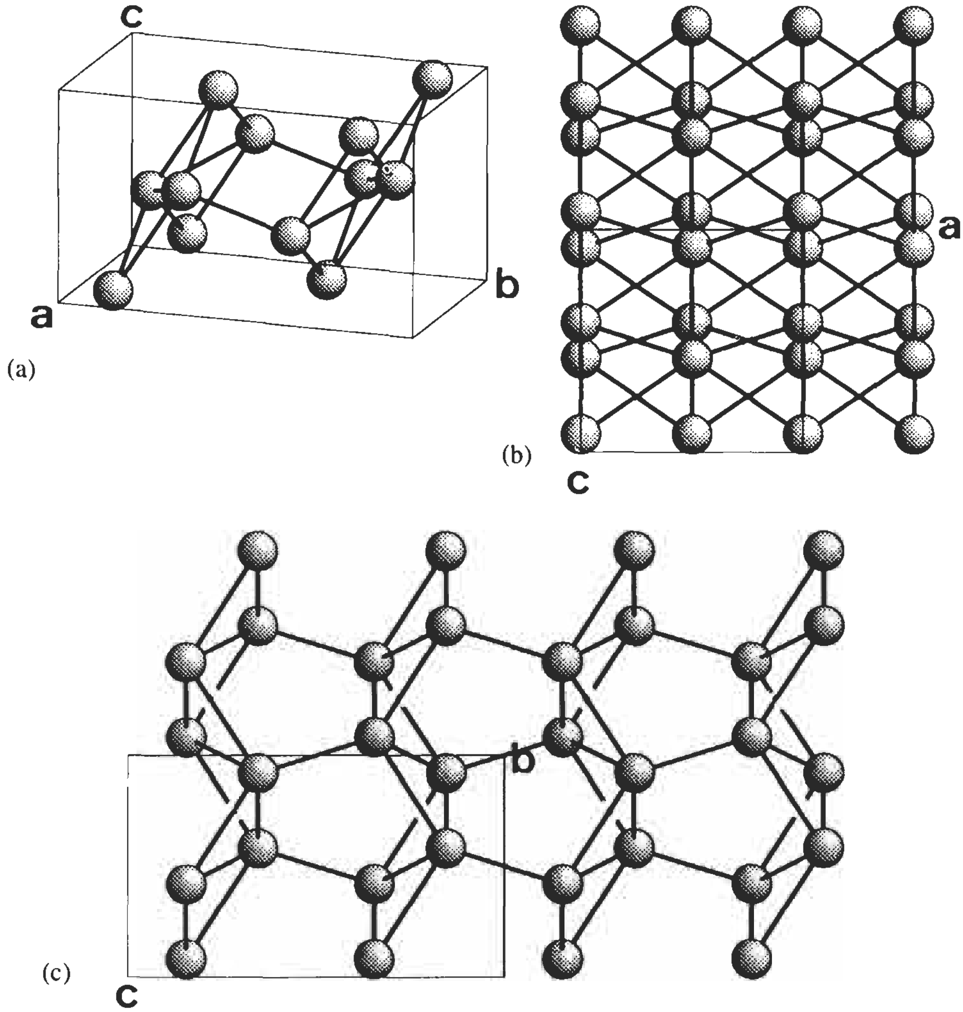

Fig. 28. The structure of oC8–Ga, Cmca, No. 64, 8f 0 0.155 0.081, (a) in a perspective view and projected upon (b) (010) and (c) (100), showing the distorted hexagonal layers.

bonding leads to low symmetry, small atomic volumes and high density in the case of the light actinides while the heavier actinides crystallize at ambient conditions in the hcp structure type. The position of plutonium at the border of itinerant and localized 5f-states causes its unusually complex phase diagram, with structures typical for both cases. Thus, monoclinic α-Pu can be considered as a distorted hcp-structure with about 20% higher packing density than cF4–Pu owing to covalent bonding contributions from 5f-electrons (fig. 36) (EK *et al.* [1993]). This ratio is quite similar to the above-mentioned one of α–Ce and γ-Ce, which are both ccp. The phase diagram of americium is very similar to

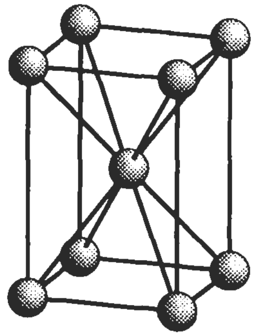

Fig. 29. The structure of tI2–In, space group I4/mmm, No. 139, 2a 0 0 0.

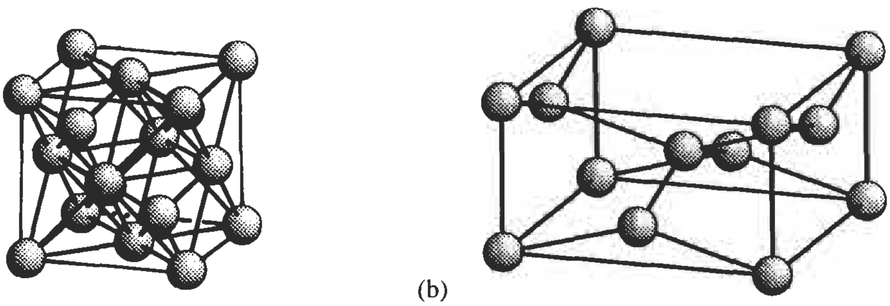

(a) (b)

Fig. 30. Relationships between the structures of the two tin allotropes: (a) grey α-Sn, cF8–C type, space group Fd$\bar{3}$m, No. 227, 8a: 0 0 0, ¾ ¼ ¾, and (b) white β-Sn, tI4–β-Sn type, space group $I4_1/amd$, No. 141, 4a: 0 0 0. Note the large difference in the minimum distances: $d_{min}^{\alpha\text{-Sn}} = 1.54$ Å and $d_{min}^{\beta\text{-Sn}} = 3.02$ Å.

those of lanthanum, proseodymium and neodymium. Owing to the localization of 5f-electrons it is the first lanthanide-like actinide element.

Both lanthanides and actinides crystallize in a great variety of polymorphic modifications (fig. 37).

Table 12

Structure information for the more metallic elements of groups 15, pnictides, and of group 16, chalcogenides. In the first line of each box the chemical symbol, atomic number Z, and the atomic volume V_{at} under ambient conditions is listed. In the second line the electronic ground state configuration is given. For each phase there is tabulated: limiting temperature T[K] and pressure P[GPa], Pearson symbol PS, prototype structure PT, and, if applicable, the lattice parameter ratio *c/a*.

	T[K]	P[GPa]	PS	PT	*c/a*		T[K]	P[GPa]	PS	PT	*c/a*
As 33 $V_{at}=21.52$ Å^3						**Se** 34 $V_{at}=27.27$ Å^3					
$1s^22s^2p^63s^2p^6d^{10}4s^2p^3$						$1s^22s^2p^63s^2p^6d^{10}4s^2p^4$					
α			hR2	α-As	2.805	α			hP3	α-Se	1.135
β		>25.0	cP1	α-Po		β		>14	mP3		
						γ		>28	tP4		
						δ		>41	hR2		
Sb 51 $V_{at}=30.21$ Å^3						**Te** 52 $V_{at}=33.98$ Å^3					
$1s^22s^2p^63s^2p^6d^{10}4s^2p^6d^{10}5s^2p^3$						$1s^22s^2p^63s^2p^6d^{10}4s^2p^6d^{10}5s^2p^4$					
α			hR2	α-As	2.617	α			hP3	α-Se	1.330
β		>8	mP4	β-Sb		β		>4.0	mP4	β-Te	
γ		>28	cI2	W		γ		>6.6	oP4		
						δ		>10.6	hR1	β-Po	
						ε		>27	cI2	W	
Bi 83 $V_{at}=35.39$ Å^3						**Po** 84 $V_{at}=38.14$ Å^3 at 311 K					
$1s^22s^2p^63s^2p^6d^{10}4s^2p^6d^{10}f^{14}5s^2p^6d^{10}6s^2p^3$						$1s^22s^2p^63s^2p^6d^{10}4s^2p^6d^{10}f^{14}5s^2p^6d^{10}6s^2p^4$					
α			hR2	α-As	2.609	α			cP1	α-Po	
β		>2.6	mC4	β-Bi		β	>327		hR1	β-Po	
γ		>3.0	mP4	β-Sb							
δ		>4.3									
ε		>9.0	cI2	W							

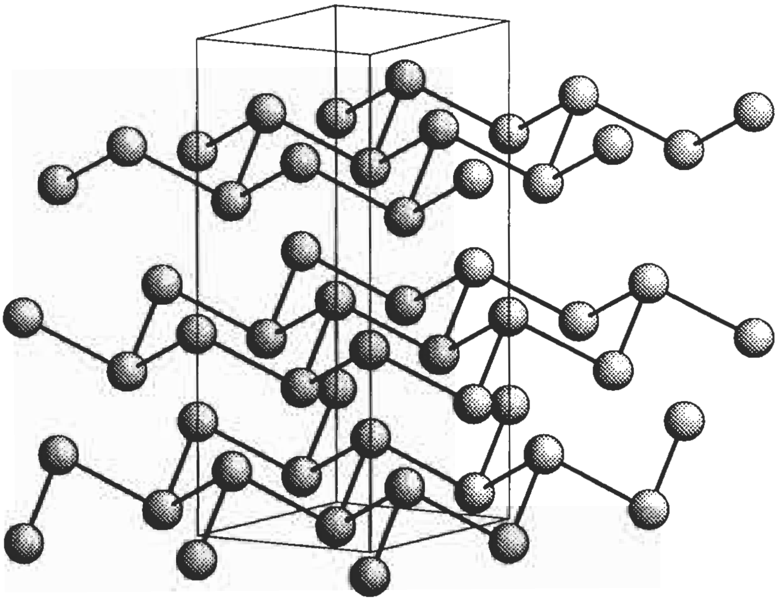

Fig. 31. The structure of hR2–As, space group R$\bar{3}$m, No. 166, 6c 0 0 0.277.

Table 13
Intralayer (d_1) and interlayer (d_2) distances in α-As-type layer structures, γ-Se-type helix structures and primitive cubic α-Po (PEARSON[1972]).

Element	Distance d_1	Distance d_2	d_2/d_1
α-As	2.51 Å	3.15 Å	1.25
α-Sb	2.87 Å	3.37 Å	1.17
α-Bi	3.10 Å	3.47 Å	1.12
γ-Se	2.32 Å	3.46 Å	1.49
γ-Te	2.86 Å	3.46 Å	1.31
α-Po	3.37 Å	3.37 Å	1.00

References: p. 45.

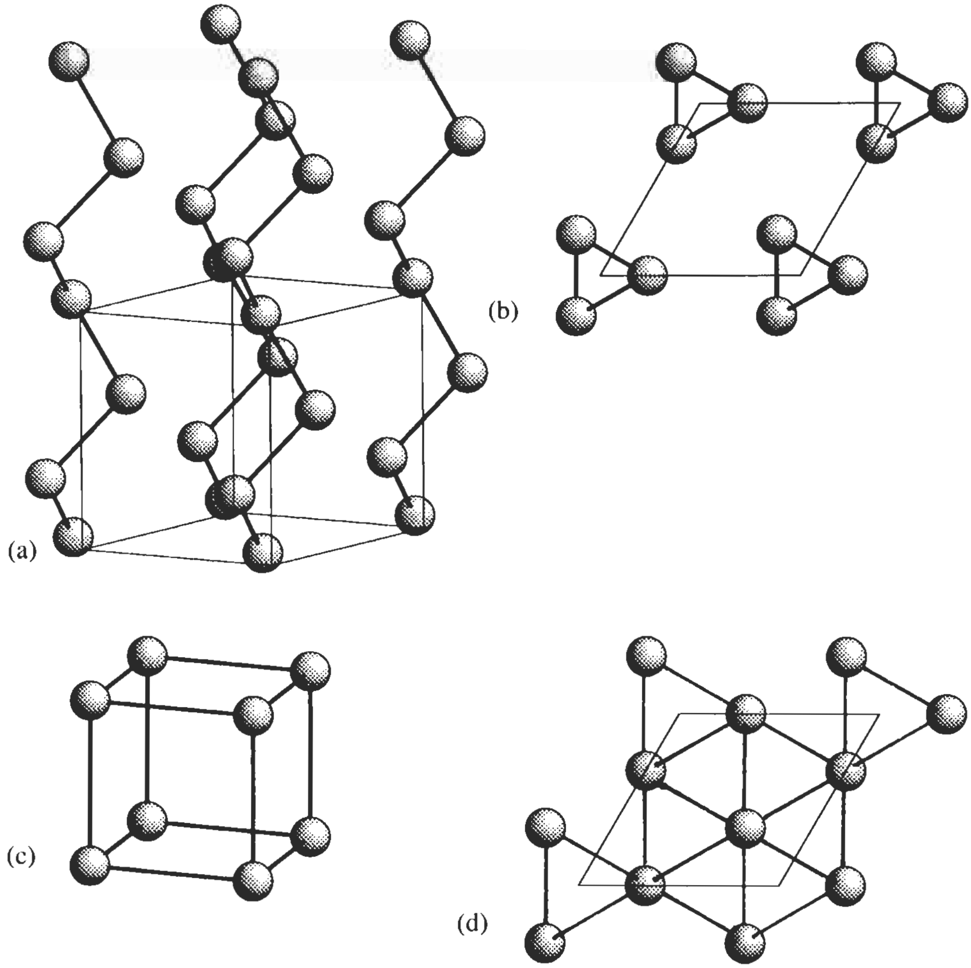

Fig. 32. (a) The structure of hP3–Se, space group $P3_121$, No. 152, 3a 0.237 0 ⅓, and (b) its projection upon (001) compared with (c) one unit cell of cP1–Po, space group $Pm\bar{3}m$, No. 221, 1a 0 0 0, and (d) its projection along [111]. The hexagonal outline of the projected cubic unit cell is drawn in.

Table 14

Structure information for the lanthanides and actinides. In the first line of each box the chemical symbol, atomic number Z, and the atomic volume V_{at} under ambient conditions is listed. In the second line the electronic ground state configuration is given. For each phase there is tabulated: limiting temperature T[K] and pressure P[GPa], Pearson symbol PS, prototype structure PT, and, if applicable, the lattice parameter ratio *c/a*.

	T[K]	P[GPa]	PS	PT	*c/a*		T[K]	P[GPa]	PS	PT	*c/a*
Ce 58 $V_{at} = 34.72$ Å^3						**Th** 90 $V_{at} = 32.87$ Å^3					
$1s^2 2s^2 p^6 3s^2 p^6 d^{10} 4s^2 p^6 d^{10} f^2 5s^2 p^6 6s^2$						$...3s^2 p^6 d^{10} 4s^2 p^6 d^{10} f^{14} 5s^2 p^6 d^{10} 6s^2 p^6 d^2 7s^2$					
α	<96		cF4	Cu		α			cF4	Cu	
β			hP4	α-La	2×1.611	β	>1633		cI2	W	
γ	>326		cF4	Cu							
δ	>999		cI2	W							
α'		>5.1	oC4	α-U?							
ε		>12.2	tI2	In							
Pr 59 $V_{at} = 35.08$ Å^3						**Pa** 91 $V_{at} = 25.21$ Å^3					
$1s^2 2s^2 p^6 3s^2 p^6 d^{10} 4s^2 p^6 d^{10} f^3 5s^2 p^6 6s^2$						$...3s^2 p^6 d^{10} 4s^2 p^6 d^{10} f^{14} 5s^2 p^6 d^{10} f^2 6s^2 p^6 d^1 7s^2$					
α			hP4	α-La	2×1.611	α			tI2	α-Pa	0.825
β	>1068		cI2	W		β	>1443		cI2	W	
γ		>3.8	cF4	Cu							
δ		>6.2	hp6	Pr	3×1.622						
ε		>20	oC4	α-U							
Nd 60 $V_{at} = 34.17$ Å^3						**U** 92 $V_{at} = 20.75$ Å^3					
$1s^2 2s^2 p^6 3s^2 p^6 d^{10} 4s^2 p^6 d^{10} f^4 5s^2 p^6 6s^2$						$...3s^2 p^6 d^{10} 4s^2 p^6 d^{10} f^{14} 5s^2 p^6 d^{10} f^3 6s^2 p^6 d^1 7s^2$					
α			hP4	α-La	2×1.612	α			oC4	α-U	
β	>1136		cI2	W		β	>941		tP30	β-U	
γ		>5.8	cF4	Cu		γ	>1049		cI2	W	
δ		>18	hp6	Pr	3×1.611						
ε		>38	mC4	?							
Pm 61 $V_{at} = 33.60$ Å^3						**Np** 93 $V_{at} = 19.21$ Å^3					
$1s^2 2s^2 p^6 3s^2 p^6 d^{10} 4s^2 p^6 d^{10} f^5 5s^2 p^6 6s^2$						$...3s^2 p^6 d^{10} 4s^2 p^6 d^{10} f^{14} 5s^2 p^6 d^{10} f^5 6s^2 p^6 7s^2$					
α			hP4	α-La	2×1.60	α			oP8	α-Np	
β	>1163		cI2	W		β	>553		tP4	β-Np	0.694
γ		>10	cF4	Cu		γ	>849		cI2	W	
δ		>18	hp6	Pr							
ε		>40	?								

Continued on next page

Table 14—*Continued*

	T[K]	P[GPa]	PS	PT	*c/a*		T[K]	P[GPa]	PS	PT	*c/a*
Sm 62 $V_{at}=33.17$ Å^3						**Pu** 94 $V_{at}=19.88$ Å^3					
$1s^2 2s^2 p^6 3s^2 p^6 d^{10} 4s^2 p^6 d^{10} f^6 5s^2 p^6 6s^2$						$...3s^2 p^6 d^{10} 4s^2 p^6 d^{10} f^{14} 5s^2 p^6 d^{10} f^6 6s^2 p^6 7s^2$					
α			hR3	α-Sm	4.5×1.605	α			mP16	α-Pu	
β	>1007		hP2	Mg	1.596	β	>388		mC34	β-Pu	
γ	>1195		cI2	W		γ	>488		oF8	γ-Pu	
δ		>4.5	hP4	α-La	2×1.611	δ	>583		cF4	Cu	
ε		>14	cF4	Cu		δ'	>725		tI2	In	1.342
ζ		>19	hp6	Pr	3×1.611	ε	>756		cI2	W	
θ		>33	mC4	?		ζ		>40.0	hP8		1.657/2
Eu 63 $V_{at}=48.10$ Å^3						**Am** 95 $V_{at}=29.27$ Å^3					
$1s^2 2s^2 p^6 3s^2 p^6 d^{10} 4s^2 p^6 d^{10} f^7 5s^2 p^6 6s^2$						$...3s^2 p^6 d^{10} 4s^2 p^6 d^{10} f^{14} 5s^2 p^6 d^{10} f^7 6s^2 p^6 7s^2$					
α			cI2	W		α			hP4	α-La	2×1.621
β		>12.5	hP2	Mg	1.553	β	>1042 or >5		cF4	Cu	
γ		>18	?			γ	>1350		cI2	W	
						δ		>12.5	mP4	δ-Am	
						ε		>15	oC4	α-U	
Gd 64 $V_{at}=33.04$ Å^3						**Cm** 96 $V_{at}=29.98$ Å^3					
$1s^2 2s^2 p^6 3s^2 p^6 d^{10} 4s^2 p^6 d^{10} f^7 5s^2 p^6 5d^1 6s^2$						$...3s^2 p^6 d^{10} 4s^2 p^6 d^{10} f^{14} 5s^2 p^6 d^{10} f^7 6s^2 p^6 d^1 7s^2$					
α			hP2	Mg	1.591	α			hP4	α-La	2×1.621
β	>1508		cI2	W		β	>1550 or >23		cF4	Cu	
γ		>2.0	hR3	α-Sm	4.5×1.61	γ		>43	oC4	α-U	
δ		>5	hP4	α-La	2×1.624						
ε		>25	cF4	Cu							
ζ		>36	hp6	Pr							
Tb 65 $V_{at}=32.04$ Å^3						**Bk** 97 $V_{at}=27.96$ Å^3					
$1s^2 2s^2 p^6 3s^2 p^6 d^{10} 4s^2 p^6 d^{10} f^9 5s^2 p^6 6s^2$						$...3s^2 p^6 d^{10} 4s^2 p^6 d^{10} f^{14} 5s^2 p^6 d^{10} f^8 6s^2 p^6 d^1 7s^2$					
α	<220		oC4	α'-Dy		α			hP4	α-La	2×1.620
α'			hP2	Mg	1.580	β	>1250 or >8		cF4	Cu	
β	>1562		cI2	W		γ		>25	oC4	α-U	
γ		>3.0	hR3	α-Sm	4.5×1.60						
δ		>6.0	hP4	α-La							
ε		>29	cF4	Cu							
ζ		>32	hp6	Pr	3×1.616						

Continued on next page

Table 14—*Continued*

	T[K]	P[GPa]	PS	PT	c/a		T[K]	P[GPa]	PS	PT	c/a
Dy 66 $V_{at} = 31.57$ Å^3						**Cf** 98 $V_{at} = 27.41$ Å^3					
$1s^22s^2p^63s^2p^6d^{10}4s^2p^6d^{10}f^{10}5s^2p^66s^2$						$...3s^2p^6d^{10}4s^2p^6d^{10}f^{14}5s^2p^6d^{10}f^{10}6s^2p^67s^2$					
α′	< 86		oC4	α′-Dy		α			hP4	α-La	2×1.625
α			hP2	Mg	1.573	β	> 863 or	> 17	cF4	Cu	
β	> 1654		cI2	W		γ		> 30	aP4	γ-Cf	
γ		> 5.0	hR3	α-Sm	4.5×1.606	δ		> 41	oC4	α-U	
δ		> 9.0	hP4	α-La							
ε		> 38	cF4	Cu							
Ho 67 $V_{at} = 31.12$ Å^3						**Es** 99					
$1s^22s^2p^63s^2p^6d^{10}4s^2p^6d^{10}f^{11}5s^2p^66s^2$						$...3s^2p^6d^{10}4s^2p^6d^{10}f^{14}5s^2p^6d^{10}f^{11}6s^2p^67s^2$					
α			hP2	Mg	1.570	α			hP4	α-La	
β	> 1660		cI2	W		β	?		cF4	Cu	
γ		> 7.0	hR3	α-Sm	4.5×1.63						
δ		> 13	hP4	α-La							
Er 68 $V_{at} = 30.65$ Å^3						**Fm** 100					
$1s^22s^2p^63s^2p^6d^{10}4s^2p^6d^{10}f^{12}5s^2p^66s^2$						$...3s^2p^6d^{10}4s^2p^6d^{10}f^{14}5s^2p^6d^{10}f^{12}6s^2p^67s^2$					
α			hP2	Mg	1.569						
β		> 7.0	hR3	α-Sm							
γ		> 13	hP4	α-La							
Tm 69 $V_{at} = 30.10$ Å^3						**Md** 101					
$1s^22s^2p^63s^2p^6d^{10}4s^2p^6d^{10}f^{13}5s^2p^66s^2$						$...3s^2p^6d^{10}4s^2p^6d^{10}f^{14}5s^2p^6d^{10}f^{13}6s^2p^67s^2$					
α			hP2	Mg	1.570						
β	> 1800		cI2	W							
γ		> 9	hR3	α-Sm							
δ		> 13	hP4	α-La	4.5×1.57						
Yb 70 $V_{at} = 41.24$ Å^3						**No** 102					
$1s^22s^2p^63s^2p^6d^{10}4s^2p^6d^{10}f^{14}5s^2p^66s^2$						$...3s^2p^6d^{10}4s^2p^6d^{10}f^{14}5s^2p^6d^{10}f^{14}6s^2p^67s^2$					
α	< 270 or	> 34	hP2	Mg	1.646						
β			cF4	Cu							
γ	> 1047 or	> 3.5	cI2	W							
Lu 71 $V_{at} = 29.52$ Å^3						**Lr** 103					
$1s^22s^2p^63s^2p^6d^{10}4s^2p^6d^{10}f^{14}5s^2p^6d^16s^2$						$...3s^2p^6d^{10}4s^2p^6d^{10}f^{14}5s^2p^6d^{10}f^{14}6s^2p^6d^17s^2$					
			hP2	Mg	1.583						
β		> 18	hR3	α-Sm	4.5×1.52						
γ		> 35	hP4	α-La							

References: p. 45.

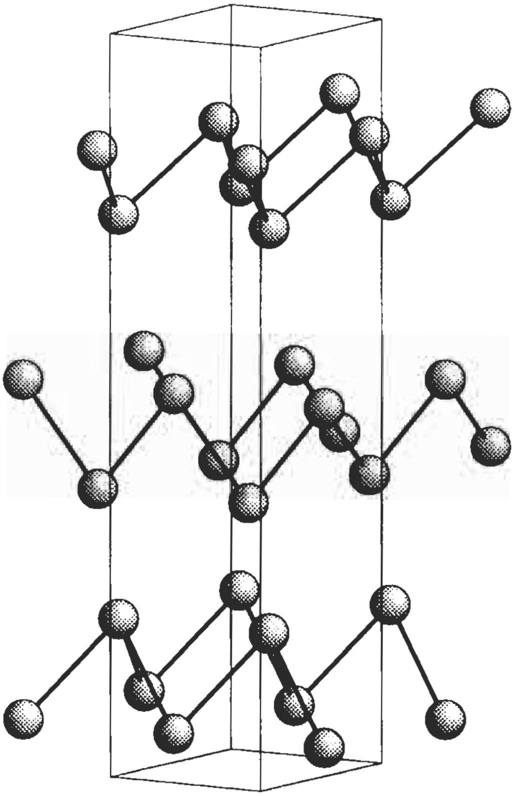

Fig. 33. The structure of hP6–Pr, space group $P3_121$, No. 152, 6c 0.28 0.28 0.772.

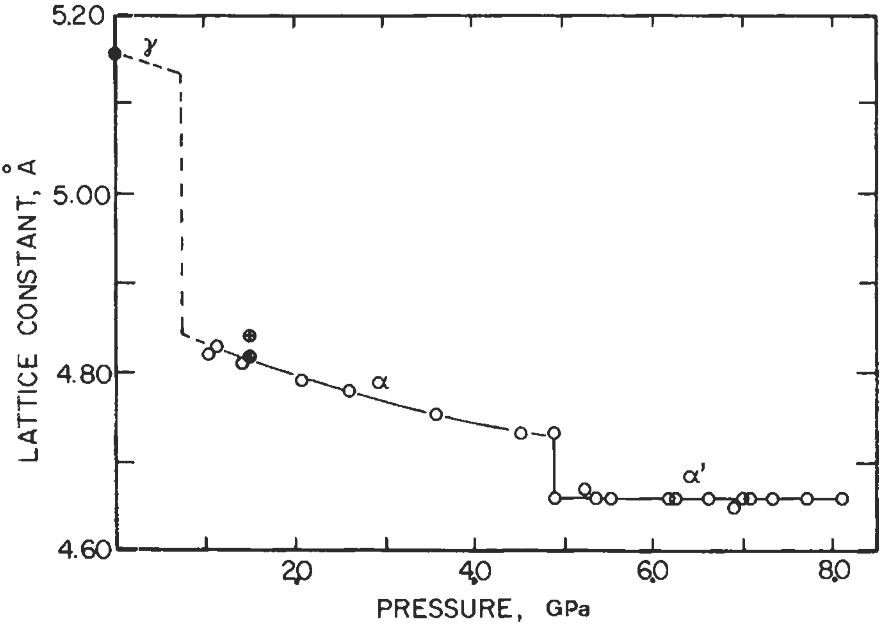

Fig. 34. Pressure dependence of the atomic volume of cerium (from DONOHUE [1974]).

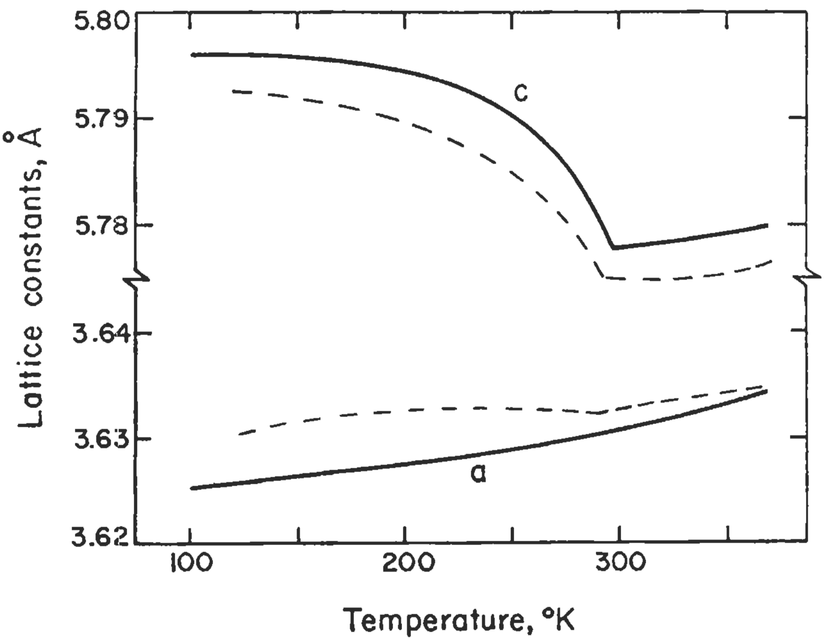

Fig. 35. Variation of the lattice parameters of gadolinium with temperature. There are no structural changes in this temperature range (from DONOHUE [1974]).

References: p. 45.

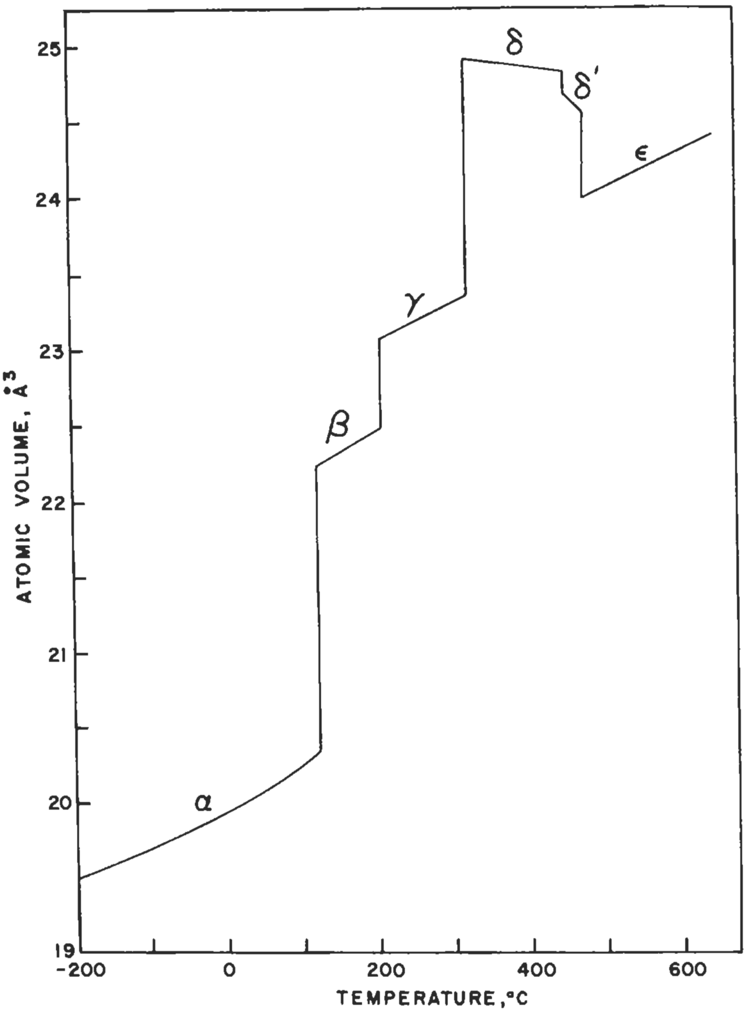

Fig. 36. The variation of the atomic volume of the various allotropes of plutonium with temperature (from DONOHUE [1974]).